Full paper

A Physcomitrella PIN protein acts in spermatogenesis and sporophyte retention

Volker M. Lüth[1], Christine Rempfer[1,2], Nico van Gessel[1], Oliver Herzog[1], Melanie Hanser[1,*], Marion Braun[1], Eva L. Decker[1] and Ralf Reski[1,2,3,4]

[1] Plant Biotechnology, Faculty of Biology, University of Freiburg, Freiburg, Germany
[2] Spemann Graduate School of Biology and Medicine (SGBM), University of Freiburg, Freiburg, Germany
[3] CIBSS – Centre for Integrative Biological Signalling Studies, University of Freiburg, Freiburg, Germany
[4] Cluster of Excellence *liv*MatS @ FIT – Freiburg Center for Interactive Materials and Bioinspired Technologies, University of Freiburg, Freiburg, Germany

Current address:
* Leibniz Institute of Vegetable and Ornamental Crops (IGZ), Großbeeren, Germany

Author for correspondence: *Ralf Reski, Email: ralf.reski@biologie.uni-freiburg.de*

Key words: auxin, bryophyte, flagellum, moss, plant development, sperm, spermatozoid

Summary

- The auxin efflux PIN-FORMED (PIN) proteins are conserved in all land plants and important players in plant development. In the moss Physcomitrella (*Physcomitrium patens*) three canonical PINs (PpPINA-C) are expressed in the leafy shoot (gametophore). PpPINA and PpPINB show functional activity in vegetative growth and sporophyte development. Here, we examined the role of PpPINC in the life cycle of Physcomitrella.
- We established reporter and knockout lines for PpPINC and analysed vegetative and reproductive tissues using microscopy and transcriptomic sequencing of moss gametangia.
- PpPINC is expressed in immature leaves, mature gametangia and during sporophyte development. The sperm cells (spermatozoids) of *pin*C knockout mutants exhibit increased motility and an altered flagella phenotype. Further, the *pin*C mutants have a higher portion of differentially expressed genes (DEGs) related to spermatogenesis, increased fertility, and an increased abortion rate of premeiotic sporophytes.
- Here, we show that PpPINC is important for spermatogenesis and sporophyte retention. We propose an evolutionary conserved way of polar growth during early moss embryo development and sporophyte attachment to the gametophore, while suggesting the mechanical function in sporophyte retention of a ring structure, the Lorch ring.

Introduction

The auxin signal transduction pathway is conserved in all land plants (Paponov *et al.*, 2009; Flores-Sandoval *et al.*, 2015; Thelander *et al.*, 2018; Cancé *et al.*, 2022). In the model moss Physcomitrella (*Physcomitrium patens*), the main auxin biosynthesis pathway is, as in Arabidopsis, the conversion of tryptophan by TAR enzymes to indole-3-pyruvate (IPyA) from where it is converted by YUC enzymes into active auxin (indole-3-acetic acid, IAA) (Landberg *et al.*, 2020). Auxin homeostasis plays an important role during the life cycle of Physcomitrella, maintaining growth and organogenesis (Ludwig-Müller *et al*., 2009; Thelander *et al.*, 2018). However, there is no indication for a polar auxin transport in the leafy moss shoot, the gametophore (Fujita *et al.*, 2008), although the protein family responsible for polar auxin transport, PIN-FORMED (PIN), is conserved in all land plants, including bryophytes (Bennett *et al.*, 2014a; Zhang *et al.*, 2020a). Instead, auxin transport appears to be diffusive in the moss gametophore (Coudert *et al.*, 2015).

Canonical PIN proteins share four highly conserved motifs in the hydrophilic loop and a strong conservation in the N'- and C'-terminal transmembrane regions, while noncanonical PINs are defined by a higher variability (Bennett *et al.*, 2014a). Structures and mechanism of auxin transport have recently been elucidated in great detail for the *Arabidopsis thaliana* PIN8 protein (Ung *et al*., 2022). The Physcomitrella genome encodes four PIN genes, the three canonical *PpPINA*, *PpPINB* and *PpPINC*, and the noncanonical *PpPIND*, with *PpPINA* and *PpPINB* being the most similar to each other (Bennett *et al.*, 2014b). The Physcomitrella PIN proteins form an outgroup with other bryophytes to vascular plants, where the canonical PpPINs cluster with PIN proteins from other mosses, while the noncanonical PpPIND is separated together with several PIN proteins of the liverwort *Marchantia polymorpha* (Bennett *et al.*, 2014a).

In the gametophore, auxin accumulates beneath the stem apex and at the stem base (Bierfreund *et al.*, 2003; Fujita *et al.*, 2008). Apical stem cells show the highest expression of *PpTAR* genes, indicating biosynthesis of IPyA (Landberg *et al.*, 2020). The growth of developing leaves (phyllids) in Physcomitrella is marked by high auxin-signalling related activity (Thelander *et al.*, 2019) with all three canonical *PpPIN* genes being active (Viaene *et al.*, 2014). While *PpPINA* is the highest expressed *PIN* gene in Physcomitrella tissues, *PpPINC* has the lowest expression level of all canonical PINs (Bennett *et al.*, 2014b). Single knockouts of *PpPIN* genes have no severe effect on gametophore growth (Viaene *et al.*, 2014), while the double knockout of *PpPINA* and *PpPINB* leads to elongated phyllids, a phenotype similar to Physcomitrella gametophores treated with excess auxin or auxin transport inhibitors (Decker *et al.*, 2006; Bennett *et al.*, 2014b).

When introduced to short day conditions with low temperatures, the monoecious moss Physcomitrella initiates the formation of sexual organs on the gametophore apex (Hohe *et al.*, 2002) with specialized stem cells for female archegonia and male antheridia development (Kofuji & Hasebe, 2014). Growth of

antheridia and archegonia is highly synchronized, beginning with the formation of the antheridia while archegonia develop later but mature faster, so that self-fertilization is possible (Cove, 2005; Landberg *et al.*, 2013). The development and growth of gametangia is controlled by the auxin-biosynthesis regulators *SHORT INTERNODE/STYLISH* (*SHI/STY*) and TAR enzymes, influencing the neck length of archegonia and growth of antheridia. During antheridia development, the expression of *PpSHI* and *PpTAR* genes overlap with the expression of *PpPINA* and the accumulation of auxin in apical cells, before spermatogenesis begins. This activity slowly declines and reaches its lowest point during spermatogenesis, indicating a process where auxin plays a minor role (Landberg *et al.*, 2013; Landberg *et al.*, 2020). Spermatogenesis in Physcomitrella is tightly regulated, producing motile, biflagellate sperm cells (spermatozoids), relying on the availability of water to swim to the egg cell (Reski, 1998; Cove, 2005; Ortiz-Ramírez *et al.*, 2017; Koshimizu *et al.*, 2018; Gu *et al.*, 2022). As in antheridia, the activity of auxin biosynthesis, signalling and accumulation are the highest in archegonia during early development. The precursor egg cell and apical neck cells show the highest activity, while there is minimal expression during egg maturation (Landberg *et al.*, 2013; Landberg *et al.*, 2020).

After fertilization of the egg cell, the zygote develops into a diploid embryo, resulting in the sporophyte (Horst *et al*., 2016). The Physcomitrella sporophyte is reduced compared to other mosses (Kirbis *et al.*, 2020), even within its own family (Ostendorf *et al.*, 2021), and consists of the sporophyte foot, a short seta and the spore capsule, which rips open after maturation to release the haploid spores (Cove, 2005). Auxin is distributed dynamically in a polar manner during sporophyte development, with an auxin maximum in the apex of the early embryo which later localizes to the foot of the young sporophyte where it slowly recedes during maturation (Fujita *et al.*, 2008). The sporophyte foot is secured in a maternal cavity (vaginula) and covered at its base with haustorial cells, important for nutrient uptake from the gametophore (Regmi *et al.*, 2017). Sporophyte formation is complex and regulated by a number of genetic elements (Sakakibara *et al.*, 2008; Mosquna *et al.*, 2009; Horst *et al.*, 2016; Ortiz-Ramírez *et al.*, 2016; Hashida *et al.*, 2020; Kirbis *et al.*, 2020; Takechi *et al.*, 2021, Landberg *et al.* 2022; Lopez-Obando *et al.*, 2022). However, auxin remains a crucial player in sporophyte development (Fujita *et al.*, 2008) through the function of the two Physcomitrella PpPINA and PpPINB proteins (Bennett *et al.*, 2014b), whereas the role of the third canonical PIN, PpPINC, remains unclear.

Here, we elucidate the role of PpPINC in the Physcomitrella life cycle. We found that PpPINC influences spermatogenesis-related gene expression, controls motility and morphology of moss sperm cells, and is important for the retention of the diploid sporophyte on the haploid gametophyte, and thus preventing early abortion of premeiotic sporophytes, while it has no obvious role in the development of the gametophyte, the protonemata and gametophores.

Material and Methods

Plant material and culture conditions

The *Physcomitrella patens* (Hedw.) Bruch & Schimp. ecotype Gransden covers several laboratory strains which are descendants of the first original cultivated single clone (Haas *et al.*, 2020) and was recently renamed to *Physcomitrium patens* (Hedw.) Mitt.. We used as wild type (WT) a fertile Gransden line, which underwent sexual reproduction regularly as a basis for all transgenic lines. Plants were cultivated using Knop medium (pH 5.8) according to Reski & Abel (1985) containing microelements according to Egener *et al.* (2002). For solid medium, 12 g/l agar (OXOID, Thermo Scientific) were added. Standard growth conditions were long day 16 hours light with 70±5 µmol m^{-2} s^{-2} at 22°C. Sporophyte induction was modified after Hohe *et al.* (2002). Plants were grown in long day conditions, before being transferred to sporophyte inducing conditions (Hohe *et al.*, 2002). At day 18 of sporophyte induction, plants were watered (H_2O dest., 10 ml for 9 cm petri dish), which was removed from the plate at day 25. All moss lines used are stored in the International Moss Stock Center (IMSC; https://www.moss-stock-center.org) with the following accession numbers: *PinCPromCit* = 40917, *pin*C#10 = 40918, *pin*C#29 = 40919, *pin*C#69 = 40420, WT = 40095.

Generation of transgenic lines

Transgenic lines were created via highly efficient homologous recombination (Hohe *et al.*, 2004) in transformed protoplasts (Hohe & Reski, 2002). For the generation of targeted *pin*C mutants the region upstream from the beginning of the first exon to the untranslated region after exon six was amplified (2915 bp) from genomic DNA using the following primers: P3-KO Fw + P3-KO Rv (Supplemental Table S1). The amplified fragment was sub-cloned into the vector *pJET1.2*. Using *SacI* and *NcoI* a fragment of the *PpPINC* gene (1696 bp) was replaced with a sulfadiazine selection cassette (Parsons *et al.*, 2012). For the generation of the transcriptional reporter line, 2.1 kb upstream of the start codon of the *PpPINC* gene were fused to the citrine CDS and nos terminator via Gibson cloning (Gibson *et al.*, 2009), using primers 5PinCprom_f+CA5 + 3PinCprom_r+Citrin (Supplemental Table S1). The expression cassette was cloned between homologous regions of the carbonic anhydrase locus (Wiedemann *et al.*, 2018), erasing the citrine expression of the parental plant when correctly integrated into the genome.

Molecular analysis of transgenic lines

Initial screening of knockout and reporter lines was done with leaflet PCR according to Schween *et al.* (2002), to test for the presence of the construct. For RT-PCR total RNA was extracted from 6-weeks-old gametophores, 21 days after the sporophyte induction started using the innuPREP Plant RNA Kit (Analytik Jena AG, Jena, Germany) and reversely transcribed using oligo-d(T)16 primers with Superscript III reverse transcriptase (Life Technologies, Thermo Fisher Scientific). Analysis for the absence of *PpPINC* RNA was performed with the gene-specific primers Pin3f_ex1-2 + Pin3r_ex2 (Supplemental Table S1). Presence of cDNA was tested with C45_fwd and C45_rev (Supplemental

Table S1) amplifying the constitutively expressed gene L21. Transgene copy numbers were tested via quantitative Real-Time PCR according to Noy-Malka *et al.* (2014). Genomic DNA was isolated from protonema one week after the last tissue disruption using the innuPREP Plant DNA Kit (Analytic Jena AG). Transgene copy numbers were determined comparing relative values of the transgene 35S promoter (35SPqPCR_f + 35SPqPCR_r; Supplemental Table S1) with the single copy transgene carbonic anhydrase line used in Wiedemann *et al.* (2018), for normalization the single copy gene CLF was used (Noy-Malka *et al.*, 2014).

Tissue isolation for gene expression analysis using SMARTseq

Triplicates of tissue samples were collected 18 days after gametophores were exposed to sporophyte-inducing conditions. Mature archegonia and antheridia were collected manually using a stereoscope (Olympus SZX7) and stored directly in TRIzol® (Fisher Scientific GmbH, Schwerte, Germany). All lines used were grown together on the same plate. For each sample eight archegonia or antheridia were collected. Tissues were homogenized using small pistils and mixed with chloroform. The aqueous phase was then processed using the Direct-zol RNA Microprep Kit (Zymo Research Europe GmbH, Freiburg, Germany). The resulting RNA was treated with RiboLock RNase Inhibitor (Fisher Scientific GmbH, Schwerte, Germany). The cDNA library was created at the Genomics Unit in the Instituto Gulbenkian de Ciencia, Portugal according to Picelli *et al.* (2014). Libraries were sequenced using the Illumina RNAseq platform from Novogene (Novogene Company Limited, Cambridge, UK).

Transcriptomic data processing

Raw data was trimmed using Trim Galore (Version 0.6.6; adapter stringency = 1 bp; minimum required sequence length for retaining a read pair = 20 bp; 3'clipping = 1 bp). All further steps were done using the Galaxy platform (Afgan *et al.*, 2018). The 150 bp paired-end reads were then mapped to the Physcomitrella genome version 3.3 downloaded from Phytozome (Goodstein *et al.*, 2012) using HISAT2 (Galaxy Version 2.1.0; spliced alignment activated). Mapped reads were counted with feature counts (Galaxy Version 2.0.1; excluding chimeric fragments; only fragments with both reads aligned, GFF feature type filter = CDS; GFF gene identifier = gene_id). Differential gene expression was analyzed using DESeq2 (Galaxy Version 2.11.40.6+galaxy1) and filtered for enriched gene ontology (GO) terms with GOEnrichment (Galaxy Version 2.0.1). Quality of mapping and read counts were controlled with MultiQC (Galaxy Version 1.11+galaxy0) and FastQC (Galaxy Version 0.73+galaxy0).

Calcium measurement in sperm cells

Sperm packets of single antheridia where extracted directly after being released from the antheridium and placed on polylysine-covered glass slides according to Horst & Reski (2017). Sperm cells where incubated in a Fluo-4 solution according to Ortiz-Ramírez *et al.* (2017) for 20 minutes, photographed (see microscopy) and pictures were then analysed using ImageJ (Schneider *et al.*, 2012).

Spermatozoid motility assessment

Mature antheridia were prepared on the moss apex, placed under a glass slide and sealed with nail polish to prevent water evaporation. Ripe antheridia opened without applying pressure, releasing sperm packets, which were then analyzed for motility.

Sporophyte count

For all lines we analysed all gametophores on the respective plate with three plates for each line. Sporophytes were counted 4 weeks after watering (see sporophyte induction culture conditions). To account for sporophytes, embryos, empty vaginulae and aborted sporophytes we removed the phyllids of the gametophore apices.

Statistical analysis

Stem length, leaf length and leaf width were tested with Student's t-Test with $p < 0.05$. Significance of motility was assessed with one-sided ANOVA and Tukey-Kramer test, flagellar phenotype with one-sided ANOVA. All tests were performed with Microsoft Excel and the XLMiner Analysis ToolPak.

Protein alignments and motif analysis

Needleman-Wunsch (Needleman & Wunsch, 1970) and multiple sequence alignments (Larkin *et al.*, 2007) with Clustal Omega (1.2.4) were performed using the European Bioinformatics Institute (EMBL-EBI) web tools (https://www.ebi.ac.uk/services) (Madeira *et al.*, 2019). Needleman-Wunsch alignments were performed with BLOSUM62, a gap penalty of 10 and extend penalty of 0.5. Multiple sequence alignments were performed with default settings.

Flow cytometry

Flow cytometry analysis was performed according to Heck *et al.* (2021) to determine ploidy of the transgenic lines (*pin*C#10, *pin*C#29, *pin*C#69, *pinCPromCit*). As there is a risk of creating diploid plants during PEG-mediated transformation of protoplasts, which could alter gene expression compared to haploid plants (Rempfer *et al.*, 2022), only haploid transgenics were analysed further.

Microscopy

For preparation of samples, we used an Olympus SZX7 stereoscope and for extraction of sperm packages a Zeiss Axiovert microscope. Fluorescence and bright-field microscopy pictures were taken with a Zeiss Axioplan 100 with a Zeiss MRc5 camera and Zeiss AxioVision software (Version 3.8.2).

Phylogenetic reconstruction and transmembrane prediction

Based on reference sequences from *A. thaliana* and *P. patens* we conducted proteome-wide sequence searches with DIAMOND (v0.9.19, Buchfink *et al.*, 2021) against *Anthoceros angustus* (Zhang *et al.*, 2020b), *Calohypnum plumiforme* (Mao *et al.*, 2020), *Chlamydomonas reinhardtii* (Merchant *et al.*,

2007), *Ceratodon purpureus* (Carey *et al.*, 2021), *Ceratopteris richardii* (Marchant *et al.*, 2022), *Funaria hygrometrica* (Kirbis *et al.*, 2021), *Klebsormidium nitens* (Hori *et al.*, 2014), *Marchantia polymorpha* (Bowman *et al.*, 2017), *Mesotaenium endlicherianum* (Cheng *et al.*, 2019), *Oryza sativa* (Ouyang *et al.*, 2006), *Picea abies* (Nystedt *et al.*, 2013), *Populus trichocarpa* (Tuskan *et al.*, 2006), *Selaginella moellendorffii* (Banks *et al.*, 2011), *Sphagnum fallax* (v1.1, DOE-JGI, http://phytozome.jgi.doe.gov/), *Sphagnum magellanicum* (v1.1, DOE-JGI, http://phytozome.jgi.doe.gov/), *Spirogloea muscicola* (Cheng *et al.*, 2019), and *Vitis vinifera* (Jaillon *et al.*, 2007). Multiple sequence alignment of protein sequences was performed with UPP/SEPP (v4.5.1, Nguyen *et al.*, 2015) and converted into a codon-aware alignment of coding sequences with PAL2NAL (v14, Suyama *et al.*, 2006). A maximum-likelihood tree was calculated with RAxML (v8.2.12, Stamatakis, 2014) using the "GTRGAMMA" model and 1,000 bootstrap replicates and visualized using R (v4.2.1, R Core Team 2022) and the ggtree package (v3.4.4, Yu *et al.*, 2017) alongside transmembrane domains which were predicted by DeepTMHMM (v1.0.15, Hallgren *et al.*, 2022).

Results

Physcomitrella PIN family

The Physcomitrella genome (Lang *et al.*, 2018) encodes three canonical PIN proteins, PpPINA (Pp3c23_10200), PpPINB (Pp3c24_2970) and PpPINC (Pp3c10_24880). These proteins are similar in structure and length (Figure 1), consisting like all canonical land plant PINs of two transmembrane regions (five helices each), separated by a hydrophilic loop (Figure 1). The transmembrane regions have the same length in all three proteins, whereas the hydrophilic loop of PpPINC is 15 amino acids (AA) shorter than those of PpPINA and PpPINB (Table 1). While PpPINA and PpPINB are very similar in their AA sequences, PpPINC differs more, especially in the hydrophilic loop (Supplemental Figure S1). While PpPINA and PpPINB share a sequence identity above 86 %, for PpPINC it is below 65 % compared to the others (Table 1, Supplemental Figure S1). Based on these findings and our phylogenetic reconstruction of PINs from selected plant species (Figure 1), we conclude that PpPINA, PpPINB and PpPINC trace back to a single sequence in the last common ancestor of the Funariaceae and originated from two gene duplication events in the genomic history of Physcomitrella (Lang *et al.*, 2018): an older one that separated PpPINC from the common ancestor of PpPINA and PpPINB and a more recent one that separated the latter two. The genomic *PpPINC* sequence is identical between the two ecotypes Gransden and Reute from the 5'UTR to the 3'UTR.

Compared to the canonical Arabidopsis PINs (AtPIN1,2,3,4,7), the hydrophilic loop of Physcomitrella PINs are between 51 and 97 AA longer, while there is strong conservation in the transmembrane regions (Supplemental Figure S1).

Table 1: Identity, similarity and length of Physcomitrella PpPIN protein motifs

	A vs B	A vs C	B vs C	PpPINA	PpPINB	PpPINC
	Identity; Similarity of AA in %			Length AA		
TM N’	96.1;98.7	87.7;93.5	88.4;93.5	155	155	155
HL	86.3;91.4	64.7;76.9	64.4;76.8	409	409	394
TM C’	95.3;98.7	80.0;88.0	77.3;86.7	150	150	150

A = PpPINA, B = PpPINB, C= PpPINC, TM N’ = N-terminal transmembrane region, HL = Hydrophilic loop, TM C’=C-terminal transmembrane region.

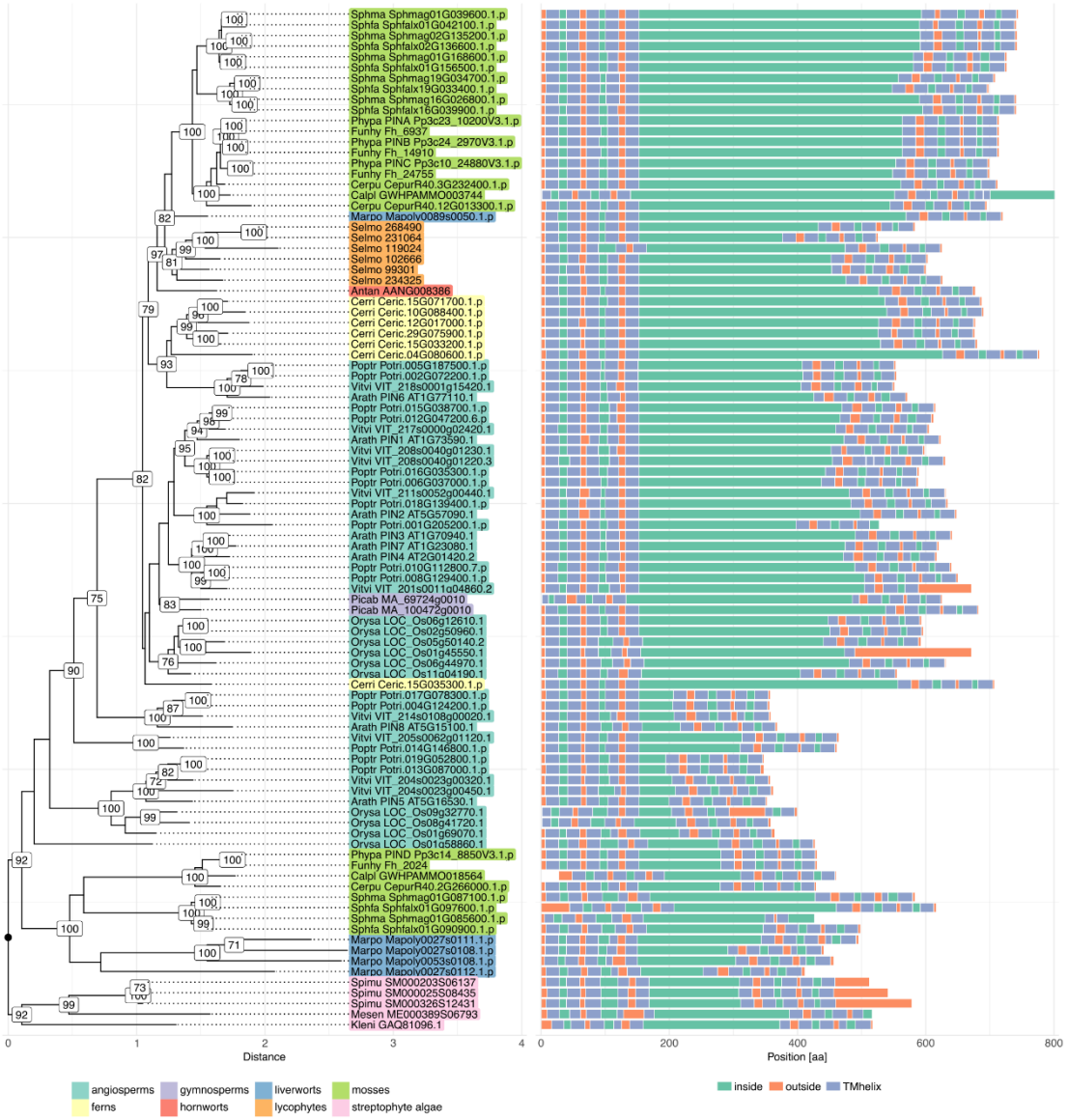

Figure 1: Phylogenetic reconstruction and transmembrane architecture of plant PIN proteins. Left: maximum-likelihood tree of a codon-aware multiple sequence alignment of PIN coding sequences annotated with bootstrap support values (>70 %) and taxonomic units, rooted at the split between streptophyte algae and embryophytes. Right: protein architecture based on DeepTMHMM transmembrane predictions. Species abbreviations: Antan, *Anthoceros angustus*; Arath, *Arabidopsis thaliana*; Calpl, *Calohypnum plumiforme*; Chlre, *Chlamydomonas reinhardtii*; Cerpu, *Ceratodon purpureus*; Cerri, *Ceratopteris richardii*; Funhy, *Funaria hygrometrica*; Kleni, *Klebsormidium nitens*; Marpo, *Marchantia polymorpha*; Mesen, *Mesotaenium endlicherianum*; Orysa, *Oryza sativa*; Phypa, *Physcomitrium patens*; Picab, *Picea abies*; Poptr, *Populus trichocarpa*; Selmo, *Selaginella moellendorffii*; Sphfa, *Sphagnum fallax*; Sphma, *Sphagnum magellanicum*; Spimu, *Spirogloea muscicola*; Vitvi, *Vitis vinifera*.

Stage-specific expression of *PpPINC*

We compared *PpPIN* expression in publicly available data (PEATmoss database; Fernandez-Pozo *et al.*, 2020) for the two Physcomitrella ecotypes Gransden and Reute in two or three datasets, respectively (Hiss *et al.*, 2014; Ortiz-Ramírez *et al.*, 2016; Perroud *et al.*, 2018). As reported in Bennett *et al.* (2014b), *PpPINA* is the highest expressed gene of the three, followed by *PpPINB* with lower, but similar expression. Consistent across the data sets, *PpPINC* is the lowest expressed of the three. While there are some differences in the expression in single tissues in the different data sets, the overall expression of *PIN* genes in both Physcomitrella ecotypes is very similar. In protonema, the expression of all three *PIN*s is the lowest, while the highest expression of *PpPINA* and *PpPINB* can be found in gametophores and developing sporophytes. For *PpPINC*, the expression in vegetative (gametophytic) tissues is very low, while there is a dynamic expression during sporophyte development in both ecotypes, which is nonetheless lower compared to the other two PINs in the same sporophytic tissues (Supplemental Figure S2).

For a closer look, we created a moss line expressing citrine (*pinCPromCit*) under the influence of the native *PpPINC* promoter region (2.1 kb upstream CDS start). This construct was targeted to the carbonic anhydrase-citrine tagged locus created by Wiedemann *et al.* (2018), because of the high expression of the carbonic anhydrase gene and the ease of selection. We screened for altered citrine signals in transformed plants compared to the ever-present citrine expression of the parental line and thus recovered a line with targeted integration of the *pinCPromCit* construct (Supplemental Figure S3). We also created knock-in reporter lines, targeting the hydrophilic loop of PpPINC, similar to localization approaches used in Arabidopsis. However, we found that the transcript of these knock-in lines stopped before the reporter sequence started, resulting in transgenics with no visible reporter signal and no perturbed phenotypes. We therefore dismissed this approach and concentrated on the native promoter strategy. Under standard growth conditions we did not observe *PpPINC*-driven citrine fluorescence,

neither in protonema, rhizoids, stems, nor in adult phyllids (Figure 2a). In contrast, citrine fluorescence was clearly visible in the apices of young phyllids. From here, fluorescence proceeds towards the base until maturation of the phyllid. Intriguingly, *PpPINC* expression was highest in parts of the midrib (costa) and in phyllid margins (Figure 2b, c).

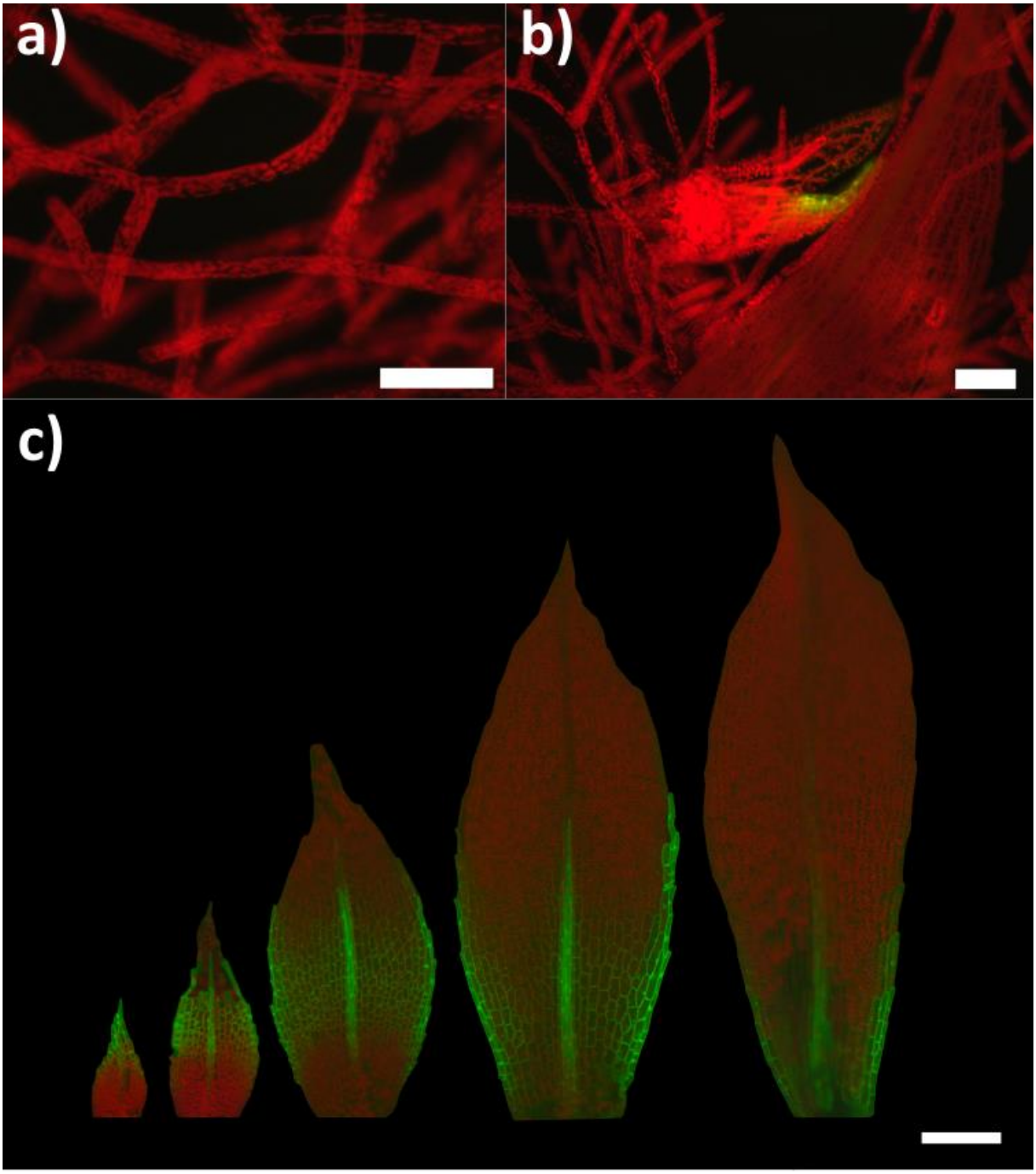

Figure 2: *PpPINC* is expressed in developing phyllids of Physcomitrella. Fluorescence microscopy to visualize citrine expression in a *PpPINC* promoter line (green). Red marks autofluorescence of chlorophyll: a) protonema (bar = 100 µm) b) budding gametophore (bar = 100 µm) c) the youngest phyllids of a moss gametophore (bar = 200 µm).

In addition, citrine expression was detectable in developing gametangia. In mature antheridia close to releasing their sperm cells (antheridium stage 9 in Landberg *et al.*, 2013), the signal was found in the foot cells separating the antheridial body from the gametophore apex (Figure 3a). In archegonia, a citrine signal was visible only after the neck canal had opened, surrounding the transition zone between canal and archegonial body above the egg cell (Figure 3b).

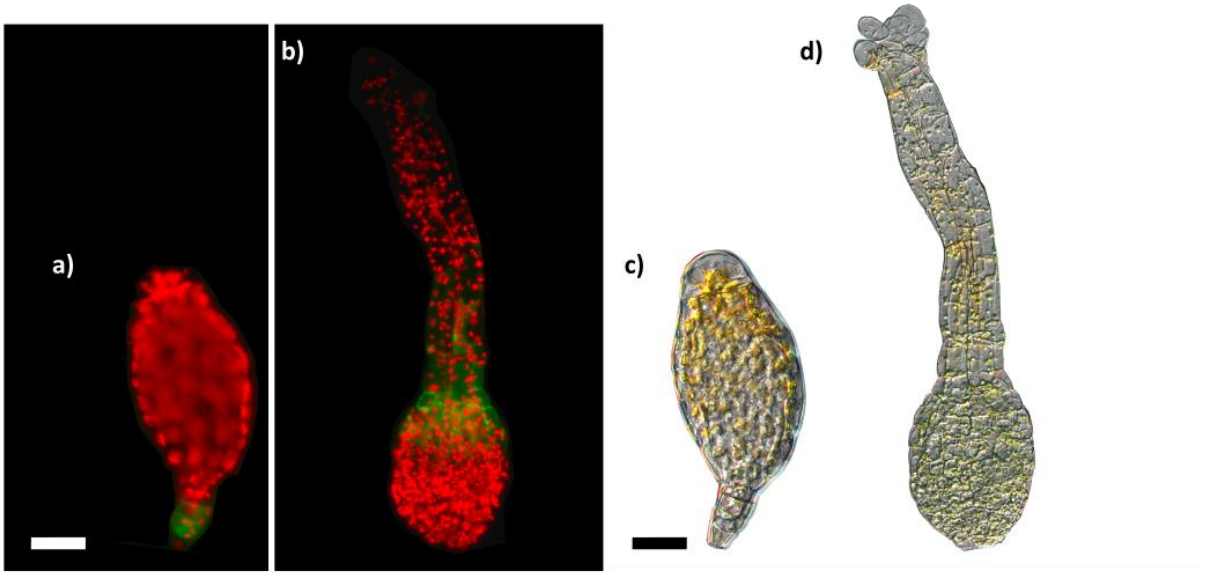

Figure 3: In Physcomitrella, *PpPINC* is dynamically expressed in reproductive organs. Fluorescence-microscopy to visualize citrine expression in a *PpPINC* promoter line (green). Red marks autofluorescence of chlorophyll: a) and c) mature antheridium shortly before sperm cells are released (scale bar = 25 µm). Sperm cells can be seen inside the antheridium in c). b) and d) mature and opened archegonium (scale bar = 50 µm).

Unaltered vegetative growth in *pin*C mutants

To understand the role of *PpPINC* in the Physcomitrella life cycle, we created targeted knockout mutants via homologous recombination in the background of a fertile Physcomitrella WT. Out of 12 targeted mutant lines devoid of *PpPINC* expression, three independent, haploid mutant lines (*pin*C#10t, *pin*C#29, *pin*C#69) with single integration of the knockout construct in the genome were chosen for further analysis (Supplemental Figure S4). Ploidy was assessed with flow cytometry (Heck *et al.*, 2021) and transgene integration numbers were assessed with the qPCR protocol established by Noy-Malka *et al.* (2014). On solid medium we could not detect obvious phenotypic differences to WT regarding stem length, leaf length and leaf width as well as overall growth (Supplemental Figure S5).

Altered sperm motility and phenotype in *pin*C mutants

When WT and *pinC* mutants were grown in gametangia-inducing conditions, i.e. 15ºC and short day (Hohe *et al*., 2002), male and female gametangia developed without any observable differences. Nevertheless, we detected an increased motility of *pin*C mutant sperm cells (spermatozoids). In WT, 38.9 ± 1 % of spermatozoids are motile 5 minutes after release from the opened antheridium. All three *pin*C mutant lines showed a significantly increased sperm motility ($p < 0.00001$) of more than 60 % compared to WT (*pin*C#10 = 64.8 ± 2.75 %, *pin*C#29 = 63.8 ± 1.51 %, *pin*C#69 = 62.3 ± 2.32 %) (Figure 4a, b, c). For a deeper analysis we focused on line *pin*C#29. When looking closer at the phenotype of the spermatozoids we observed that a majority of WT spermatozoids have coiled flagella (59.8 ± 11.96 % coiled) (Figure 4d, g, h), while in the mutant *pin*C#29 the vast majority of spermatozoids have non-coiled flagella (94.48 ± 5.22 %) (Figure 4e, f). It was shown by Ortiz-Ramírez *et al.* (2017) that calcium concentration in Physcomitrella sperm cells can alter their motility. However, staining with the calcium-sensitive dye Fluo-4 did not reveal differences in calcium concentrations inside the sperms of WT and mutant *pin*C#29 (Supplemental Figure S6).

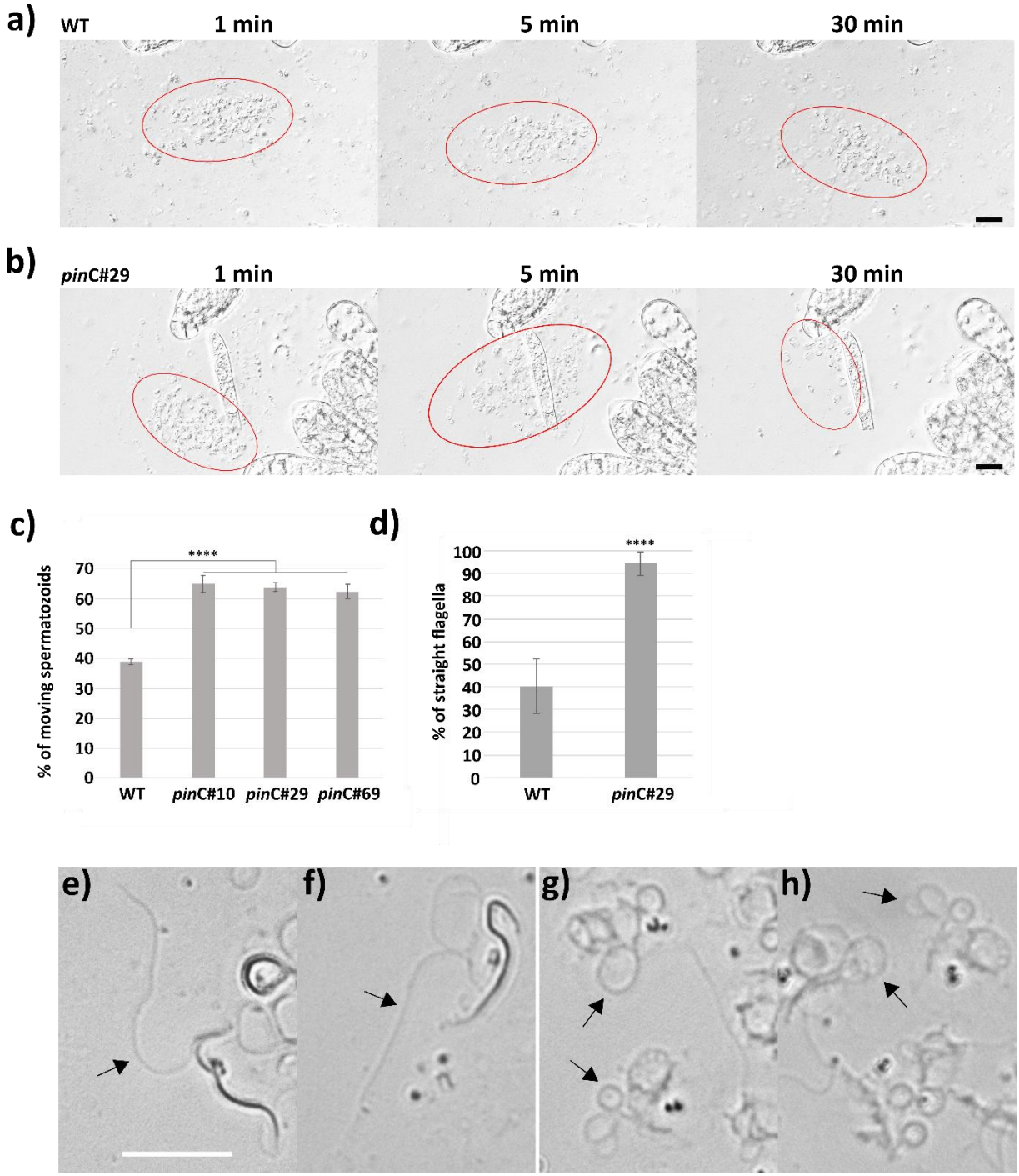

Figure 4: Sperm morphology and motility in Physcomitrella WT and *pin*C mutants. Mutant sperm cells are more motile and have less coiled flagella compared to WT sperm cells. a) WT and b) *pin*C#29 spermatozoids one, five and 30 minutes after being released from a single antheridium, respectively (bar = 20 µm). Areas circled in red highlight spermatozoids after release. c) Percentage of moving spermatozoids after being released from the antheridium (n = 10). d) Percentage of non-coiled flagella compared to coiled flagella (WT: n = 7 antheridia, *pin*C#29: n = 9 antheridia). Asterisks in c) and d) = $p \leq 0.0001$, one-sided ANOVA. e) and f) *pin*C#29 spermatozoids with non-coiled flagella marked by arrows. g) and h) WT spermatozoids with coiled flagella marked by arrows. e) – h) bar = 10 µm. For better resolution of sperm cells pictures in a, b, e-h are stacked pictures.

Organ-specific differential gene expression

To identify genes underlying the differences in sperm flagella phenotype, we performed RNAseq analysis on WT and mutant gametangia. We collected mature archegonia and antheridia from WT and the *pinC*#29 mutant, cultivated on the same plate, 20 days after start of sporophyte induction. Using RNAseq protocols designed for single cell transcriptomics for each line and organ, we pooled eight mature gametangia per sample which were collected on three different occasions (three samples per organ and line). With this approach we could use handpicked gametangia at a specific point in their development. Mapping of sequenced samples resulted in alignment rates of 71.8 – 93.8 % with version 3.3 of the Physcomitrella genome (Lang *et al.*, 2018), which is in line with results on Physcomitrella phyllid cells (Kubo *et al.*, 2019) and is comparable to alignment rates for the human genome (Dobin *et al.*, 2013). With 150 bp paired-end Illumina platform-based sequencing, we reached read counts between 19 and 39.8 million for the feature coding sequence (CDS) (Supplemental Figure S7). No reads could be mapped to the deleted area of *PpPINC* in mutant *pin*C#29, which confirms the gene knockout (Supplemental Figure S8). Between all mutant and all WT samples, we could not find significant differences in gene expression and no gene that may have been affected by a possible off-target integration of the knockout construct. In contrast, we found a clear separation between male and female gametangia, while the difference between WT and *pin*C mutant was not strong (Figure 5a). When comparing the samples to each other, we found that for the male samples (WT antheridia WM vs. mutant antheridia PM) there were two upregulated (*Pp3c26_6020, Pp3c26_3990*) and nine downregulated genes (*Pp3c9_8920, Pp3c14_8940, Pp3c20_22670, Pp3c1_22810, Pp3c19_15670, Pp3c3_4950, Pp3c3_11110, Pp3c21_8410, Pp3c12_11710*) ($p \leq 0.05$, Fold change (FC) > ± 2, Table 2) (Supplemental Table S2a). Three of the downregulated genes are not annotated so far, while the other genes show counts only in a local part of the gene or exhibit obscure gene structures consisting of only one exon or 22 micro exons. Comparing the female samples, we found one upregulated (*Pp3c11_4360*) and two downregulated (*Pp3c7_8820, Pp3c6_26100)* genes (Supplemental Table S2b), while these genes also show expression only in one part of the gene or show unusual gene structures. When comparing samples derived from antheridia against archegonia, we observed a strong upregulation of genes in male gametangia of both lines, but no change in expression of genes related to female development. The ratio of upregulated to downregulated genes is higher than 4. The highest number of upregulated genes was found in the comparison between all male and all female samples with 1920 genes upregulated and 397 downregulated genes (Table 2). The results of all differentially expressed genes (DEGs) are compiled in Supplemental Table S3.

Table 2: Upregulated and downregulated genes in male (M) and female (F) tissue samples from Physcomitrella WT (W) and *pin*C#29 (P).

	Upregulated genes	Downregulated genes
PM vs. WM	2	9
PF vs. WF	1	2
***pinC*#29 vs. WT**	0	0
PM vs. PF	1361	245
WM vs. WF	1323	298
Male vs. Female	1920	397

We analysed the gene ontology (GO) terms of the DEGs for accumulation of specific terms for all experiments (p-value cut off 0.01). Enriched GO terms occurred in the comparisons between sexes, especially in upregulated genes (Figure 5b). For the comparison of WT antheridia against WT archegonia (WM vs. WF) we found a weak enrichment of the GO term axonemal dynein complex (0.08 %). In the experiment PM vs. PF (mutant antheridia vs. mutant archegonia) we found that five GO terms were most prominent, three are associated with spermatogenesis and one each with energy consumption and DNA synthesis (Cellular Components: cilium = 0.36 %, microtubule organizing center = 0.23 %; Biological Process: carbohydrate catabolic process = 7.2 %, cilium assembly = 1.3 %, purine ribonucleotide metabolic process = 7 %). The same is true for the comparison of all antheridia samples with all archegonia samples, where four spermatogenesis-related GO terms were overrepresented (Cellular Components: cilium = 3.9 %, dynein complex = 2.2 %, intraciliary transport particle B = 0.84 %; Biological Process: cell projection organization = 1.3 %) (Supplemental Table S1).

In consequence, we detected more spermatogenesis-related DEGs in the comparison between mutant antheridia and archegonia than in the comparison of WT gametangia. Most of the upregulated DEGs found in the comparison of the sexes were shared between WT and mutant (Figure 5c). The number of DEGs found exclusively in the mutant was similar between upregulated and downregulated genes (119 / 117). The WT shared the least downregulated genes with the mutant, while contributing more downregulated DEGs to the comparison between male and female (Figure 5d). We identified some single DEGs, which had been reported to play roles in flagella formation or auxin homeostasis. The coiled coil-like protein *Ppccdc39* (Meyberg *et al.*, 2020) was upregulated almost 3-fold (FC) in male samples compared to female samples (FC = 2.98). While it is also significantly upregulated in the comparison of WT male against female gametangia (FC = 2.4, p = 0.0005), the fold change was even larger in the mutant samples, but due to high variation in the male samples not statistically significant. The arl13b homologue *Pp3c1_40600*, which is involved in flagella stability, was significantly upregulated in the comparison of male against female gametangia (FC = 3.44, p = 0.025), which is also upregulated in the Reute ecotype compared to Gransden (Meyberg *et al.*, 2020). In all comparisons of male against female tissues the arabinogalactan 31 homologue *Pp3c5_9210*, found to be active during spermatogenesis (Meyberg *et al.*, 2020), was upregulated with a higher fold change in PM vs. PF (FC = 7.24, p = 2.06E-10) than in WM vs WF (FC = 4.62, p = 1.20E-07) (male vs. female FC = 5.34, p =

1.61E-08). Furthermore, the embryogenesis-related transcription factor *PpBELL2* (Horst *et al.*, 2016) was significantly downregulated in all male samples compared to female samples (PM vs. PF: FC = -7.53, p = 8.17E-09; WM vs. WF: FC = -3.07, p = 0.013, male vs. female: FC = -3.85, p = 0.0029). The two PHD clade IIa genes *PpMS1A* and *PpMS1B* are expressed significantly higher in male tissues compared to female (*PpMS1A*: male vs. female FC = 2.35, p = 0.029, *PpMS1B*: male vs. female FC = 2.81, p = 0.036, WM vs WF FC = 2.04, p = 0.035), which is in accordance with Landberg *et al*. (2022).

While not being differentially expressed, we observed expression of all six *PpTAR* genes in antheridia and archegonia. We could also find higher expression levels of *PpYUCB* and *PpYUCF* in antheridia and archegonia compared to the other *PpYUC* genes, while *PpYUCD* showed a very low, but significantly upregulated expression in archegonia (PM vs. PF FC = -4.69, p = 0.02, Male vs. Female FC = -4.65, p = 0.0008). This indicates active auxin synthesis in mature gametangia. While our transcriptomic data reveal trends in general gene expression, we could not identify a single DEG that might account for the difference in sperm flagella phenotype in the comparison of WT and mutant, but found more spermatogenesis-related DEGs in the *pin*C mutant.

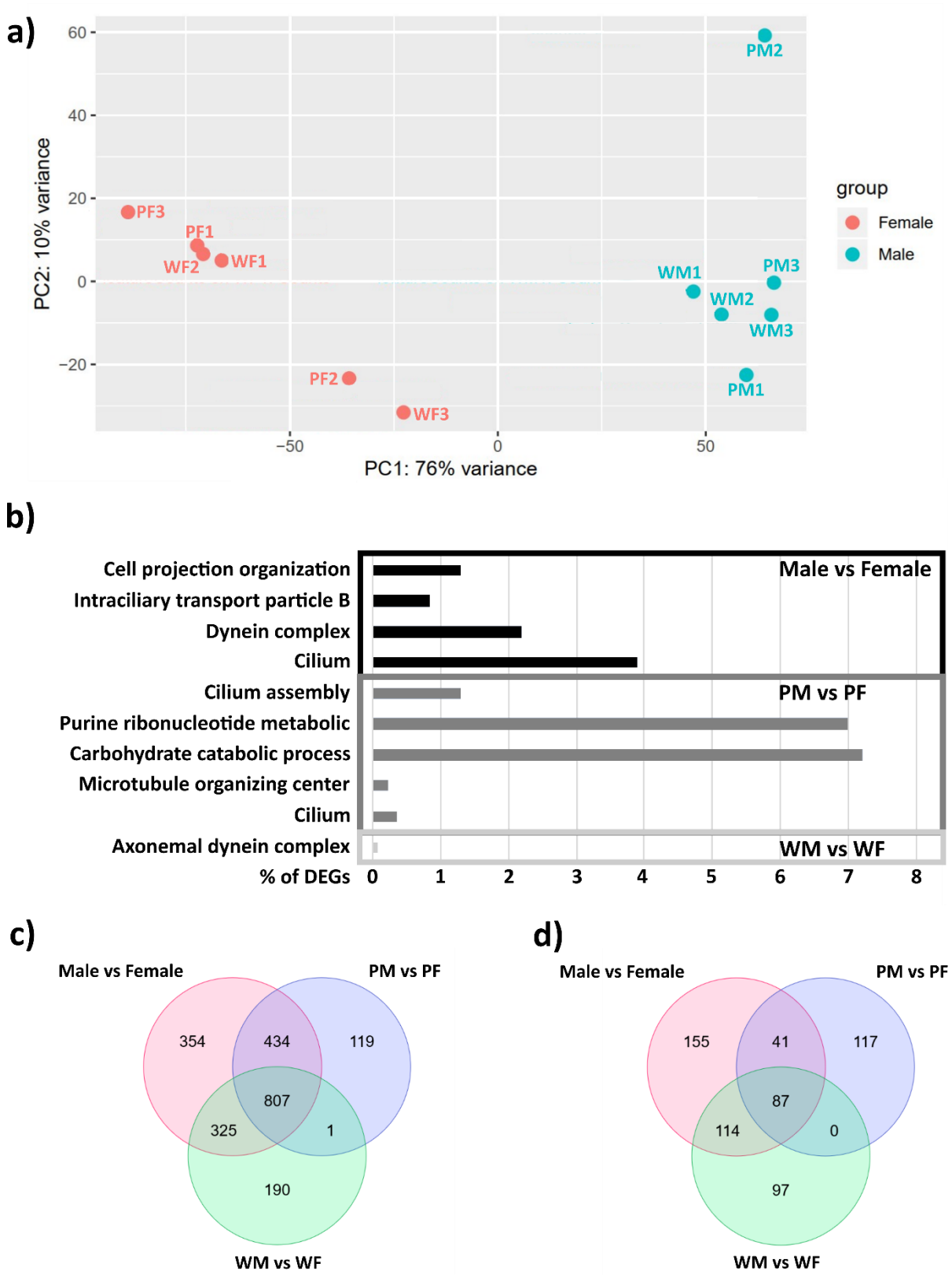

Figure 5: Transcriptomic analysis of Physcomitrella WT and mutant gametangia. a) Variance of all samples. Samples group together into male and female, but there is no clear separation between WT and mutant samples. M = male (antheridia), F = female (archegonia), W = wild type, P = *pin*C#29. b)

All enriched gene ontology terms in upregulated DEGs in the comparison of all male against all female samples (male vs. female), all WT male against WT female (WM vs. WF) and mutant male against mutant female samples (PM vs. PF). c) Venn diagram of all upregulated and d) downregulated genes in the comparisons of male and female samples.

Altered fertility and abortion rate

We did not observe any differences in the morphology of mature spore capsules or spore germination rates between WT and mutant (Supplemental Figure S9). In contrast, in addition to the higher motility of mutant spermatozoids, we found a significantly higher fertility rate in all three mutant lines (Figure 6). Low fertility rates of the Gransden ecotype have been reported (Perroud *et al.*, 2011; Hiss *et al.*, 2017; Meyberg *et al.*, 2020), and in our experiments 5.5 ± 0.4 % of all WT gametophores produced a sporophyte. In contrast, all *pin*C mutants developed significantly more sporophytes, with 39.8 ± 1.6 % for *pin*C#10, 63.2 ± 4.5 % for *pin*C#29 and 14.5 ± 0.6 % for *pin*C#69.

In addition to increased fertility, we detected an increased abortion rate of sporophytes in the mutants. For this we examined every gametophore apex of a colony and counted sporophytes, empty vaginulae and apices with no gametangia. Abortion rate was determined for each colony by calculating the percentage of aborted sporophytes per gametophore per colony. Subsequently, we calculated the abortion rates in WT and mutants to be WT = 0.1 ± 0.03 %, *pin*C#10 = 8.7 ± 1.3 %, *pin*C#29 = 35.4 ± 1.7 %, and *pin*C#69 = 6.5 ± 0.2 % (Supplemental Table S4). The aborted sporophytes were no longer attached to the maternal tissue (vaginula). Abortion happened around two weeks after fertilization of the egg cell, when the sporogenic tissue starts to expand (Stage S3 in Ortiz-Ramírez *et al.*, 2016; day 12-16 in Lopez-Obando *et al.*, 2022).

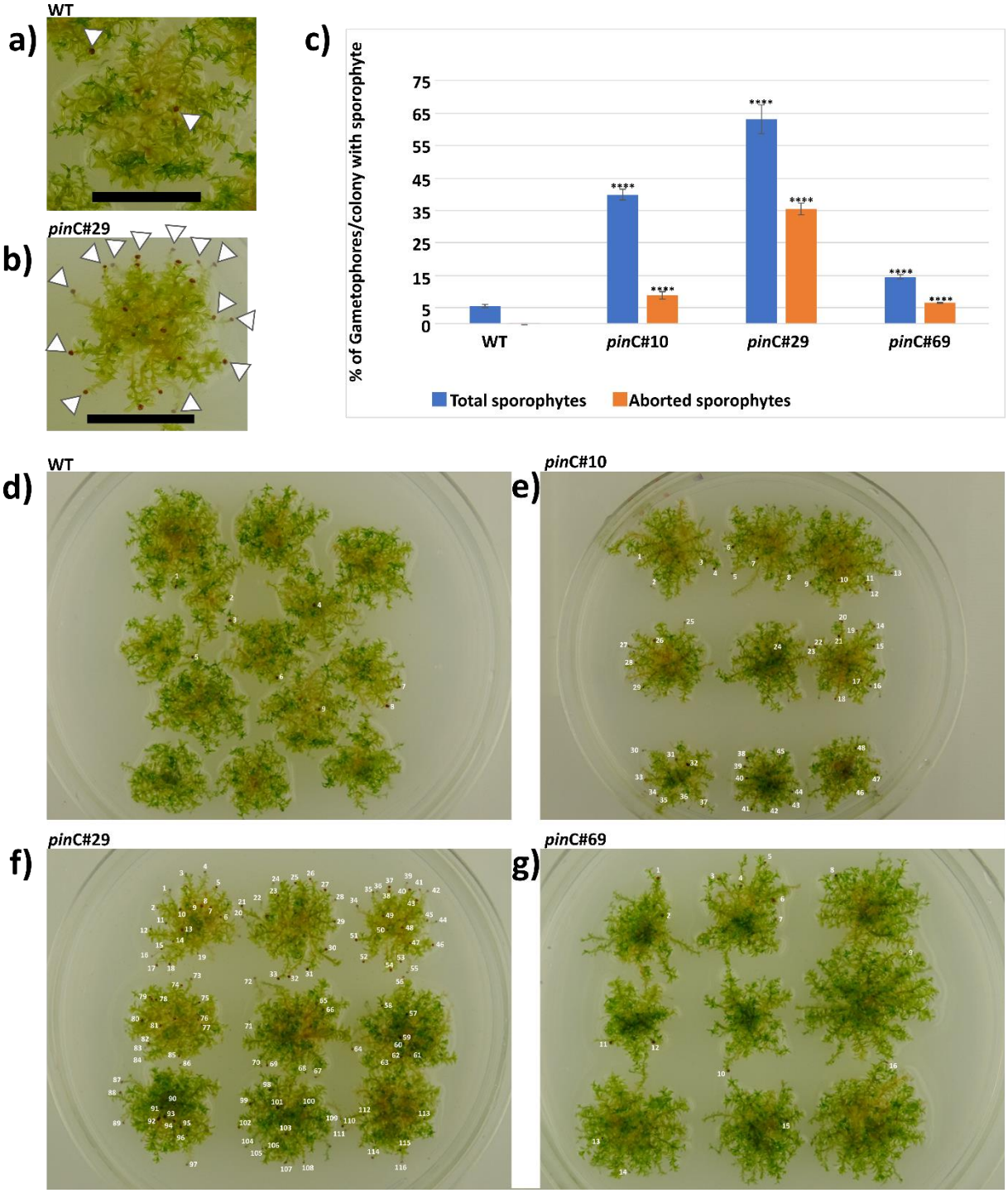

Figure 6: Spore capsule numbers. Physcomitrella spore capsules in a) WT and b) *pin*C#29 mutant, white arrows mark sporophytes (for visibility reasons, not all sporophytes in b) are marked while all visible sporophytes are marked in a)). bar = 1cm. c) Percentage of gametophores with a sporophyte per colony. Total number of sporophytes (adult + aborted) in blue, only aborted sporophytes in orange. Asterisks = $p<0.00005$ (Student's t-test) of mutant lines against WT, n (colonies) = WT (41), *pin*C#10 (30), *pin*C#29 (42), *pin*C#69 (32) d) WT plate with 9 sporophytes counted. e) *pin*C#10 plate with 48 sporophytes. f) *pin*C#29 plate with 116 sporophytes. g) *pin*C#69 with 16 sporophytes.

In the early embryo, *PpPINC* was active in the lower half, excluding the basal tip cells, as well as in the walls of the maternal tissue that surrounds the young embryo (epigonium) (Figure 7a). Development of the sporophyte foot and the maternal tissue are highly synchronized. When the embryo has doubled in size and the foot is secured in the now fully developed vaginula (Figure 7b), the seta forms and rips apart the surrounding tissue of the epigonium, while the later developing spore capsule also starts to separate (Figure 7c), splitting the epigonium into the calyptra at the apex and the vaginula at the basis of the premeiotic sporophyte. The expression of *PpPINC* slowly declines in the foot of the embryo (Figure 7a-c), while it increases in the maternal tissue during sporophyte foot growth, forming a distinct ring structure at the border of maternal and sporophytic tissue (Figure 7b). After the growth spurt, *PpPINC* expression can be found only in the apophysis (region between seta and premeiotic tissue), while excluding the stomata cells (Figure 7d). We found that Physcomitrella develops a true-type vaginula, where the foot of the sporophyte does not penetrate the gametophore tissue under the vaginula (Figure 7e, f). Sporophyte development is polar in Physcomitrella, where the foot of the sporophyte develops faster than the seta or premeiotic spore capsule. The basis of the foot was not in direct contact with the maternal cells, which is in line with an earlier report (Regmi *et al.*, 2017), while the vaginula tightened at its apical border to the sporophyte, which is visible as a reddish-brown coloured ring after the emergence of the premeiotic sporophyte (Figure 7g, i). In the mature sporophyte, no *PpPINC* expression was detectable.

Aborted sporophytes in WT and mutants were in the premeiotic phase after the separation of the epigonium (comparable to stage shown in Figure 7g), and no longer attached to the vaginula. No visible defects could be detected, apart from the separation from the gametophore. On one occasion we could observe a sporophyte slipping out of the cavity of the vaginula, not losing contact as the basis of the foot was stuck in the tighter apical end (Figure 7h). Empty vaginulae clearly showed the coloured ring formation at the apical opening (Figure 7i). The aborted sporophytes had fully developed foot structures, with haustorium cells at the basis, seta, stomata cells and a depression between seta and haustorium cells, which we believe results from the securement of the sporophyte by the coloured ring formation (Figure 7j). We could find no morphological differences in the aborted sporophytes between mutants and WT, except for an increase in the number and percentage of abortions in the *pin*C mutants. The calyptra could be removed without resistance, some aborted sporophytes had already lost them (Figure 7k, l).

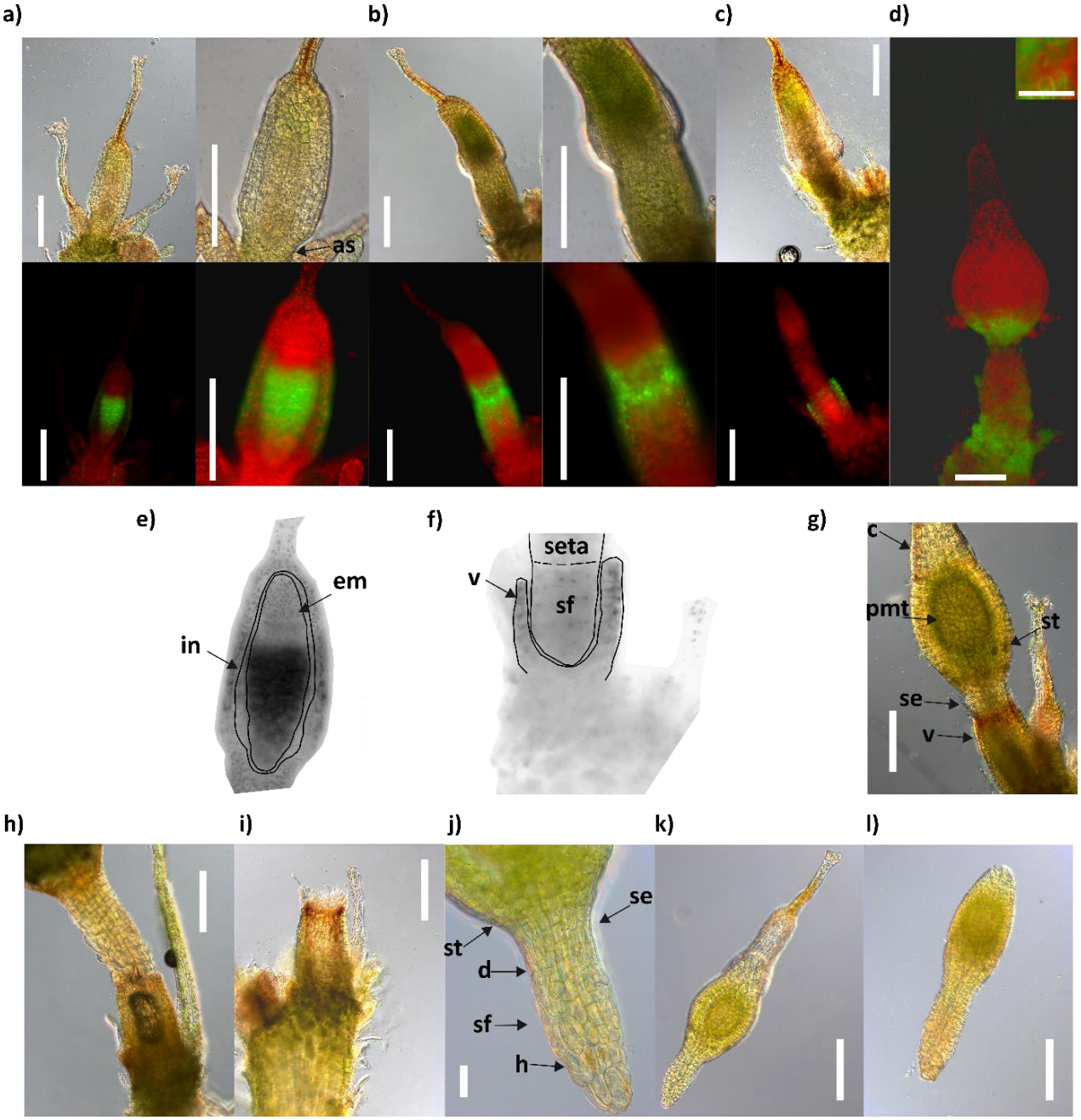

Figure 7: Sporophyte development in Physcomitrella. a)-d) Bright-field and fluorescent microscopy pictures of Physcomitrella PpPINC reporter line. a) Embryo (probably 128 cell stadium) inside the epigonium, as = archegonial stalk. b) Embryo has doubled in size, vaginula and sporophyte foot are fully developed. c) Growth phase of seta, epigonium is about to rupture. d) Premeiotic sporophyte around 14 days post fertilization. The fluorescent signal is concentrated in the apophysis excluding stomata cells (smaller picture, bar = 25 µm). e) and f) = Negative grayscale cut out of a) = e) and c) = f), e) em = embryo, and in = inner wall epigonium are outlined in black. f) Fully developed vaginula (v) with sporophyte foot (sf) and growing seta are indicated by black lines. g) Premeiotic sporophyte, after the epigonium has split into the calyptra (c) and vaginula (v), pmt = premeiotic tissue, se = seta, st = stomata. h) Premeiotic sporophyte slips out of vaginula. i) Empty vaginula after abortion. j) Lower half of an aborted premeiotic sporophyte, d = depression, h = haustorium cells, se = seta, sf = sporophyte foot, st

= stomata). k) Aborted premeiotic sporophyte covered by calyptra. h) – k) = *pin*C#29 mutant. l) Aborted premeiotic sporophyte from WT, not attached to calyptra. Bars in a), c), d), g), h), i), k), and l) = 200 µm. Bar in j) = 50 µm.

Discussion

Auxin plays crucial roles in plant development (Santner & Estelle, 2009; Weijers & Wagner, 2016), including Physcomitrella development (Decker *et al.*, 2006; Menand *et al*., 2007; Fujita *et al.*, 2008; Coudert *et al*., 2017; Nemec-Venza *et al*., 2022) and biotechnology (Ruiz-Molina *et al*., 2022). Although PIN proteins are central in auxin transport and action (Adamowski & Friml, 2015; Sauer & Kleine-Vehn, 2019; Ung *et al*., 2022), only two of the three canonical Physcomitrella PIN proteins have been fully characterized; the similar and relatively highly expressed PpPINA and PpPINB. In contrast, little was known about the function of the more divergent and less expressed PpPINC. Here, we strived to close this knowledge gap.

Our data on the expression of *PpPIN*C in young Physcomitrella phyllids is in line with an earlier report (Viaene *et al.*, 2014), as well as the absence of the signal in stem, rhizoids and older phyllids. It was known that the single knockout of *PpPINA* or *PpPINB* has no visible effect on the morphology of the gametophore or phyllids (Bennett *et al.*, 2014b), and this is also true for *PpPINC*, as we have shown here. However, a double knockout of *PpPINA* and *PpPINB* lead to elongated phyllids and stems, similar to treatments with exogenous auxin or auxin transport inhibitors (Bennett *et al.*, 2014b). This means that while *PpPINA* or *PpPINB* together with *PpPINC* can rescue the knockout of either *A* or *B*, *PpPINC* alone cannot replace the function of both proteins in a double knockout line.

The publicly available expression data for canonical PIN proteins in the two Physcomitrella ecotypes Gransden and Reute is not always comparable, as they are different experimental data sets describing specific tissue stages. However, all three canonical PINs have a similar expression pattern regarding tissue and ecotype. All three PINs are expressed in gametophores and sporophytes, with PpPINA and PpPINB being more highly expressed than PpPINC. The expression of all three PINs in vegetative (gametophytic) tissue has been reported (Viaene *et al.*, 2014), as well as the important role of PpPINA and PpPINB in sporophyte formation (Bennett *et al.*, 2014b). We could not find any differences between the expression of *PpPINC* in the Gransden and Reute data sets. Further, we did not observe any vegetative phenotype alteration in *PpPINC* knockout mutants. While Viaene *et al*. (2014) showed expression of all three canonical PIN proteins in Physcomitrella protonema apical cells, we could not find such expression. This might be due to differences in targeting, reporter construct or culture conditions. In contrast, we could identify PpPINC as an important regulator of spermatogenesis and sporophyte retention. We therefore conclude that PpPINC is functionally active only in gametangia and sporophytic tissues, contrary to the other two canonical Physcomitrella PIN proteins. Consequently, the

*pin*AB double mutants are affected in gametophytic as well as sporophytic development (Bennett *et al.*, 2014b), while this is not the case in the *pin*C mutants analysed here.

It has been reported that the low fertility of the Physcomitrella ecotype Gransden is based on reduced male fertility (Perroud *et al.*, 2011). This is partially caused by coiled flagella of spermatozoids, which results in low sperm motility (Meyberg *et al.*, 2020). We confirm this phenotype for the Gransden ecotype, with a high percentage of coiled flagella and a motility of under 50 %, resulting in a very low sporophyte production rate. In contrast, the *pin*C mutants, which we generated in the Gransden background, resemble the Reute ecotype in sperm morphology and fertility rate, as it has no coiled flagella, a high sperm motility and a high sporophyte rate (Hiss *et al.*, 2017; Meyberg *et al.*, 2020). While the fertility rate of the three *pin*C mutant lines varied, it was significantly higher in all three lines than in WT. There are many biological factors at play which could influence fertilization success on the female side. However, one essential factor for successful fertilization is the ability of sperm cells to swim to an egg cell. Therefore, it is evident that higher sperm motility leads to higher fertilization rates, as we observed here in the *pin*C mutants. The Gransden ecotype was introduced by Engel (1968) as a laboratory strain from one single spore from the UK, and has been propagated mostly vegetatively in laboratories around the world since, while the Reute ecotype was introduced relatively recently as a collection from Germany (Hiss *et al.*, 2017). Compared to Reute, Gransden accumulated somatic, epigenetic mutations, probably leading to faults in spermatogenesis (Haas *et al.*, 2020).

Here, we found more spermatogenesis-related DEGs in mature antheridia of a *pin*C knockout mutant compared to WT (WT: axonemal dynein complex = 0.08 %, *pin*C#29: cilium = 0.36 %, microtubule organizing center = 0.23 % cilium assembly = 1.3 %), but we could not find changes regarding female or egg-cell related differences in expression in mature mutant and WT archegonia. Activity of a *TAR* gene and *PpPINA* in the apical cells of the mature antheridium has been reported (Landberg *et al.*, 2013; Landberg *et al.*, 2020), while there are no reports of phenotypically different gametangia in *PpPINA* mutants. Here, we also found evidence for expression of auxin synthesis-genes in mature gametangia. With *PpPINC* being expressed in the foot of the mature antheridium, contrary to *PpPINA* in the apical tip cell, it seems to be more important for spermatogenesis to control auxin homeostasis at the bottom of the antheridium than at the tip. Whether this mode of action is part of a polar auxin homeostasis in a moss organ controlled by PIN proteins needs further clarification.

Gaining the ability to move the flagellum is one of the final steps of spermatogenesis before spermatozoids are released and activated. In mammals, this ability is gained in the epididymis, and is controlled by different external and internal factors (Pereira *et al.*, 2017; O'Flaherty, 2019; Björkgren & Sipilä, 2019). Due to the complexity of the process and a large number of influences, sperm populations are not homogenous, but vary regarding phenotype, motility or activity (Gómez Montoto *et al.*, 2011; Genau *et al.*, 2021; Martins-Bessa *et al.*, 2021). A key role in metazoan and Physcomitrella spermatogenesis is played by the evolutionary conserved DNA Topoisomerase 1α, which facilitates

chromatin condensation towards the compact sperm head (Gu *et al*., 2022). Activation of the flagella of released spermatozoids depends on changes in pH, calcium concentration, or the presence of a chemoattractant released by the egg cell (Nakajima, 2005; Suarez, 2008; Morita *et al.*, 2009). While mammalian spermatozoids are transported through the epididymis during maturation, spermatogenesis in the moss antheridium is stationary. This increases pressure on the exact spatio-temporal expression of spermatogenesis-related genes. As in mammals, Physcomitrella releases heterogeneous sperm populations from one antheridium. This was true for WT where motility (~40 %) and non-coiled flagella (~40 %) seem to fit nicely, whereas in the *pin*C#29 mutant over 90 % of all spermatozoids were straight, with an overall motility of 60 %. While the phenotype of the spermatozoids changed drastically in the mutant, motility did not increase at the same rate. As we have shown, *PpPINC* is expressed only shortly before sperm cells are released, reducing the time it can influence spermatogenesis to a short window. Therefore, alterations in duration and strength of expression, which are likely to occur after somatic mutations, could explain the differences in sperm morphology between the two ecotypes Gransden and Reute. The *PpPINC* gDNA sequence between the Gransden ecotype (v3.3 Phytozome genome ID:318) and Reute (SRX1528135; Hiss *et al.*, 2017) is identical. Given that the mutant antheridia exhibit a higher portion of spermatogenesis-related DEGs compared to WT, together with an overall increased motility and fertility, we suggest that PpPINC acts in repression of spermatogenesis. The repression of spermatogenesis at the end of the whole process could be a molecular signal for sperm release or activation of flagella. The difference in expression between both ecotypes would be an earlier repression in Gransden, halting spermatogenesis when most of the flagella are coiled and not yet ready for release, while the signal in Reute comes later, when spermatogenesis has progressed to a majority of non-coiled sperm flagella. The unknown activating signal of *PpPINC* expression could therefore be the culprit responsible for reduced male fertility in the Gransden ecotype. The identification of such regulators is in its infancy, with WAV3 in the regulation of Arabidopsis PIN2 being the first (Konstantinova *et al.*, 2022).

Male sexuality is reduced in many bryophytes, with a female-biased sex ratio (Cameron & Wyatt, 1990; Stark *et al.*, 2010; Pépin *et al.*, 2013; Bisang *et al.*, 2015; de Jong *et al.*, 2018), or size of the plants, with the occurrence of dwarf males (nannandry), which are unique in bryophytes among land plants (Pedersen *et al.*, 2006; Rosengren & Cronberg, 2014; Rosengren *et al.*, 2016; Lang *et al.*, 2021). Dwarf males grow on the leaves of female plants (Pichonet & Gradstein, 2012; Rosengren & Cronberg, 2014; Rosengren *et al.*, 2016; Lang *et al.*, 2021) and increase fertilization success (Hedenäs & Bisang 2012; Rosengren & Cronberg, 2014), in the absence of a female, male spores develop normally. In *Macromitrium japonicum*, dwarf males grew in culture on medium containing auxin, but developed normally on auxin-free medium (Une, 1985). Dioecious mosses grow mostly vegetatively and sporophyte production can be rare due to absence of a sexual partner, while monoecious mosses produce sporophytes more frequently, as the chances for fertilization are higher (Haig, 2016). However, self-fertilization leads to homozygous spores, while self-produced sperm are rarely outcompeted by non-self

sperm (Taylor *et al.*, 2007; Rosengren *et al.*, 2016). Reducing male fertility in a monoecious moss increases the chance for outcrossing and could therefore be an internal mechanism, controlling the need to refresh genetic material (McDaniel *et al*., 2010; Haig, 2016; Szövényi *et al*., 2017). In a monoecious moss like Physcomitrella with a very short life cycle (3-6 months) (Cove, 2005), pressure on mutations regarding the sexual life cycle is strong, as changes in fertility would be lethal (Haig, 2016). Cultivation in vegetative culture in laboratories around the world (Haas *et al.*, 2020) could reduce this pressure on fertility, increasing the risk for severe mutations in the sexual signalling cascade (Meyberg *et al.*, 2020; Haas *et al.*, 2020). As male gametes need more energy and are more complex to build than female gametes (Rydgren & Økland, 2003; Stark *et al.*, 2000, 2009; Horsley *et al.*, 2011; Santos *et al.*, 2022), risk for mutations is higher. This cost calculation would also favour intentionally reducing male rather than female fertility, as more energy is required to constantly produce sperm cells rather than egg cells, which are waiting for fertilization, ending the gamete production cycle and starting the growth of propagules.

In Arabidopsis, the expression of PIN proteins plays an important role during pollen development, together with anther-specific expression of YUCCA genes (Cecchetti *et al.*, 2008; Dal Bosco *et al.*, 2012). PIN8 locates to the ER and regulates auxin homeostasis with a rate-limiting activity during pollen grain development and pollen tube growth. It is functionally active only during male gametophyte development and a knockout of PIN8 leads to misshaped and aborted pollen (Ding *et al.*, 2012; Dal Bosco *et al.*, 2012). The activity of PIN proteins in male gametophytic tissues is also reported in algae, in *Chara vulgaris* a PIN2-like protein is expressed during spermatogenesis (Żabka *et al.*, 2016). Together with our findings it seems plausible that PIN proteins can play important roles during male gametophytic development in all plants. However, the exclusive function of PIN1 in Arabidopsis in the formation of floral organs could not be rescued by the Physcomitrella PpPINA protein expressed under the PIN1 promoter, while it complements the vegetative phenotype of the knockout (Zhang *et al.*, 2020a).

The abortion of embryos is a natural process. Unfavourable environmental conditions, genetic mutations, injury of the embryo or of maternal tissue can trigger abortion. In mosses, the normal abortion rate differs among species (Stark & Stephenson, 1983; Stark *et al.*, 2009; Rosengren *et al.*, 2016; Hedenäs & Bisang, 2019) and seems to be resource-limited (Stark *et al.*, 2000). Mosses have to allocate their energy between clonal regeneration and sexual reproduction (Stark *et al.*, 2009), and sporophyte survival positively correlates with vegetative growth prior to fertilization (Stark & Stephenson, 1983). In these cases, aborted sporophytes were no longer supported with nutrients and stopped growing inside the vaginula, contrary to the active abortion we observed here in the *pin*C mutant.

The haustorium cells of the sporophyte foot are not pressed against the vaginula tissue but surrounded by a placenta-like space, while both tissues are separated by a diffusion barrier (Uzawa & Higuchi, 2010; Regmi *et al.*, 2017). The foot of the sporophyte is wider than the seta with a small depression between

seta and foot, while vital sporophytes are tightly attached to the gametophore. We observed a clear polarity during early embryo development favouring growth of the foot, while the upper part of the embryo starts to increase only after the foot is secured in the vaginula. *PpPINC* is active in the maternal tissues which will form the vaginula and the sclerotized ring structure after the sporophyte ruptures the epigonium. Premeiotic sporophytes were aborted after the epigonium had ruptured and the sporophyte foot had to be secured in the vaginula. The significantly increased abortion rate in our *pin*C mutants, combined with the activity of *PpPINC* at the vaginula-seta junction, point to a regulation of sporophyte securement controlled at least partially by *PpPINC*. This sporophyte abortion phenotype was not observed with the *pin*AB double mutants, which have malformed sporophytes that are nevertheless firmly attached to the gametophore (Bennett *et al*., 2014b). Based on our observations, we suggest that the sclerotized, brown ring structure at the vaginula-seta junction has the mechanical function of securing the sporophyte foot. It is well-known that auxin can have a loosening effect on cell walls (Cosgrove, 2021), regulated by complex molecular signalling (Xiong *et al.*, 2021; Varapparambath *et al.*, 2022). Thus, changes in auxin distribution or concentration in the ring structure could lead to a loosening of the ring and subsequently to the loss of the sporophyte.

The polarity of early embryo development we observed here in Physcomitrella as well as the functional significance of the sclerotized ring structure is in line with the findings of Lorch (1909) in the moss family Polytrichaceae. He reported that the sporophyte foot develops first, before the seta subsequently elongates, and as the lumen in the vaginula is not completely filled by the foot, the sclerotized ring structure must secure the sporophyte (Lorch, 1909). As we could not find a name for this ring structure in the literature, we propose to name the reddish-brown ring structure, formed at the junction of vaginula and seta, the Lorch ring.

One important step in the evolution of land plants was the retention of the product of fertilization, the zygote, on the haploid gametophyte (Reski, 2018). This “zygote retention” already occurs in streptophyte algae (Becker & Marin, 2009) and is a prerequisite for the development of the alternation of generations that is characteristic for all land plants (Horst & Reski, 2016). Our data presented here suggest that the structure that mechanically ensures sporophyte retention is the Lorch ring, and that retention and abortion of the sporophyte can be regulated by auxin via PpPINC.

Taken together, the canonical Physcomitrella PINC protein is functional in reproductive tissues only, an important regulator of late spermatogenesis, sperm motility and of retention and active abortion of premeiotic sporophytes. Thus, it may integrate environmental signals with developmental programs to regulate sexual reproduction, at least in moss gametangia and early stages of embryo development.

Acknowledgements: We gratefully acknowledge Richard Haas for expert technical advice and assistance extracting RNA from gametangia, and Anne Katrin Prowse for proof-reading of the

manuscript. We gratefully acknowledge funding by the Deutsche Forschungsgemeinschaft (DFG, German Research Foundation) under Germany's Excellence Strategy EXC-2189 (CIBSS to RR) and EXC-2193/1 – 390951807 (*liv*MatS to RR).

Author contributions: VML, CR, ELD and RR planned and designed the research. VML did most of the experimental work. NvG performed sequence search and alignment, phylogenetic reconstruction and transmembrane prediction. Data analysis of transcriptomic sequences was done by VML, guided by CR. MB created the knockout constructs and first knockout plants. OH took pictures of spermatozoids and aborted sporophytes. MH did measurements of stems and leaves, while data analysis for this was done by VML. ELD and RR supervised research. RR acquired funding for this work. VML wrote the manuscript with the help of ELD and RR. All authors read and approved the manuscript.

Declaration: All authors declare that they have no competing interests.

ORCID IDs

VLM: 0000-0002-2923-4236; CR: 0000-0002-0672-3897; NvG: 0000-0002-0606-246X; OH: 0000-0003-3958-5061; MH: 0000-0002-2659-3372; MB: 0000-0002-3601-5250; ELD: 0000-0002-9151-1361; RR: 0000-0002-5496-6711

Data availability: All RNA-seq samples as well as the DEG experiments created in this study are available via the NCBI GEO project **GSE205257**. All moss lines used are available via the International Moss Stock Center (IMSC; https://www.moss-stock-center.org) with the following accession numbers: WT = 40095, *PinCPromCit* = 40917, *pin*C#10 = 40918, *pin*C#29 = 40919, *pin*C#69 = 40420.

References

Adamowski M, Friml J. **2015**. PIN-dependent auxin transport: Action, regulation, and development. *Plant Cell* **27**: 20–32.

Afgan E, Baker D, Batut B, van den Beek M, Bouvier D, Cech M, Chilton J, et al. 2018. The Galaxy platform for accessible, reproducible and collaborative biomedical analyses: 2018 update. *Nucleic Acid Research* **46:** W537-W544.

Banks JA, Nishiyama T, Hasebe M, Bowman JL, Gribskov M, DePamphilis C, Albert VA, Aono N, Aoyama T, Ambrose BA, *et al.* 2011. The *Selaginella* genome identifies genetic changes associated with the evolution of vascular plants. *Science* **332**: 960–963.

Becker B, Marin B. 2009. Streptophyte algae and the origin of embryophytes. *Annals of Botany* **103**: 999-1004.

Bennett T, Brockington SF, Rothfels C, Graham SW, Stevenson D, Kutchan T, Rolf M, Thomas P, Wong GK-S, Leyser O, *et al.* 2014a. Paralogous radiations of PIN proteins with multiple origins of noncanonical PIN structure. *Molecular Biology and Evolution* **31**: 2042–2060.

Bennett TA, Liu MM, Aoyama T, Bierfreund NM, Braun M, Coudert Y, Dennis RJ, O'Connor D, Wang XY, White CD, *et al.* 2014b. Plasma membrane-targeted PIN proteins drive shoot development in a moss. *Current Biology* **24**: 2776–2785.

Bierfreund NM, Reski R, Decker EL. **2003**. Use of an inducible reporter gene system for the analysis of auxin distribution in the moss *Physcomitrella patens*. *Plant Cell Reports* **21**: 1143–1152.

Bisang I, Ehrlén J, Korpelainen H, Hedenäs L. **2015**. No evidence of sexual niche partitioning in a dioecious moss with rare sexual reproduction. *Annals of Botany* **116**: 771–779.

Björkgren I, Sipilä P. **2019**. The impact of epididymal proteins on sperm function. *Reproduction* **158**: 155–167.

Bowman JL, Kohchi T, Yamato KT, Jenkins J, Shu S, Ishizaki K, Yamaoka S, Nishihama R, Nakamura Y, Berger F, *et al.* 2017. Insights into land plant evolution garnered from the *Marchantia polymorpha* genome. *Cell* **171**: 287-304.e15.

Buchfink B, Reuter K, Drost HG. 2021. Sensitive protein alignments at tree-of-life scale using DIAMOND. *Nature Methods* **18**: 366–368.

Cameron RG, Wyatt R. **1990**. Spatial patterns and sex ratios in dioecious and monoecious mosses of the genus *Splachnum*. *Bryologist* **93**: 161-166.

Cancé C, Martin-Arevalillo R, Boubekeur K, Dumas R. **2022**. ARFs are keys to the many auxin doors. *New Phytologist* **235**: 402-419.

Carey SB, Jenkins J, Lovell JT, Maumus F, Sreedasyam A, Payton AC, Shu S, Tiley GP, Fernandez-Pozo N, Healey A, *et al.* 2021. Gene-rich UV sex chromosomes harbor conserved regulators of sexual development. *Science Advances* **7**: eabh2488.

Cecchetti V, Altamura MM, Falasca G, Costantino P, Cardarelli M. **2008**. Auxin regulates *Arabidopsis* anther dehiscence, pollen maturation, and filament elongation. *Plant Cell* **20**: 1760–1774.

Cheng S, Xian W, Fu Y, Marin B, Keller J, Wu T, Sun W, Li X, Xu Y, Zhang Y, *et al.* 2019. Genomes of subaerial Zygnematophyceae provide insights into land plant evolution. *Cell* **179**: 1057-1067.e14.

Cosgrove DJ. 2021. Expanding wheat yields with expansin. *New Phytologist* **230**: 403-405.

Coudert Y, Palubicki W, Ljung K, Novak O, Leyser O, Harrison CJ. 2015. Three ancient hormonal cues co-ordinate shoot branching in a moss. *ELIFE* **4**: e06808.

Coudert Y, Bell NE, Edelin C, Harrison CJ. **2017**. Multiple innovations underpinned branching form diversification in mosses. *New Phytologist* **215**: 840-850.

Cove D. **2005**. The moss *Physcomitrella patens*. *Annual Review of Genetics* **39**: 339-358.

Dal Bosco C, Dovzhenko A, Liu X, Woerner N, Rensch T, Eismann M, Eimer S, Hegermann J, Paponov IA, Ruperti B, *et al.* 2012. The endoplasmic reticulum localized PIN8 is a pollen-specific auxin carrier involved in intracellular auxin homeostasis. *Plant Journal* **71**: 860–870.

Decker EL, Frank W, Sarnighausen E, Reski R. **2006**. Moss systems biology *en route*: Phytohormones in Physcomitrella development. *Plant Biology* **8**: 397–405.

Ding Z, Wang B, Moreno I, Dupláková N, Simon S, Carraro N, Reemmer J, Pěnčík A, Chen X, Tejos R, *et al.* 2012. ER-localized auxin transporter PIN8 regulates auxin homeostasis and male gametophyte development in Arabidopsis. *Nature Communications* **3**: 941.

Dobin A, Davis CA, Schlesinger F, Drenkow J, Zaleski C, Jha S, Batut P, Chaisson M, Gingeras TR. 2013. STAR: ultrafast universal RNA-seq aligner. *Bioninformatics* **29**: 15-21.

Engel PP. 1968. The induction of biochemical and morphological mutants in the moss *Physcomitrella patens*. *American Journal of Botany* **55**: 438-446.

Egener T, Granado J, Guitton M-C, Hohe A, Holtorf H, Lucht JM, Rensing SA, Schlink K, Schulte J, Schween G, *et al.* 2002. High frequency of phenotypic deviations in *Physcomitrella patens* plants transformed with a gene-disruption library. *BMC Plant Biology* **2**: 6.

Fernandez-Pozo N, Haas FB, Meyberg R, Ullrich KK, Hiss M, Perroud P, Hanke S, Kratz V, Powell AF, Vesty EF, *et al.* 2020. PEATmoss (*Physcomitrella* Expression Atlas Tool): a unified gene expression atlas for the model plant *Physcomitrella patens*. *Plant Journal* **102**: 165–177.

Flores-Sandoval E, Eklund DM, Bowman JL. **2015**. A simple auxin transcriptional response system regulates multiple morphogenetic processes in the liverwort *Marchantia polymorpha*. *PLOS Genetics* **11**: e1005207.

Fujita T, Sakaguchi H, Hiwatashi Y, Wagstaff SJ, Ito M, Deguchi H, Sato T, Hasebe M. **2008**. Convergent evolution of shoots in land plants: lack of auxin polar transport in moss shoots. *Evolution & Development* **10**: 176–186.

Genau AC, Li Z, Renzaglia KS, Pozo NF, Nogué F, Haas FB, Wilhelmson PKI, Ullrich KK, Schreiber M, Meyberg R, et al. **2021**. HAG1 and SWI3A/B control of male germ line development in *P. patens* suggests conservation of epigenetic reproductive control across land plants. *Plant Reproduction* **34**: 149–173.

Gibson DG, Young L, Chuang RY, Venter JC, Hutchinson III CA, Smith HO. 2009. Enzymatic assembly of DNA molecules up to several hundred kilobases. *Nature Methods* **6:** 343-345.

Goodstein DM, Shu S, Howson R, Neupane R, Hayes RD, Fazo J, Mitros T, Dirks W, Hellsten U, et al. 2012. Phytozome: a comparative platform for green plant genomics. *Nucleic Acid Research* **40:** D1178-D1186.

Gómez Montoto L, Magaña C, Tourmente M, Martín-Coello J, Crespo C, Luque-Larena JJ, Gomendio M, Roldan ERS. **2011**. Sperm competition, sperm numbers and sperm quality in muroid rodents. *PLOS ONE* **6**: e18173.

Gu N, Chen C, Kabeya Y, Hasebe M, Tamada Y. **2022**. Topoisomerase 1α is required for synchronous spermatogenesis in *Physcomitrium patens*. *New Phytologist* **234**: 137–148.

Haas FB, Fernandez-Pozo N, Meyberg R, Perroud PF, Göttig M, Stingl N, Saint-Marcoux D, Langdale JA, Rensing SA. 2020. Single nucleotide polymorphism charting of *P. patens* reveals accumulation of somatic mutations during *in vitro* culture on the scale of natural variation by selfing. *Frontiers in Plant Science* **11:** 813.

Haig D. **2016**. Living together and living apart: the sexual lives of bryophytes. *Philosophical Transactions of the Royal Society B: Biological Sciences* **371**: 20150535.

Hallgren J, Tsirigos KD, Damgaard Pedersen M, Juan J, Armenteros A, Marcatili P, Nielsen H, Krogh A, Winther O. 2022. DeepTMHMM predicts alpha and beta transmembrane proteins using deep neural networks. *bioRxiv*: 2022.04.08.487609.

Hashida Y, Takechi K, Abiru T, Yabe N, Nagase H, Hattori K, Takio S, Sato Y, Hasebe M, Tsukaya H, *et al.* 2020. Two *ANGUSTIFOLIA* genes regulate gametophore and sporophyte development in *Physcomitrella patens*. *Plant Journal* **101**: 1318–1330.

Heck MA, Lüth VM, van Gessel N, Krebs M, Kohl M, Prager A, Joosten H, Decker EL, Reski R. 2021. Axenic *in vitro* cultivation of 19 peat moss (*Sphagnum* L.) species as a resource for basic biology, biotechnology and paludiculture. *New Phytologist* **229**: 861-876.

Hedenäs L, Bisang I. **2012**. Sex expression and sex ratios in dwarf male-producing pleurocarpous mosses – have we missed something? *Plant Ecology & Diversity* **5**, 387 – 393.

Hedenäs L, Bisang I. **2019**. Episodic but ample sporophyte production in the moss *Drepanocladus turgescens* (Bryophyta: Amblystegiaceae) in SE Sweden. *Acta Musei Silesiae, Scientiae Naturales* **68**: 83–93.

Hiss M, Laule O, Meskauskiene RM, Arif MA, Decker EL, Erxleben A, Frank W, Hanke ST, Lang D, Martin A, *et al.* 2014. Large-scale gene expression profiling data for the model moss *Physcomitrella patens* aid understanding of developmental progression, culture and stress conditions. *Plant Journal* **79**: 530–539.

Hiss M, Meyberg R, Westermann J, Haas FB, Schneider L, Schallenberg-Rüdinger M, Ullrich KK, Rensing SA. **2017**. Sexual reproduction, sporophyte development and molecular variation in the model moss *Physcomitrella patens*: introducing the ecotype Reute. *Plant Journal* **90**: 606–620.

Hohe A, Reski R. **2002**. Optimisation of a bioreactor culture of the moss *Physcomitrella patens* for mass production of protoplasts. *Plant Science* **163**: 69–74.

Hohe A, Rensing SA, Mildner M, Lang D, Reski R. **2002**. Day length and temperature strongly influence sexual reproduction and expression of a novel MADS-box gene in the moss *Physcomitrella patens*. *Plant Biology* **4**: 595–602.

Hohe A, Egener T, Lucht JM, Holtorf H, Reinhard C, Schween G, Reski R. **2004**. An improved and highly standardised transformation procedure allows efficient production of single and multiple targeted gene-knockouts in a moss, *Physcomitrella patens*. *Current Genetics* **44**: 339–347.

Hori K, Maruyama F, Fujisawa T, Togashi T, Yamamoto N, Seo M, Sato S, Yamada T, Mori H, Tajima N, *et al.* 2014. *Klebsormidium flaccidum* genome reveals primary factors for plant terrestrial adaptation. *Nature Communications* **5**: 3978.

Horsley K, Stark LR, McLetchie DN. 2011. Does the silver moss *Bryum argenteum* exhibit sex-specific patterns in vegetative growth rate, asexual fitness or prezygotic reproductive investment? *Annals of Botany* **107:** 897-907.

Horst NA, Reski R. **2016**. Alternation of generations – unravelling the underlying molecular mechanism of a 165-year-old botanical observation. *Plant Biology* **18**: 549-551.

Horst NA, Reski R. **2017**. Microscopy of *Physcomitrella patens* sperm cells. *Plant Methods* **13**: 33.

Horst NA, Katz A, Pereman I, Decker EL, Ohad N, Reski R. **2016**. A single homeobox gene triggers phase transition, embryogenesis and asexual reproduction. *Nature Plants* **2**: 15209.

Jaillon O, Aury JM, Noel B, Policriti A, Clepet C, Casagrande A, Choisne N, Aubourg S, Vitulo N, Jubin C, *et al.* 2007. The grapevine genome sequence suggests ancestral hexaploidization in major angiosperm phyla. *Nature* **449**: 463–467.

de Jong TJ, During HJ, Shmida A. **2018**. Differences and similarities of sex ratios between dioecious angiosperms and dioicous bryophytes. *Evolutionary Ecology Research* **19**: 365–386.

Kirbis A, Waller M, Ricca M, Bont Z, Neubauer A, Goffinet B, Szövényi P. **2020**. Transcriptional landscapes of divergent sporophyte development in two mosses, *Physcomitrium* (Physcomitrella) *patens* and *Funaria hygrometrica*. *Frontiers in Plant Science* **11**: 747.

Kofuji R, Hasebe M. **2014**. Eight types of stem cells in the life cycle of the moss *Physcomitrella patens*. *Current Opinion in Plant Biology* **17**: 13–21.

Konstantinova N, Hörmayer L, Glanc M, Keshkeih R, Tan S, Di Donato M, Retzer K, Moulinier-Anzola J, Schwihla M, Korbei B, *et al*. 2022. WAVY GROWTH Arabidopsis E3 ubiquitin ligases affect apical PIN sorting decisions. *Nature Communications* **13**: 5147.

Koshimizu S, Kofuji R, Sasaki-Sekimoto Y, Kikkawa M, Shimojima M, Ohta H, Shigenobu S, Kabeya Y, Hiwatashi Y, Tamada Y, *et al.* 2018. Physcomitrella MADS-box genes regulate water supply and sperm movement for fertilization. *Nature Plants* **4**: 36–45.

Kubo M, Nishiyama T, Tamada Y, Sano R, Ishikawa M, Murata T, Imai A, Lang D, Demura T, Reski R, Hasebe M. 2019. Single-cell transcriptome analysis of Physcomitrella leaf cells during reprogramming using microcapillary manipulation. *Nucleic Acids Research* **47**: 4539-4553.

Landberg K, Pederson ERA, Viaene T, Bozorg B, Friml J, Jonsson H, Thelander M, Sundberg E. **2013**. The moss *Physcomitrella patens* reproductive organ development is highly organized, affected by the two SHI/STY genes and by the level of active auxin in the SHI/STY expression domain. *Plant Physiology* **162**: 1406–1419.

Landberg K, Šimura J, Ljung K, Sundberg E, Thelander M. **2020**. Studies of moss reproductive development indicate that auxin biosynthesis in apical stem cells may constitute an ancestral function for focal growth control. *New Phytologist* **229**: 845-860.

Landberg K, Lopez-Obando M, Sanchez Vera V, Sundberg E, Thelander M. 2022. *MS1/MMD1* homologs in the moss *Physcomitrium patens* are required for male and female gametogenesis. *New Phytologist* **236**: 512-524.

Lang D, Ullrich KK, Murat F, Fuchs J, Jenkins J, Haas FB, Piednoel M, Gundlach H, Van Bel M, Meyberg R, *et al.* 2018. The *Physcomitrella patens* chromosome-scale assembly reveals moss genome structure and evolution. *Plant Journal* **93**: 515–533.

Lang AS, Gehrmann T, Cronberg N. **2021**. Genetic diversity and population structure in bryophyte with facultative nannandry. *Frontiers in Plant Science* **12**: 517547.

Larkin MA, Blackshields G, Brown NP, Chenna R, McGettigan PA, McWilliam H, Valentin F, Wallace IM, Wilm A, Lopez R, *et al.* 2007. Clustal W and Clustal X version 2.0. *Bioinformatics* **23**: 2947–2948.

Ludwig-Müller J, Jülke S, Bierfreund NM, Decker EL, Reski R. **2009**. Moss (*Physcomitrella patens*) GH3 proteins act in auxin homeostasis. *New Phytologist* **181**: 323–338.

Lopez-Obando M, Landberg K, Sundberg E, Thelander M. **2022**. Dependence on clade II bHLH transcription factors for nursing of haploid products by tapetal-like cells is conserved between moss sporangia and angiosperm anthers. *New Phytologist* **235**: 718-731.

Lorch W. **1909**. Die Polytrichaceen. Eine biologische Monographie. *Abhandlungen der Bayerischen Akademie der Wissenschaften - Mathematisch-naturwissenschaftliche Klasse*: 445–546.

Madeira F, Park YM, Lee J, Buso N, Gur T, Madhusoodanan N, Basutkar P, Tivey ARN, Potter SC, Finn RD, Lopez R. 2019. The EMBL-EBI search and sequence analysis tools APIs in 2019. *Nucleic Acids Research* **47**: W636–W641.

Mao L, Kawaide H, Higuchi T, Chen M, Miyamoto K, Hirata Y, Kimura H, Miyazaki S, Teruya M, Fujiwara K, *et al.* 2020. Genomic evidence for convergent evolution of gene clusters for momilactone biosynthesis in land plants. *Proceedings of the National Academy of Sciences (USA)* **117**: 12472–12480.

Marchant DB, Chen G, Cai S, Chen F, Schafran P, Jenkins J, Shu S, Plott C, Webber J, Lovell JT, *et al.* 2022. Dynamic genome evolution in a model fern. *Nature Plants* **8**: 1038–1051.

Martins-Bessa A, Quaresma M, Leiva B, Calado A, Navas González FJ. **2021**. Bayesian linear regression modelling for sperm quality parameters using age, body weight, testicular morphometry, and combined biometric indices in donkeys. *Animals* **11**: 176.

McDaniel SF, von Stackelberg M, Richardt S, Quatrano RS, Reski R, Rensing SA. **2010**. The speciation history of the *Physcomitrium-Physcomitrella* species complex. *Evolution* **64**: 217-231.

Menand B, Yi KK, Jouannic S, Hoffmann L, Ryan E, Linstead P, Schaefer DG, Dolan L. **2020**. An ancient mechanism controls the development of cells with a rooting function in land plants. *Science* **316**: 1477-1480.

Merchant SS, Prochnik SE, Vallon O, Harris EH, Karpowicz SJ, Witman GB, Terry A, Salamov A, Fritz-Laylin LK, Maréchal-Drouard L, *et al.* 2007. The *Chlamydomonas* genome reveals the evolution of key animal and plant functions. *Science* **318**: 245–251.

Meyberg R, Perroud PF, Haas FB, Schneider L, Heimerl T, Renzaglia KS, Rensing SA. **2020**. Characterization of evolutionarily conserved key players affecting eukaryotic flagellar motility and fertility using a moss model. *New Phytologist* **227**: 440-454.

Morita M, Kitamura M, Nakajima A, Sri Susilo E, Takemura A, Okuno M. **2009**. Regulation of sperm flagellar motility activation and chemotaxis caused by egg-derived substance(s) in sea cucumber. *Cell Motility and the Cytoskeleton* **66**: 202–214.

Mosquna A, Katz A, Decker EL, Rensing SA, Reski R, Ohad N. **2009**. Regulation of stem cell maintenance by the Polycomb protein FIE has been conserved during land plant evolution. *Development* **136**: 2433–2444.

Nakajima A. **2005**. Increase in intracellular pH induces phosphorylation of axonemal proteins for activation of flagellar motility in starfish sperm. *Journal of Experimental Biology* **208**: 4411–4418.

Needleman SB, Wunsch CD. **1970**. A general method applicable to the search for similarities in the amino acid sequence of two proteins. *Journal of Molecular Biology* **48**: 443–453.

Nemec-Venza Z, Madden C, Stewart A, Liu W, Novak O, Pencik A, Cuming AC, Kamisugi Y, Harrison CJ. **2022**. CLAVATA modulates auxin homeostasis and transport to regulate stem cell identity and plant shape in a moss. *New Phytologist* **234**: 149–163.

Nguyen NPD, Mirarab S, Kumar K, Warnow T. 2015. Ultra-large alignments using phylogeny-aware profiles. *Genome Biology* **16**: 124.

Noy-Malka C, Yaari R, Itzhaki R, Mosquna A, Auerbach Gershovitz N, Katz A, Ohad N. **2014**. A single CMT methyltransferase homolog is involved in CHG DNA methylation and development of *Physcomitrella patens*. *Plant Molecular Biology* **84**: 719–735.

Nystedt B, Street NR, Wetterbom A, Zuccolo A, Lin YC, Scofield DG, Vezzi F, Delhomme N, Giacomello S, Alexeyenko A, *et al.* 2013. The Norway spruce genome sequence and conifer genome evolution. *Nature* **497**: 579–584.

O'Flaherty C. **2019**. Orchestrating the antioxidant defenses in the epididymis. *Andrology* **7**: 662-668.

Ortiz-Ramírez C, Hernandez-Coronado M, Thamm A, Catarino B, Wang M, Dolan L, Feijó JA, Becker JD. **2016**. A transcriptome atlas of *Physcomitrella patens* provides insights into the evolution and development of land plants. *Molecular Plant* **9**: 205–220.

Ortiz-Ramírez C, Michard E, Simon AA, Damineli DSC, Hernández-Coronado M, Becker JD, Feijó JA. **2017**. GLUTAMATE RECEPTOR-LIKE channels are essential for chemotaxis and reproduction in mosses. *Nature* **549**: 91–95.

Ostendorf AK, van Gessel N, Malkowsky Y, Sabovljevic MS, Rensing SA, Roth-Nebelsick A, Reski R. **2021**. Polyploidization within the Funariaceae—a key principle behind speciation, sporophyte reduction and the high variance of spore diameters? *Bryophyte Diversity and Evolution* **43**: 164-179.

Ouyang S, Zhu W, Hamilton J, Lin H, Campbell M, Childs K, Thibaud-Nissen F, Malek RL, Lee Y, Zheng L, *et al.* 2007. The TIGR Rice Genome Annotation Resource: improvements and new features. *Nucleic Acids Research* **35**: D883–D887.

Paponov IA, Teale W, Lang D, Paponov M, Reski R, Rensing SA, Palme K. **2009**. The evolution of nuclear auxin signalling. *BMC Evolutionary Biology* **9**: 126.

Parsons J, Altmann F, Arrenberg CK, Koprivova A, Beike AK, Stemmer C, Gorr G, Reski R, Decker EL. **2012**. Moss-based production of asialo-erythropoietin devoid of Lewis A and other plant-typical carbohydrate determinants: Lewis A-free recombinant EPO from moss. *Plant Biotechnology Journal* **10**: 851–861.

Pedersen N, Russell SJ, Newton AE, Ansell SW. **2006**. A novel molecular protocol for the rapid extraction of DNA from bryophytes and the utility of direct amplification of DNA from a single dwarf male. *Bryologist* **109**: 257–264.

Pépin F, Hugonnot V, Celle J. **2013**. Sex ratio patterns and fertility of *Hamatocaulis vernicosus* (Mitt.) Hedenäs at different spatial scales. *Journal of Bryology* **35**: 20–26.

Pereira R, Sá R, Barros A, Sousa M. **2017**. Major regulatory mechanisms involved in sperm motility. *Asian Journal of Andrology* **19**: 5-14.

Perroud PF, Cove DJ, Quatrano RS, McDaniel SF. **2011**. An experimental method to facilitate the identification of hybrid sporophytes in the moss *Physcomitrella patens* using fluorescent tagged lines. *New Phytologist* **191**: 301–306.

Perroud PF, Haas FB, Hiss M, Ullrich KK, Alboresi A, Amirebrahimi M, Barry K, Bassi R, Bonhomme S, Chen H, *et al.* 2018. The *Physcomitrella patens* gene atlas project: large-scale RNA-seq based expression data. *Plant Journal* **95**: 168–182.

Picelli S, Faridani OR, Björklund ÅK, Winberg G, Sagasser S, Sandberg R. **2014**. Full-length RNA-seq from single cells using Smart-seq2. *Nature Protocols* **9**: 171–181.

R Core Team. 2022. *R: A language and environment for statistical computing.* Vienna, Austria: R foundation for Statistical Computing. URL https://www.R-project.org/.

Regmi KC, Li L, Gaxiola RA. **2017**. Alternate modes of photosynthate transport in the alternating generations of *Physcomitrella patens*. *Frontiers in Plant Science* **8**: 1956.

Rempfer C, Wiedemann G, Schween G, Kerres KL, Lucht JM, Horres R, Decker EL, Reski R. 2022. Autopolyploidization affects transcript patterns and gene targeting frequencies in *Physcomitrella. Plant Cell Reports* **41**: 153-173.

Reski R. **1998**. Development, genetics and molecular biology of mosses. *Botanica Acta* **111**: 1–15.

Reski R. **2018**. Enabling the water-to-land transition. *Nature Plants* **4**: 67–68.

Reski R, Abel WO. **1985**. Induction of budding on chloronemata and caulonemata of the moss, *Physcomitrella patens*, using isopentenyladenine. *Planta* **165**: 354–358.

Rosengren F, Cronberg N. **2014**. The adaptive background of nannandry: dwarf male distribution and fertilization in the moss *Homalothecium lutescens*. *Biological Journal of the Linnean Society* **113**: 74–84.

Rosengren F, Cronberg N, Hansson B. **2016**. Balance between inbreeding and outcrossing in a nannandrous species, the moss *Homalothecium lutescens*. *Heredity* **116**: 107–113.

Ruiz-Molina N, Parsons J, Schroeder S, Posten C, Reski R, Decker EL. **2022**. Process engineering of biopharmaceutical production in moss bioreactors *via* model-based description and evaluation of phytohormone impact. *Frontiers in Bioengineering and Biotechnology* **10**: 837965.

Rydgren K, Økland RH. 2003. Short-term cost of sexual reproduction in the clonal moss *Hylocomium splendens. Bryologist* **106:** 212-220.

Sakakibara K, Nishiyama T, Deguchi H, Hasebe M. 2008. Class 1 KNOX genes are not involved in shoot development in the moss *Physcomitrella patens* but do function in sporophyte development. *Evolution & Development* **10:** 555-566.

Santner A, Estelle M. **2009**. Recent advances and emerging trends in plant hormone signalling. *Nature* **459**: 1071–1078.

Santos WL, Pôrto KC, Pinheiro F 2022. Sex-specific differences in reproductive life-history traits of the moss *Weissia jamaicensis*. *American Journal of Botany* **109**: 645-654.

Sauer M, Kleine-Vehn J. **2019**. PIN-FORMED and PIN-LIKES auxin transport facilitators. *Development* **146**: dev168088.

Schneider CA, Rasband WS, Eliceiri KW. 2012. NIH Image to ImageJ: 25 years of image analysis. *Nature Methods* **9:** 671-675.

Schween G, Fleig S, Reski R. **2002**. High-throughput-PCR screen of 15,000 transgenic Physcomitrella plants. *Plant Molecular Biology Reporter* **20**: 43–47.

Stamatakis A. 2014. RAxML version 8: a tool for phylogenetic analysis and post-analysis of large phylogenies. *Bioinformatics* **30**: 1312–1313.

Stark LR, Stephenson AG. **1983**. Reproductive biology of *Entodon cladorrhizans* (Bryopsida, Entodontaceae). II. Resource-limited reproduction and sporophyte abortion. *Systematic Botany* **8**: 389-394.

Stark LR, Mishler BD, McLetchie DN. **2000**. The cost of realized sexual reproduction: assessing patterns of reproductive allocation and sporophyte abortion in a desert moss. *American Journal of Botany* **87**: 1599–1608.

Stark LR, Brinda JC, McLetchie DN. **2009**. An experimental demonstration of the cost of sex and a potential resource limitation on reproduction in the moss *Pterygoneurum* (Pottiaceae). *American Journal of Botany* **96**: 1712–1721.

Stark LR, McLetchie DN, Eppley SM. **2010**. Sex ratios and the shy male hypothesis in the moss *Bryum argenteum* (Bryaceae). *Bryologist* **113**: 788–797.

Suarez SS. **2008**. Control of hyperactivation in sperm. *Human Reproduction Update* **14**: 647–657.

Suyama M, Torrents D, Bork P. 2006. PAL2NAL: robust conversion of protein sequence alignments into the corresponding codon alignments. *Nucleic Acids Research* **34**: W609–W612.

Szövényi P, Ullrich KK, Rensing SA, Lang D, van Gessel N, Stenoien HK, Conti E, Reski R. **2017**. Selfing in haploid plants and efficacy of selection: Codon usage bias in the model moss *Physcomitrella patens*. *Genome Biology and Evolution* **9**: 1528–1546.

Takechi K, Nagase H, Furuya T, Hattori K, Sato Y, Miyajima K, Higuchi T, Matsuda R, Takio S, Tsukaya H, *et al.* 2021. Two atypical ANGUSTIFOLIA without a plant-specific C-terminus regulate gametophore and sporophyte shapes in the moss *Physcomitrium* (*Physcomitrella*) *patens*. *Plant Journal* **105**: 1390–1399.

Taylor PJ, Eppley SM, Jesson LK. 2007. Sporophytic inbreeding depression in mosses occurs in a species with separate sexes but not in a species with combined sexes. *American Journal of Botany* **94:** 1853-1859.

Thelander M, Landberg K, Sundberg E. **2018**. Auxin-mediated developmental control in the moss *Physcomitrella patens*. *Journal of Experimental Botany* **69**: 277–290.

Thelander M, Landberg K, Sundberg E. **2019**. Minimal auxin sensing levels in vegetative moss stem cells revealed by a ratiometric reporter. *New Phytologist* **224**: 775-788.

Tuskan GA, DiFazio S, Jansson S, Bohlmann J, Grigoriev I, Hellsten U, Putnam M, Ralph S, Rombauts S, Salamov A, *et al.* 2006. The genome of black cottonwood, *Populus trichocarpa* (Torr. & Gray). *Science* **313**: 1596–1604.

Une K. 1985. Sexual dimorphism in the Japanese species of *Macromitrium* Brid. (Musci: Orthotrichaceae). *Journal of the Hattori Botanical Laboratory* **59**: 487-514.

Ung KL, Winkler M, Schulz L, Kolb M, Janacek DP, Dedic E, Stokes DL, Hammes UZ, Pedersen BP. 2022. Structures and mechanism of the plant PIN-FORMED auxin transporter. *Nature* **609**: 605-610.

Uzawa M, Higuchi M. **2010**. Comparative development of the sporophyte–gametophyte junction in six moss species. *Journal of Plant Research* **123**: 777–787.

Varapparambath V, Mathew MM, Shanmukhan AP, Radhakrishnan D, Kareem A, Verma S, Ramalho JJ, Manoj B, Vellandath AR, Aiyaz M, Radha RK, Landge AN, Mähönen AP, Heisler MG, Weijers D, Prasad K. 2022. Mechanical conflict caused by a cell-wall-loosening enzyme activates *de novo* shoot regeneration. *Developmental Cell* **57**: 2063-2080.e10.

Viaene T, Landberg K, Thelander M, Medvecka E, Pederson E, Feraru E, Cooper ED, Karimi M, Delwiche CF, Ljung K, *et al.* 2014. Directional auxin transport mechanisms in early diverging land plants. *Current Biology* **24**: 2786–2791.

Weijers D, Wagner D. **2016**. Transcriptional responses to the auxin hormone. *Annual Review of Plant Biology* **67**: 539–574.

Wiedemann G, van Gessel N, Köchl F, Hunn L, Schulze K, Maloukh L, Nogué F, Decker EL, Hartung F, Reski R. **2018**. RecQ helicases function in development, DNA repair, and gene targeting in *Physcomitrella patens*. *Plant Cell* **30**: 717–736.

Xiong Y, Wu B, Du F, Guo X, Tian C, Hu J, Lü S, Long M, Zhang L, Wang Y, Jiao Y. 2021. A crosstalk between auxin and brassinosteriod regulates leaf shape by modulating growth anisotropy. *Molecular Plant* **14**: 949-962.

Yu G, Smith DK, Zhu H, Guan Y, Lam TTY. 2017. ggtree: an r package for visualization and annotation of phylogenetic trees with their covariates and other associated data. *Methods in Ecology and Evolution* **8**: 28–36.

Żabka A, Polit JT, Winnicki K, Paciorek P, Juszczak J, Nowak M, Maszewski J. **2016**. PIN2-like proteins may contribute to the regulation of morphogenetic processes during spermatogenesis in *Chara vulgaris*. *Plant Cell Reports* **35**: 1655–1669.

Zhang Y, Rodriguez L, Li L, Zhang X, Friml J. **2020a**. Functional innovations of PIN auxin transporters mark crucial evolutionary transitions during rise of flowering plants. *Science Advances* **6**: eabc8895.

Zhang J, Fu X-X, Li R-Q, Zhao X, Liu Y, Li M-H, Zwaenepoel A, Ma H, Goffinet B, Guan Y-L, *et al.* 2020b. The hornwort genome and early land plant evolution. *Nature Plants* **6**: 107–118.

Supporting Information

Supplemental Figure S1: Alignments of protein sequences of Physcomitrella and Arabidopsis PIN proteins

Supplemental Figure S2: Expression data of Physcomitrella PIN genes from PEATmoss database

Supplemental Figure S3: Molecular evaluation of *pinCPromCit*

Supplemental Figure S4: Molecular analysis of Physcomitrella *pin*C mutant lines

Supplemental Figure S5: Phenotypical characterization of vegetative tissue for Physcomitrella wild type (WT) and *pin*C mutant lines

Supplemental Figure S6: Calcium concentration in Physcomitrella spermatozoids

Supplemental Figure S7: Quality control RNAseq

Supplemental Figure S8: Proof of *PpPINC* mutation in *pin*C#29

Supplemental Figure S9: Size of spore capsules and spore germination rate

Supplemental Table S1: Primers used in Physcomitrella WT and mutant lines

Supplemental Table S2: Differentially expressed genes in Physcomitrella WT and mutant

Supplemental Table S3: All DEG experiments, including table of single genes already identified in other publications

Supplemental Table S4: Number of vital and aborted sporophytes counted in Physcomitrella WT and *pin*C mutant lines

a)

PpPINA HL and PpPINB HL

Length: 409
Identity: 353/409 (86.3%)
Similarity: 374/409 (91.4%)
Gaps: 2/409 (0.5%)
Score: 1819.0

```
PINALOOP          1 AAKILIMQQFPENAASIVSFKVDSDVMSLDGREPVLTEAEIGDDGKLHVK     50
                    ||||||||||||||.||||||||||||||||||||||||||||||||||||
PINBLOOP          1 AAKILIMQQFPENAGSIVSFKVDSDVMSLDGREPVLTEAEIGDDGKLHVK     50

PINALOOP         51 VRRSVSSRSQGMHSAHHSMPSSKALTPRPSNLTGAEIYSMHSSVNLTPRD    100
                    ||||||||||||||||||||||||||||||||||||||||||||||||||
PINBLOOP         51 VRRSVSSRSQGMHSAHHSMPSSKALTPRPSNLTGAEIYSMHSSVNLTPRD    100

PINALOOP        101 SSFNQGEFHSMMSQRSPHRQSNFDTSDVYSLQSSRGPTPRSSNFNEENSK    150
                    |||||||:.|||:||||||||||||.||||||||||||||||:|||||||||
PINBLOOP        101 SSFNQGEYFSMMAQRSPHRQSNFDISDVYSLQSSRGPTPRTSNFNEENSK    150

PINALOOP        151 DIHTHHRGLNMNSPRFAPPLYRNGMGARMFTPRPGLGGIGVPGTDCTGHG    200
                    |:||||||||:.||||.||||||..|.|||.||.||||:.|.|.|.||||
PINBLOOP        151 DMHTHHRGLNLTSPRFVPPLYRNVAGGRMFMPRTGLGGLPVHGNDPTGHG    200

PINALOOP        201 TLSTLGAPGMGPDGRTIYPGSQTAINILTLGGAANVNATAPSTAVNTQIV    250
                    :|||||.||||||||||||||||:::|.||..|: ||..|:::||||||
PINBLOOP        201 SLSTLGTPGMGPDGRTIYPGSQTAISLVTPGGTGNI-ATPLSSSLNTQIV    249

PINALOOP        251 NPVYSPQASQIAKKVKDPKASPRADEDAKELHMFVWSANASPVSEAGLHV    300
                    ||||||:||||||||||.:.||::||||||||||||||||||||||||||
PINBLOOP        250 NPVYSPRASQIAKKVKDTRTSPKSDEDAKELHMFVWSANASPVSEAGLHV    299

PINALOOP        301 FGGNDTSANLQQRFDPKEVRMLVHPQLDRGLAAASPRTYDEYTREDFSFG    350
                    ||||||||||.|.||||||||||||||.|.....|:||||||.|.:||||||
PINBLOOP        300 FGGNDTSANLHQSFDPKEVRMLVHPQSDLRHPEANPRTYDNYAQEDFSFG    349

PINALOOP        351 NRNDLKLEDLDKDGPRLD-KFGSTSTAELTPKLAEDEAKKSMPPSAVMIK    399
                    |||||||||||||||||| |||||||||||||:.||||||||||||||||
PINBLOOP        350 NRNDLKLEDLDKDGPRLDNKFGSTSTAELTPKVPEDEAKKSMPPSAVMIK    399

PINALOOP        400 LIAVMTFRK    408
                    |||||||||
PINBLOOP        400 LIAVMTFRK    408
```

PpPINA HL and PpPINC HL

Length: 411
Identity: 266/411 (64.7%)
Similarity: 316/411 (76.9%)
Gaps: 21/411 (5.1%)
Score: 1312.5

```
PINALOOP          1 AAKILIMQQFPENAASIVSFKVDSDVMSLDGREPVLTEAEIGDDGKLHVK     50
                    ||:||||.:||||||||||||||:||||||||.:|||||||..:||||||:
PINCLOOP          1 AARILIMHRFPENAASIVSFKVESDVMSLDGPDPVLTEAEFRNDGKLHVR     50

PINALOOP         51 VRRSVSSRSQGMHSAHHSMPSSKALTPRPSNLTGAEIYSMHSSVNLTPRD    100
                    |||||||||||:|||:||:|||||||||.|||:.||||||:||||||||.
PINCLOOP         51 VRRSVSSRSQGVHSANHSIPSSKALTPRASNLSNAEIYSMNSSVNLTPRG    100

PINALOOP        101 SSFNQGEFHSMMSQRSPHRQSNFDTSDVYSLQSSRGPTPRSSNFNEENSK    150
                    |||::||..|.|:.|.|:|:|||||||:||||||||||||:|||||||||
PINCLOOP        101 SSFDRGEDCSTMAHRDPNRKSNFDTSDIYSLQSSRGPTPRNSNFNEENSK    150

PINALOOP        151 DIHTHHRGLNMNSPRFAPPLYRNGMGARMFTPRPGLGGIGVPGTDCTGHG    200
                    ::|.|...||:|.||||||||||||.|.|:|..|..|||:|....:...|
```

```
PINCLOOP         151 EVHNHRGALNVNIPRFAPPLYRNGSGGRLFMARSDLGGVGALSFEPAAH-    199

PINALOOP         201 TLSTLGAPGMGPDGRTIYPGSQTAINILTLGGAANVNATAPSTAVNTQIV    250
                             .|||||||||||    |.::|     |..|..|::.|:|.|:
PINCLOOP         200 --------SMGPDGRTIYPG----ITVVT-----NSVAAVPASGVSTHII    232

PINALOOP         251 NPVYSPQASQIAKKVKDPKAS-PRADEDAKELHMFVWSANASPVSEAGLH    299
                     |||:||..||:||||.||:|| |:.||:||||||||.|||.:.|||..||
PINCLOOP         233 NPVFSPLVSQVAKKVNDPRASIPKTDEEAKELHMFVSSANPTSVSEGELH    282

PINALOOP         300 VFGGNDTSANLQQRFDPKEVRMLVHPQLDRGL-AAASPRTYDEYTREDFS    348
                     ||||:|.|.||||..:|||:.:.||||.:..| .||:.:|.||:.|:.||
PINCLOOP         283 VFGGSDISINLQQSVNPKELHVHVHPQSEHHLPGAANHKTQDEHARQGFS    332

PINALOOP         349 FGNRNDLKLEDLDKDGPRLD-KFGSTSTAELTPKLAEDEAKKSMPPSAVM    397
                     ||||.|||:||:|.:|.:|| ||.|..||||.||...||.|.||||||:||
PINCLOOP         333 FGNRRDLKVEDVDNNGSKLDKKFRSILTAELAPKHPMDEGKTSMPPSSVM    382

PINALOOP         398 IKLIAVMTFRK    408
                     ||||.||||||
PINCLOOP         383 IKLICVMTFRK    393
```

PpPINB HL and PpPINC HL

Length: 410
Identity: 264/410 (64.4%)
Similarity: 315/410 (76.8%)
Gaps: 19/410 (4.6%)
Score: 1306.0

```
PINBLOOP           1 AAKILIMQQFPENAGSIVSFKVDSDVMSLDGREPVLTEAEIGDDGKLHVK     50
                     ||:||||.:|||||.|||||||:||||||||.:|||||||..:||||||:
PINCLOOP           1 AARILIMHRFPENAASIVSFKVESDVMSLDGPDPVLTEAEFRNDGKLHVR     50

PINBLOOP          51 VRRSVSSRSQGMHSAHHSMPSSKALTPRPSNLTGAEIYSMHSSVNLTPRD    100
                     |||||||||||:|||:||:||||||||.|||:.||||||:||||||||.
PINCLOOP          51 VRRSVSSRSQGVHSANHSIPSSKALTPRASNLSNAEIYSMNSSVNLTPRG    100

PINBLOOP         101 SSFNQGEYFSMMAQRSPHRQSNFDISDVYSLQSSRGPTPRTSNFNEENSK    150
                     |||::||..|.||.|.|:|:||||.||:||||||||||||.|||||||||
PINCLOOP         101 SSFDRGEDCSTMAHRDPNRKSNFDTSDIYSLQSSRGPTPRNSNFNEENSK    150

PINBLOOP         151 DMHTHHRGLNLTSPRFVPPLYRNVAGGRMFMPRTGLGGLPVHGNDPTGHG    200
                     ::|.|...||:..|||.||||||.:|||:||.|:.|||:.....:|..|
PINCLOOP         151 EVHNHRGALNVNIPRFAPPLYRNGSGGRLFMARSDLGGVGALSFEPAAH-    199

PINBLOOP         201 SLSTLGTPGMGPDGRTIYPGSQTAISLVTPGGTGNIATPLSSSLNTQIVN    250
                             .|||||||||||    |::|    |.::|...:|.::|.|:|
PINCLOOP         200 --------SMGPDGRTIYPG----ITVV----TNSVAAVPASGVSTHIIN    233

PINBLOOP         251 PVYSPRASQIAKKVKDTRTS-PKSDEDAKELHMFVWSANASPVSEAGLHV    299
                     ||:||..||:||||.|.|.| ||:||:||||||||.|||.:.|||..|||
PINCLOOP         234 PVFSPLVSQVAKKVNDPRASIPKTDEEAKELHMFVSSANPTSVSEGELHV    283

PINBLOOP         300 FGGNDTSANLHQSFDPKEVRMLVHPQSDLRHP-EANPRTYDNYAQEDFSF    348
                     |||:|.|.||.||.:|||:.:.|||||:...| .||.:|.|.:|::.|||
PINCLOOP         284 FGGSDISINLQQSVNPKELHVHVHPQSEHHLPGAANHKTQDEHARQGFSF    333

PINBLOOP         349 GNRNDLKLEDLDKDGPRLDNKFGSTSTAELTPKVPEDEAKKSMPPSAVMI    398
                     |||.|||:||:|.:|.:||.||.|..||||.||.|.||.|.||||||:|||
PINCLOOP         334 GNRRDLKVEDVDNNGSKLDKKFRSILTAELAPKHPMDEGKTSMPPSSVMI    383

PINBLOOP         399 KLIAVMTFRK    408
                     |||.||||||
PINCLOOP         384 KLICVMTFRK    393
```

PpPINA TM1 and PpPINB TM1

Length: 155
Identity: 149/155 (96.1%)

Similarity: 153/155 (98.7%)
Gaps: 0/155 (0.0%)
Score: 792.0

```
PINATM1            1 MINGHDIYNVLSAMVPLYVAMMLAYGSVKWWGILTPQQCGGINRFVSIFA     50
                     ||||||||||||||||||||||||||||||||||||||||||||||||||
PINBTM1            1 MINGHDIYNVLSAMVPLYVAMMLAYGSVKWWGILTPQQCGGINRFVSIFA     50

PINATM1           51 VPLLSFQFISGNNPYAMNFKFIAADAVSKVLVLLCLGLWARYAKRGSLEW    100
                     ||||||||||||||||||:||||||||||.||||||||||||:|||||||
PINBTM1           51 VPLLSFQFISGNNPYAMNFRFIAADAVSKVFVLLCLGLWARYSKRGSLEW    100

PINATM1          101 MITLFVLITIPNTLVMGTPLLAAMYGAGPGDLTVQAVVLQCIIWYTLLLV    150
                     ||||||||||||||||||||||||||.||||||:||||||||||||||:
PINBTM1          101 MITLFVLITIPNTLVMGTPLLAAMYGPGPGDLTIQAVVLQCIIWYTLLLL    150

PINATM1          151 MYEYR    155
                     |||||
PINBTM1          151 MYEYR    155
```

PpPINA TM1 and PpPINC TM1

Length: 155
Identity: 136/155 (87.7%)
Similarity: 145/155 (93.5%)
Gaps: 0/155 (0.0%)
Score: 726.0

```
PINATM1            1 MINGHDIYNVLSAMVPLYVAMMLAYGSVKWWGILTPQQCGGINRFVSIFA     50
                     ||.|||:||||||||||||||||||.||||||||||||||.||||||||||
PINCTM1            1 MITGHDMYNVLSAMVPLYVAMMLAYASVKWWGILTPQQCDGINRFVSIFA     50

PINATM1           51 VPLLSFQFISGNNPYAMNFKFIAADAVSKVLVLLCLGLWARYAKRGSLEW    100
                     ||||||||:||||||.|||:||||||||||.||.||||||.|::||||||||
PINCTM1           51 VPLLSFQFVSGNNPYEMNFRFIAADAVSKVFVLSCLGLWVRFSKRGSLEW    100

PINATM1          101 MITLFVLITIPNTLVMGTPLLAAMYGAGPGDLTVQAVVLQCIIWYTLLLV    150
                     :||||:|.|||||||:||||||||||:.||.||||||||||||||||||
PINCTM1          101 VITLFMLTTIPNTLVIGTPLLAAMYGSKPGQLTVQAVVLQCIIWYTLLLV    150

PINATM1          151 MYEYR    155
                     |||||
PINCTM1          151 MYEYR    155
```

PpPINB TM1 and PpPINC TM1

Length: 155
Identity: 137/155 (88.4%)
Similarity: 145/155 (93.5%)
Gaps: 0/155 (0.0%)
Score: 732.0

```
PINBTM1            1 MINGHDIYNVLSAMVPLYVAMMLAYGSVKWWGILTPQQCGGINRFVSIFA     50
                     ||.|||:||||||||||||||||||.||||||||||||||.||||||||||
PINCTM1            1 MITGHDMYNVLSAMVPLYVAMMLAYASVKWWGILTPQQCDGINRFVSIFA     50

PINBTM1           51 VPLLSFQFISGNNPYAMNFRFIAADAVSKVFVLLCLGLWARYSKRGSLEW    100
                     ||||||||:||||||.||||||||||||||||||.||||||.|:||||||||
PINCTM1           51 VPLLSFQFVSGNNPYEMNFRFIAADAVSKVFVLSCLGLWVRFSKRGSLEW    100

PINBTM1          101 MITLFVLITIPNTLVMGTPLLAAMYGPGPGDLTIQAVVLQCIIWYTLLLL    150
                     :||||:|.|||||||:||||||||||..||.||:|||||||||||||||:
PINCTM1          101 VITLFMLTTIPNTLVIGTPLLAAMYGSKPGQLTVQAVVLQCIIWYTLLLV    150

PINBTM1          151 MYEYR    155
                     |||||
PINCTM1          151 MYEYR    155
```

PpPINA TM2 and PpPINB TM2

Length: 150
Identity: 143/150 (95.3%)
Similarity: 148/150 (98.7%)
Gaps: 0/150 (0.0%)
Score: 739.0

```
PINATM2            1 LVWNPNTYSSLLGVIWSLVANRWHLSMPLILYKSVHILSDAGLGMAMFSL     50
                     |||||||||||||||||||||||||.:||||||||||||||||||||||||
PINBTM2            1 LVWNPNTYSSLLGVIWSLVANRWHFTMPLILYKSVHILSDAGLGMAMFSL     50

PINATM2           51 GLFMGLGDRIIVCGTKMAVFGMALRFLAGPAVFAAASYLVGLRGVPLKVS    100
                     ||||||||||:|||.|||:|||:||||||||||||||||||||||||||||
PINBTM2           51 GLFMGLGDRIVVCGRKMAIFGMSLRFLAGPAVFAAASYLVGLRGVPLKVS    100

PINATM2          101 IVQAALPQGIVPFVFAKEYGVHPEILSTAVIFGMLIALPITMVYYILLGL    150
                     |||||||||||||||||||||||||:||||||||||||||||||||||||||
PINBTM2          101 IVQAALPQGIVPFVFAKEYGVHPEMLSTAVIFGMLIALPITMVYYILLGL    150
```

PpPINA TM2 and PpPINC TM2

Length: 150
Identity: 120/150 (80.0%)
Similarity: 132/150 (88.0%)
Gaps: 0/150 (0.0%)
Score: 621.0

```
PINATM2            1 LVWNPNTYSSLLGVIWSLVANRWHLSMPLILYKSVHILSDAGLGMAMFSL     50
                     |..|||||||||||:|||::.:.||.||||||||.||:||||:|||||||
PINCTM2            1 LTRNPNTYSSLLGVVWSLISFKCHLDMPLILYKSYHIISDAGIGMAMFSL     50

PINATM2           51 GLFMGLGDRIIVCGTKMAVFGMALRFLAGPAVFAAASYLVGLRGVPLKVS    100
                     |||||:|||||.||||.|:|.|.||||.||||||||||||||||.|.||
PINCTM2           51 GLFMGMGDRIIACGTKHALFAMLLRFLVGPAVFAAASYLVGLRGVSLNVS    100

PINATM2          101 IVQAALPQGIVPFVFAKEYGVHPEILSTAVIFGMLIALPITMVYYILLGL    150
                     .||||||||||||||||||.|||||||||||||::.||..::|||||||
PINCTM2          101 TVQAALPQGIVPFVFAKEYNVHPEILSTAVIFGMIVTLPTALLYYILLGL    150
```

PpPINB TM2 and PpPINC TM2

Length: 150
Identity: 116/150 (77.3%)
Similarity: 130/150 (86.7%)
Gaps: 0/150 (0.0%)
Score: 606.0

```
PINBTM2            1 LVWNPNTYSSLLGVIWSLVANRWHFTMPLILYKSVHILSDAGLGMAMFSL     50
                     |..|||||||||||:|||::.:.|..||||||||.||:||||:|||||||
PINCTM2            1 LTRNPNTYSSLLGVVWSLISFKCHLDMPLILYKSYHIISDAGIGMAMFSL     50

PINBTM2           51 GLFMGLGDRIVVCGRKMAIFGMSLRFLAGPAVFAAASYLVGLRGVPLKVS    100
                     |||||:||||:.||.|.|:|.|.||||.||||||||||||||||.|.||
PINCTM2           51 GLFMGMGDRIIACGTKHALFAMLLRFLVGPAVFAAASYLVGLRGVSLNVS    100

PINBTM2          101 IVQAALPQGIVPFVFAKEYGVHPEMLSTAVIFGMLIALPITMVYYILLGL    150
                     .||||||||||||||||||.||||:|||||||||::.||..::|||||||
PINCTM2          101 TVQAALPQGIVPFVFAKEYNVHPEILSTAVIFGMIVTLPTALLYYILLGL    150
```

1334

b)

```
Pp3c10_24880V3.1.p      EENSKEVHNHRGALNVNIPRFAPPLYRNGSGGRLFMARSDLGGVGALSFEPAA-------  353
Pp3c23_10200V3.1.p      EENSKDIHTHHRGLNMNSPRFAPPLYRNGMGARMFTPRPGLGGIGVPGTDCTGHGTLSTL  360
Pp3c24_2970V3.1.p       EENSKDMHTHHRGLNLTSPRFVPPLYRNVAGGRMFMPRTGLGGLPVHGNDPTGHGSLSTL  360
                        *****::*.*: .**:. ***.******  *.*:*  * .***: . . : :.
Pp3c10_24880V3.1.p      --HSMGPDGRTIYPGITVVTNSV---------AAVPASGVSTHIINPVFSPLVSQVAKKV  402
Pp3c23_10200V3.1.p      GAPGMGPDGRTIYPGSQTAINILTLGGAANVNATAPSTAVNTQIVNPVYSPQASQIAKKV  420
Pp3c24_2970V3.1.p       GTPGMGPDGRTIYPGSQTAISLVTPGGTGNIAT-PLSSSLNTQIVNPVYSPRASQIAKKV  419
                           .***********  .. . :         :   ::.:.*:*:***:** .**:****
```

c)

```
CLUSTAL O(1.2.4) multiple sequence alignment


Pp3c10_24880V3.1.p      MITGHDMYNVLSAMVPLYVAMMLAYASVKWWGILTPQQCDGINRFVSIFAVPLLSFQFVS  60
Pp3c23_10200V3.1.p      MINGHDIYNVLSAMVPLYVAMMLAYGSVKWWGILTPQQCGGINRFVSIFAVPLLSFQFIS  60
Pp3c24_2970V3.1.p       MINGHDIYNVLSAMVPLYVAMMLAYGSVKWWGILTPQQCGGINRFVSIFAVPLLSFQFIS  60
AT5G57090.1             MITGKDMYDVLAAMVPLYVAMILAYGSVRWWGIFTPDQCSGINRFVAVFAVPLLSFHFIS  60
AT1G73590.1             MITAADFYHVMTAMVPLYVAMILAYGSVKWWKIFTPDQCSGINRFVALFAVPLLSFHFIA  60
AT2G01420.2             MITWHDLYTVLTAVVPLYVAMILAYGSVQWWKIFSPDQCSGINRFVAIFAVPLLSFHFIS  60
AT1G70940.1             MISWHDLYTVLTAVIPLYVAMILAYGSVRWWKIFSPDQCSGINRFVAIFAVPLLSFHFIS  60
AT1G23080.1             MITWHDLYTVLTAVIPLYVAMILAYGSVRWWKIFSPDQCSGINRFVAIFAVPLLSFHFIS  60
                        **.  *:* *::*::******:***.**:** *::*:**.******::********:*::

Pp3c10_24880V3.1.p      GNNPYEMNFRFIAADAVSKVFVLSCLGLWVRFSKRGSLEWVITLFMLTTIPNTLVIGTPL  120
Pp3c23_10200V3.1.p      GNNPYAMNFKFIAADAVSKVLVLLCLGLWARYAKRGSLEWMITLFVLITIPNTLVMGTPL  120
Pp3c24_2970V3.1.p       GNNPYAMNFRFIAADAVSKVFVLLCLGLWARYSKRGSLEWMITLFVLITIPNTLVMGTPL  120
AT5G57090.1             SNDPYAMNYHFLAADSLQKVVILAALFLWQAFSRRGSLEWMITLFSLSTLPNTLVMGIPL  120
AT1G73590.1             ANNPYAMNLRFLAADSLQKVIVLSLLFLWCKLSRNGSLDWTITLFSLSTLPNTLVMGIPL  120
AT2G01420.2             TNDPYAMNFRFVAADTLQKIIMLVLLALWANLTKNGSLEWMITIFSLSTLPNTLVMGIPL  120
AT1G70940.1             TNNPYAMNLRFIAADTLQKIIMLSLLVLWANFTRSGSLEWSITIFSLSTLPNTLVMGIPL  120
AT1G23080.1             SNNPYAMNLRFIAADTLQKLIMLTLLIIWANFTRSGSLEWSITIFSLSTLPNTLVMGIPL  120
                         *:** ** :*:***::.*:.:*  * :*   :: ***:* **:* * *:*****:* **

Pp3c10_24880V3.1.p      LAAMYGSKPGQLTVQAVVLQCIIWYTLLLVMYEYRAARILIMHRFPENAASIVSFKVESD  180
Pp3c23_10200V3.1.p      LAAMYGAGPGDLTVQAVVLQCIIWYTLLLVMYEYRAAKILIMQQFPENAASIVSFKVDSD  180
Pp3c24_2970V3.1.p       LAAMYGPGPGDLTIQAVVLQCIIWYTLLLLMYEYRAAKILIMQQFPENAGSIVSFKVDSD  180
AT5G57090.1             LRAMYGDFSGNLMVQIVVLQSIIWYTLMLFLFEFRGAKLLISEQFPETAGSITSFRVDSD  180
AT1G73590.1             LKGMYGNFSGDLMVQIVVLQCIIWYTLMLFLFEYRGAKLLISEQFPDTAGSIVSIHVDSD  180
AT2G01420.2             LIAMYGTYAGSLMVQVVVLQCIIWYTLLLFLFEYRGAKLLIMEQFPETGASIVSFKVESD  180
AT1G70940.1             LIAMYGEYSGSLMVQIVVLQCIIWYTLLLFLFEFRGAKMLIMEQFPETAASIVSFKVESD  180
AT1G23080.1             LIAMYGEYSGSLMVQIVVLQCIIWYTLLLFLFEYRGAKILIMEQFPETGASIVSFKVESD  180
                        * .***   *.* :* ****.******:*.::*:*.*::** .:**:...**.*::*:**

Pp3c10_24880V3.1.p      VMSLDGPDPVLTEAEFRNDGKLHVRVRRSVSSRSQGV--HSANHSIPSSKALTPRASNLS  238
Pp3c23_10200V3.1.p      VMSLDGREPVLTEAEIGDDGKLHVKVRRSVSSRSQGM--HSAHHSMPSSKALTPRPSNLT  238
Pp3c24_2970V3.1.p       VMSLDGREPVLTEAEIGDDGKLHVKVRRSVSSRSQGM--HSAHHSMPSSKALTPRPSNLT  238
AT5G57090.1             VISLNGREPLQTDAEIGDDGKLHVVVRRSSAASSMISSFNKSHGGGLNSSMITPRASNLT  240
AT1G73590.1             IMSLDGRQPLETEAEIKEDGKLHVTVRRSNASRSDIY------SRRSQGLSATPRPSNLT  234
AT2G01420.2             VVSLDGHDFLETDAEIGNDGKLHVTVRKSNASRRSL--------------MMTPRPSNLT  226
AT1G70940.1             VVSLDGHDFLETDAEIGDDGKLHVTVRKSNASRRSFC------G-----PNMTPRPSNLT  229
AT1G23080.1             VVSLDGHDFLETDAQIGDDGKLHVTVRKSNASRRSFY------GG--GGTNMTPRPSNLT  232
                        ::**:* : : *:*:: :****** **:* ::                    *** ***:

Pp3c10_24880V3.1.p      NAEIYSMNSSVNLTPRGSSFDRGEDCSTMAHRDPNRKSN------------FDTSDIYSL  286
Pp3c23_10200V3.1.p      GAEIYSMHSSVNLTPRDSSFNQGEFHSMMSQRSPHRQSN------------FDTSDVYSL  286
Pp3c24_2970V3.1.p       GAEIYSMHSSVNLTPRDSSFNQGEYFSMMAQRSPHRQSN------------FDISDVYSL  286
AT5G57090.1             GVEIYSVQSSREPTPRASSFNQTDFYAMFNASK-APSPRHGYTNSYGGAGAGPGGDVYSL  299
AT1G73590.1             NAEIYSLQSSRNPTPRGSSFNHTDFYSMMASGG-GRNSN------------FGPGEA--V  279
AT2G01420.2             GAEIYSLS----STPRGSNFNHSDFYSVMGFPG-GRLSN------------FGPADLYSV  269
AT1G70940.1             GAEIYSLS----TTPRGSNFNHSDFYNMMGFPG-GRLSN------------FGPADMYSV  272
AT1G23080.1             GAEIYSLN----TTPRGSNFNHSDFYSMMGFPG-GRLSN------------FGPADMYSV  275
                        ..****:      *** *.*:: :    :         .               .:   :

Pp3c10_24880V3.1.p      QSSRGPTPRNSNFNEENSKEVHNHRGALNVNIPRFAPPLYRNGSGGRLFMARSDLGGVGA  346
Pp3c23_10200V3.1.p      QSSRGPTPRSSNFNEENSKDIHTHHRGLNMNSPRFAPPLYRNGMGARMFTPRPGLGGIGV  346
Pp3c24_2970V3.1.p       QSSRGPTPRTSNFNEENSKDMHTHHRGLNLTSPRFVPPLYRNVAGGRMFMPRTGLGGLPV  346
AT5G57090.1             QSSKGVTPRTSNFDEEVMKTAKKAG-R-GGRS-----------------MSGELYNNN--  338
AT1G73590.1             FGSKGPTPRPSNYEEDGGPAKPTAAGT-AAGAGRF------------HYQSG-GSGGG--  323
AT2G01420.2             QSSRGPTPRPSNFEENNAV--------------KY------------GFYNNTNSSVP--  301
AT1G70940.1             QSSRGPTPRPSNFEENCAMASSP----------RF------------GYYPG-----G--  303
AT1G23080.1             QSSRGPTPRPSNFEESCAMASSP----------RF------------GYYPG-----G--  306
                         .*:* *** **::*.
```

```
Pp3c10_24880V3.1.p      LSFEPAA---------HSMGPDGRTIYPGITVVTNSV---------AAVPASGVSTHIIN  388
Pp3c23_10200V3.1.p      PGTDCTGHGTLSTLGAPGMGPDGRTIYPGSQTAINILTLGGAANVNATAPSTAVNTQIVN  406
Pp3c24_2970V3.1.p       HGNDPTGHGSLSTLGTPGMGPDGRTIYPGSQTAISLVTPGGTGNIAT-PLSSSLNTQIVN  405
AT5G57090.1             -----------------------SVPSYPPPNPMFTGSTSGASGVK-KK------------  363
AT1G73590.1             -----------------------GGAHYPAPNPGMFSPNTGGGGGTAAK-----------G  350
AT2G01420.2             -----------------------AAGSYPAPNPEFSTGTGVS------T-----------K  322
AT1G70940.1             -----------------------GAGSYPAPNPEFSSTTTSTANKSVNK-----------N  330
AT1G23080.1             -----------------------APGSYPAPNPEFSTGNKTG-----SK-----------A  328
                                                .   **

Pp3c10_24880V3.1.p      PVFSPLVSQVAKKVNDPRASIPKTDEEAKELHMFVSSANPTSVSEGE-LHVFGGS-DISI  446
Pp3c23_10200V3.1.p      PVYSPQASQIAKKVKDPKAS-PRADEDAKELHMFVWSANASPVSEAG-LHVFGGN-DTSA  463
Pp3c24_2970V3.1.p       PVYSPRASQIAKKVKDTRTS-PKSDEDAKELHMFVWSANASPVSEAG-LHVFGGN-DTSA  462
AT5G57090.1             ------ES-----GGGGSGGGVGVGGQNKEMNMFVWSSSASPVSEANAKNAMTRGSSTD-  411
AT1G73590.1             --------------NAPVVGGKRQDGNGRDLHMFVWSSSASPVSDVFGGG----GGNHHA  392
AT2G01420.2             PNKIPKEN-----QQQLQEKDSKASHDAKELHMFVWSSSASPVSDVFG----GGAGDNVA  373
AT1G70940.1             PKDVNTNQ-----QTTLPTGGKSNSHDAKELHMFVWSSNGSPVSDRAGLNVFGGAPDNDQ  385
AT1G23080.1             PKE------------NHHHVGKSNSNDAKELHMFVWGSNGSPVSDRAGLQVDNGANE-QV  375
                                                 . : ::::*** .:. : **:           .

Pp3c10_24880V3.1.p      --NLQQSVNPKELHVHVHPQSEHHLPGA-ANHKTQDEHARQGFSFGNRRDLKVEDVDNNG  503
Pp3c23_10200V3.1.p      --NLQQRFDPKEVRMLVHPQLDRGLAAA--SPRTYDEYTREDFSFGNRNDLKLEDLDKDG  519
Pp3c24_2970V3.1.p       --NLHQSFDPKEVRMLVHPQSDLRHPEA--NPRTYDNYAQEDFSFGNRNDLKLEDLDKDG  518
AT5G57090.1             --------VSTDPKVSIPPHDNLA-TKAMQNLIENMSPG-------RKGHVE----M--D  449
AT1G73590.1             DYSTATNDHQKDVKISVPQG----------NSNDNQYVEREEFSFGNKDDDSKVLAT---  439
AT2G01420.2             --TEQSEQGAKEIRMVVSDQPRKSNARGGGDDI----GGL------DSGEGEREIEK--A  419
AT1G70940.1             --GGRSDQGAKEIRMLVPDQSHNGETKAVAHPASGDFGGEQQFSFAGKEEEAERPKD--A  441
AT1G23080.1             --GKSDQGGAKEIRMLISDHTQNGENKA--GPMNGDYGGE---------EESERVKE--V  420
                                  .: :: :                                  .

Pp3c10_24880V3.1.p      SKLDKKFRSILTAELAPKHPMD----EGKTSMPPSSVMIKLICVMTFRKLTRNPNTYSSL  559
Pp3c23_10200V3.1.p      PRLD-KFGSTSTAELTPKLAED----EAKKSMPPSAVMIKLIAVMTFRKLVWNPNTYSSL  574
Pp3c24_2970V3.1.p       PRLDNKFGSTSTAELTPKVPED----EAKKSMPPSAVMIKLIAVMTFRKLVWNPNTYSSL  574
AT5G57090.1             QDGNNGGK-SPYMGKKGSDVEDGGPGPRKQQMPPASVMTRLILIMVWRKLIRNPNTYSSL  508
AT1G73590.1             -D---------------GGNNISNKTTQAKVMPPTSVMTRLILIMVWRKLIRNPNSYSSL  483
AT2G01420.2             TAGLNKMGSNSTAELEAAGGDGGG--NNGTHMPPTSVMTRLILIMVWRKLIRNPNTYSSL  477
AT1G70940.1             ENGLNKLAPNSTAALQSKTGLGGAEASQRKNMPPASVMTRLILIMVWRKLIRNPNTYSSL  501
AT1G23080.1             PNGLHKLRCNSTAELNPKEAIETGETVPVKHMPPASVMTRLILIMVWRKLIRNPNTYSSL  480
                                                  ***::** :** :*.:***  ***:****

Pp3c10_24880V3.1.p      LGVVWSLISFKCHLDMPLILYKSYHIISDAGIGMAMFSLGLFMGMGDRIIACGTKHALFA  619
Pp3c23_10200V3.1.p      LGVIWSLVANRWHLSMPLILYKSVHILSDAGLGMAMFSLGLFMGLGDRIIVCGTKMAVFG  634
Pp3c24_2970V3.1.p       LGVIWSLVANRWHFTMPLILYKSVHILSDAGLGMAMFSLGLFMGLGDRIVVCGRKMAIFG  634
AT5G57090.1             FGLAWSLVSFKWNIKMPTIMSGSISILSDAGLGMAMFSLGLFMALQPKIIACGKSVAGFA  568
AT1G73590.1             FGITWSLISFKWNIEMPALIAKSISILSDAGLGMAMFSLGLFMALNPRIIACGNRRAAFA  543
AT2G01420.2             IGLIWALVAYRWHVAMPKILQQSISILSDAGLGMAMFSLGLFMALQPKIIACGNSVATFA  537
AT1G70940.1             IGLIWALVAFRWHVAMPKIIQQSISILSDAGLGMAMFSLGLFMALQPKLIACGNSVATFA  561
AT1G23080.1             IGLIWALVAFRWDVAMPKIIQQSISILSDAGLGMAMFSLGLFMALQPKLIACGNSTATFA  540
                        :*: *:*:: : .. ** ::  *  *:****:***********.:  :::.**   * *.

Pp3c10_24880V3.1.p      MLLRFLVGPAVFAAASYLVGLRGVSLNVSTVQAALPQGIVPFVFAKEYNVHPEILSTAVI  679
Pp3c23_10200V3.1.p      MALRFLAGPAVFAAASYLVGLRGVPLKVSIVQAALPQGIVPFVFAKEYGVHPEILSTAVI  694
Pp3c24_2970V3.1.p       MSLRFLAGPAVFAAASYLVGLRGVPLKVSIVQAALPQGIVPFVFAKEYGVHPEMLSTAVI  694
AT5G57090.1             MAVRFLTGPAVIAATSIAIGIRGDLLHIAIVQAALPQGIVPFVFAKEYNVHPDILSTAVI  628
AT1G73590.1             AAMRFVVGPAVMLVASYAVGLRGVLLHVAIIQAALPQGIVPFVFAKEYNVHPDILSTAVI  603
AT2G01420.2             MAVRFITGPAIMAVAGIAIGLHGDLLRIAIVQAALPQGIVPFVFAKEYNVHPTILSTGVI  597
AT1G70940.1             MAVRFLTGPAVMAVAAIAIGLRGDLLRVAIVQAALPQGIVPFVFAKEYNVHPAILSTGVI  621
AT1G23080.1             MAVRFFTGPAVMAVAAMAIGLRGDLLRVAIVQAALPQGIVPFVFAKEYNVHPAILSTGVI  600
                          :**..***:: .:.  :*::*  *.:: :*****************.*** :***.**

Pp3c10_24880V3.1.p      FGMIVTLPTALLYYILLGL     698
Pp3c23_10200V3.1.p      FGMLIALPITMVYYILLGL     713
Pp3c24_2970V3.1.p       FGMLIALPITMVYYILLGL     713
AT5G57090.1             FGMLVALPVTVLYYVLLGL     647
AT1G73590.1             FGMLIALPITLLYYILLGL     622
AT2G01420.2             FGMLIALPITLVYYILLGL     616
AT1G70940.1             FGMLIALPITLVYYILLGL     640
AT1G23080.1             FGMLIALPITLVYYILLGL     619
```

Supplemental Figure S1: Alignments of protein sequences of Physcomitrella and Arabidopsis PIN proteins. a) Needleman-Wunsch (Needleman & Wunsch, 1970) alignments of the hydrophilic loop (HL) as well as N'- and C'-terminal transmembrane regions (TM) of the three canonical Physcomitrella PIN proteins. b) Differences in the middle of the loop

structure of the three canonical PIN proteins in Physcomitrella. c) Multiple sequence alignment (Madeira *et al.*, 2019) of the canonical PIN proteins of Physcomitrella and Arabidopsis. Cyan blue = fully conserved, yellow = conserved in two of three; (*) = fully conserved (:) = conservation between amino acid groups of similar properties; (.) = conservation between amino acid groups with weak similar properties.

1488

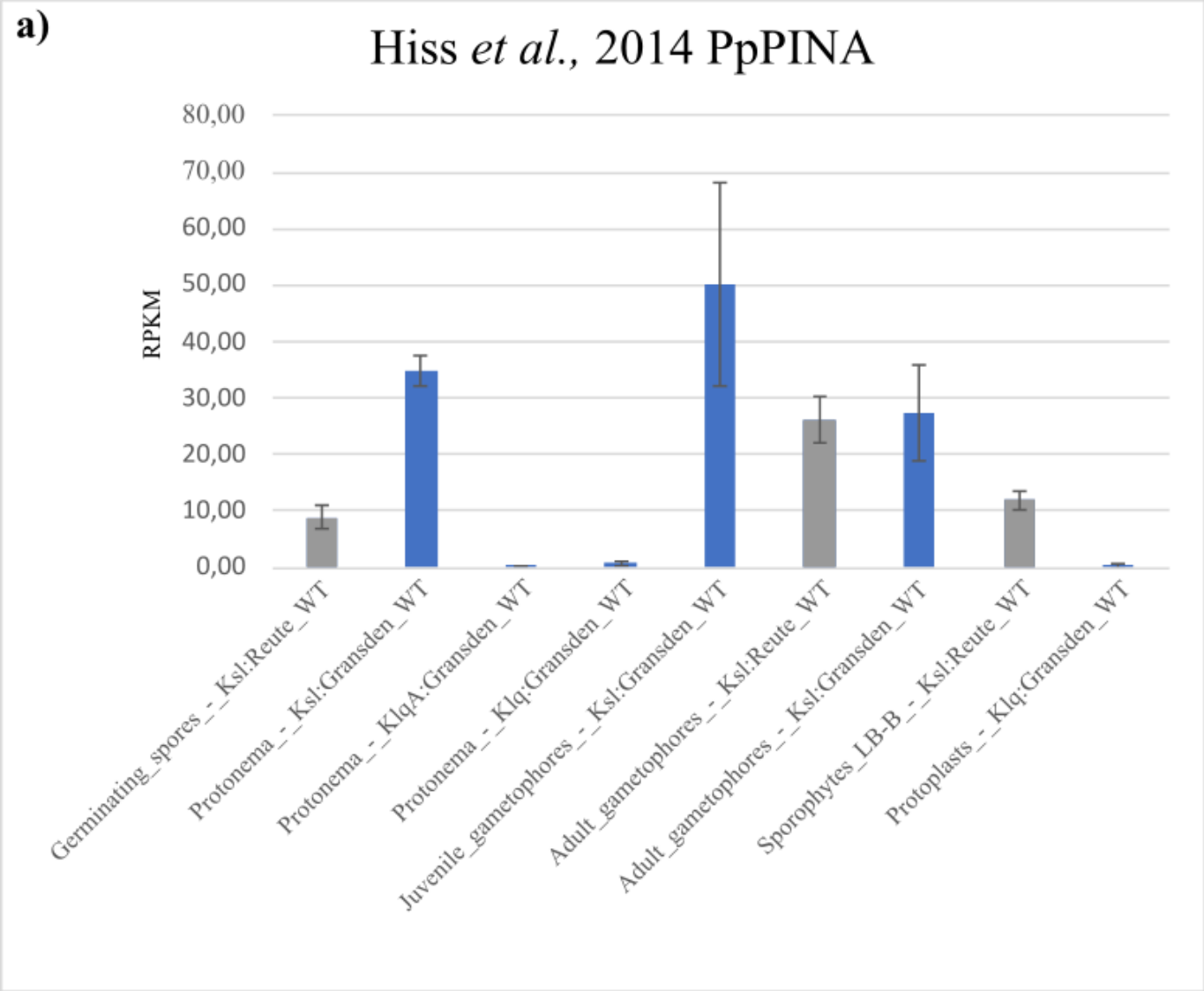
a)
Hiss et al., 2014 PpPINA
RPKM
80,00
70,00
60,00
50,00
40,00
30,00
20,00
10,00
0,00
Germinating_spores_-_Ksl:Reute_WT
Protonema_-_Ksl:Gransden_WT
Protonema_-_KlqA:Gransden_WT
Protonema_-_Klq:Gransden_WT
Juvenile_gametophores_-_Ksl:Gransden_WT
Adult_gametophores_-_Ksl:Reute_WT
Adult_gametophores_-_Ksl:Gransden_WT
Sporophytes_LB-B_-_Ksl:Reute_WT
Protoplasts_-_Klq:Gransden_WT

1489

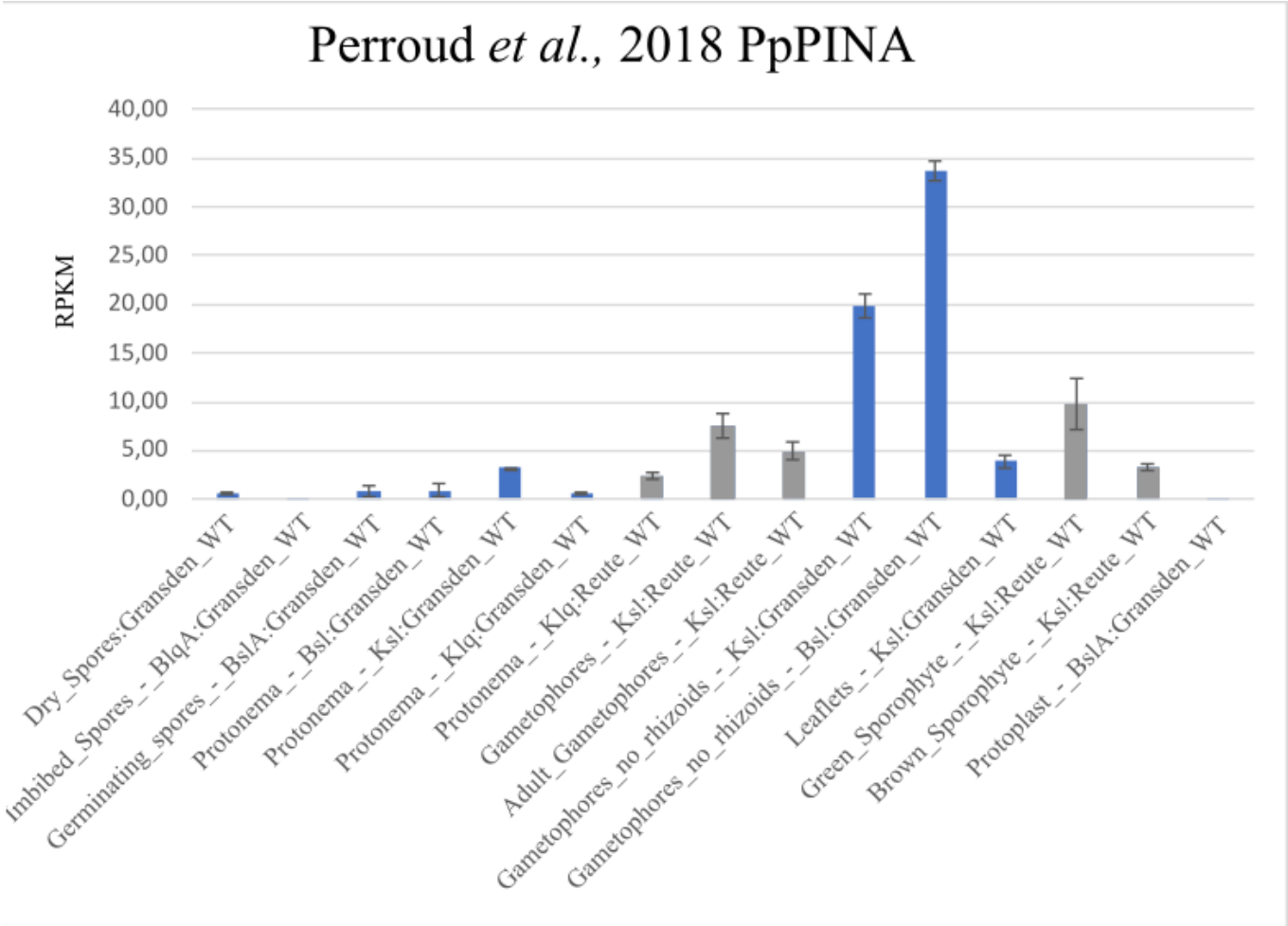
Perroud *et al.*, 2018 PpPINA
RPKM
40,00
35,00
30,00
25,00
20,00
15,00
10,00
5,00
0,00
Dry_Spores:Gransden_WT
Imbibed_Spores_-_BlqA:Gransden_WT
Germinating_spores_-_BslA:Gransden_WT
Protonema_-_Bsl:Gransden_WT
Protonema_-_Ksl:Gransden_WT
Protonema_-_Klq:Gransden_WT
Protonema_-_Klq:Reute_WT
Gametophores_-_Ksl:Reute_WT
Adult_Gametophores_-_Ksl:Reute_WT
Gametophores_no_rhizoids_-_Ksl:Gransden_WT
Gametophores_no_rhizoids_-_Bsl:Gransden_WT
Leaflets_-_Ksl:Gransden_WT
Green_Sporophyte_-_Ksl:Reute_WT
Brown_Sporophyte_-_Ksl:Reute_WT
Protoplast_-_BslA:Gransden_WT

1490

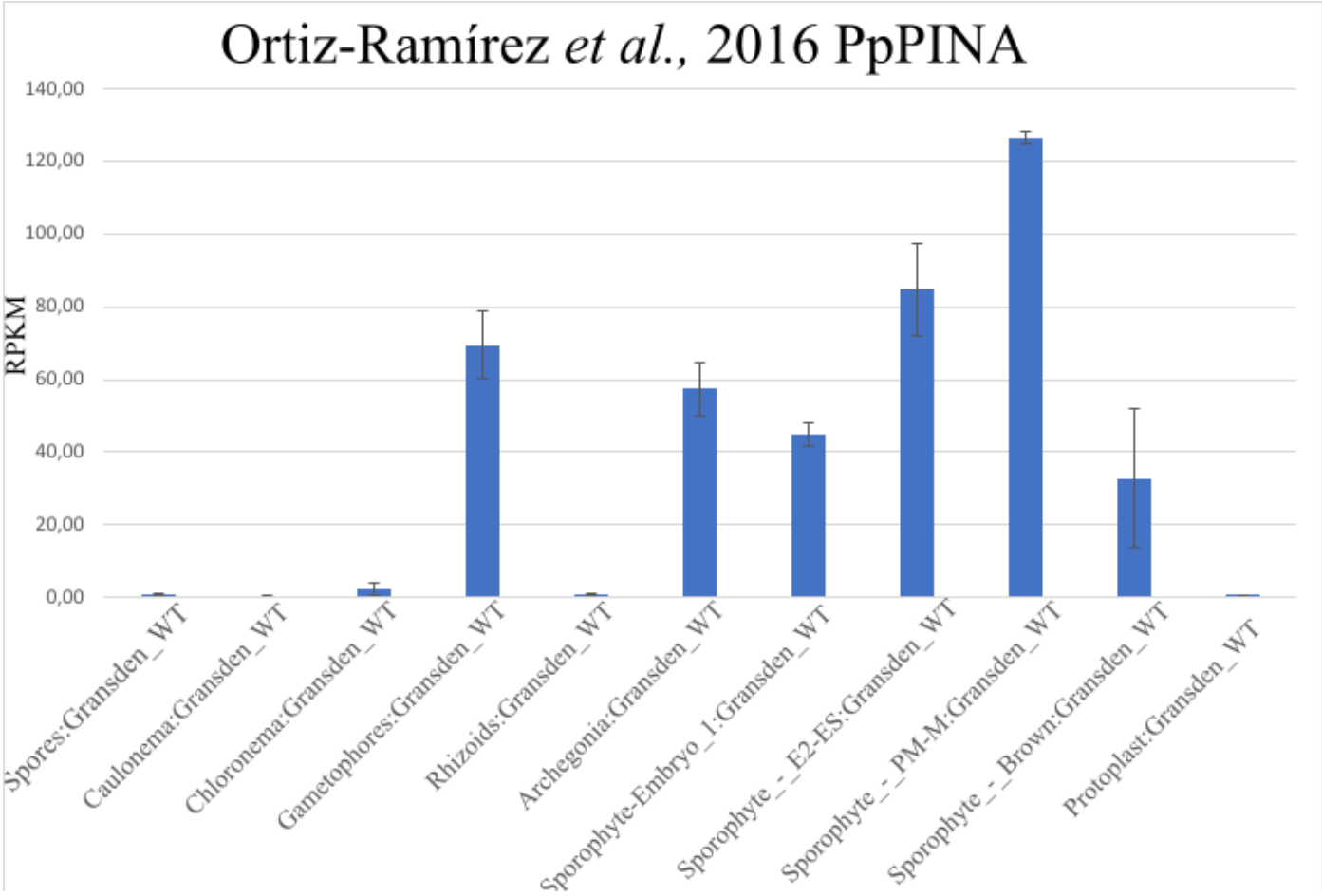
Ortiz-Ramírez et al., 2016 PpPINA
RPKM
140,00
120,00
100,00
80,00
60,00
40,00
20,00
0,00
Spores:Gransden_WT
Caulonema:Gransden_WT
Chloronema:Gransden_WT
Gametophores:Gransden_WT
Rhizoids:Gransden_WT
Archegonia:Gransden_WT
Sporophyte-Embryo_1:Gransden_WT
Sporophyte_-_E2-ES:Gransden_WT
Sporophyte_-_PM-M:Gransden_WT
Sporophyte_-_Brown:Gransden_WT
Protoplast:Gransden_WT

1491

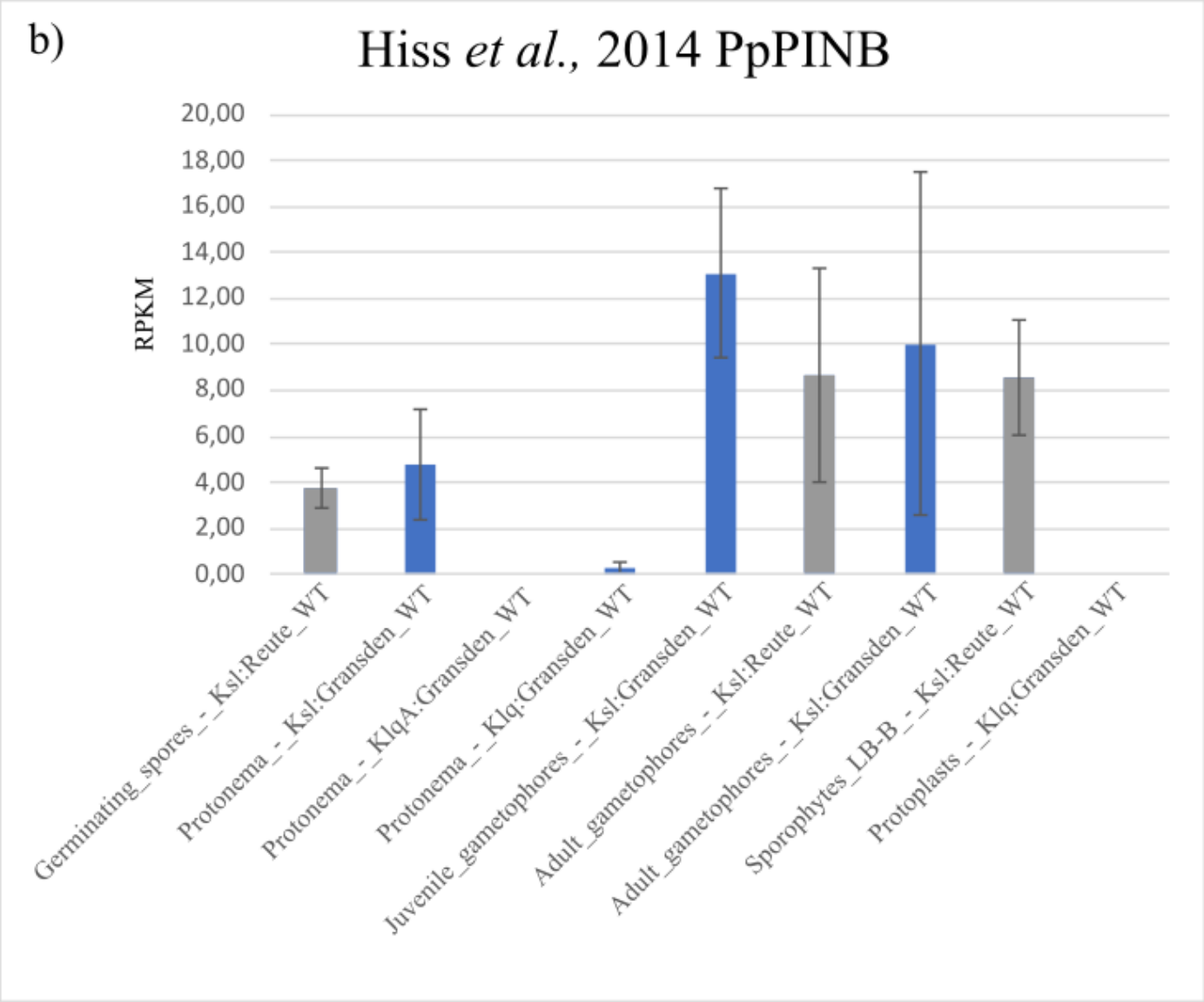
b)
Hiss et al., 2014 PpPINB
RPKM
20,00
18,00
16,00
14,00
12,00
10,00
8,00
6,00
4,00
2,00
0,00
Germinating_spores_-_Ksl:Reute_WT
Protonema_-_Ksl:Gransden_WT
Protonema_-_KlqA:Gransden_WT
Protonema_-_Klq:Gransden_WT
Juvenile_gametophores_-_Ksl:Gransden_WT
Adult_gametophores_-_Ksl:Reute_WT
Adult_gametophores_-_Ksl:Gransden_WT
Sporophytes_LB-B_-_Ksl:Reute_WT
Protoplasts_-_Klq:Gransden_WT

1492

1493

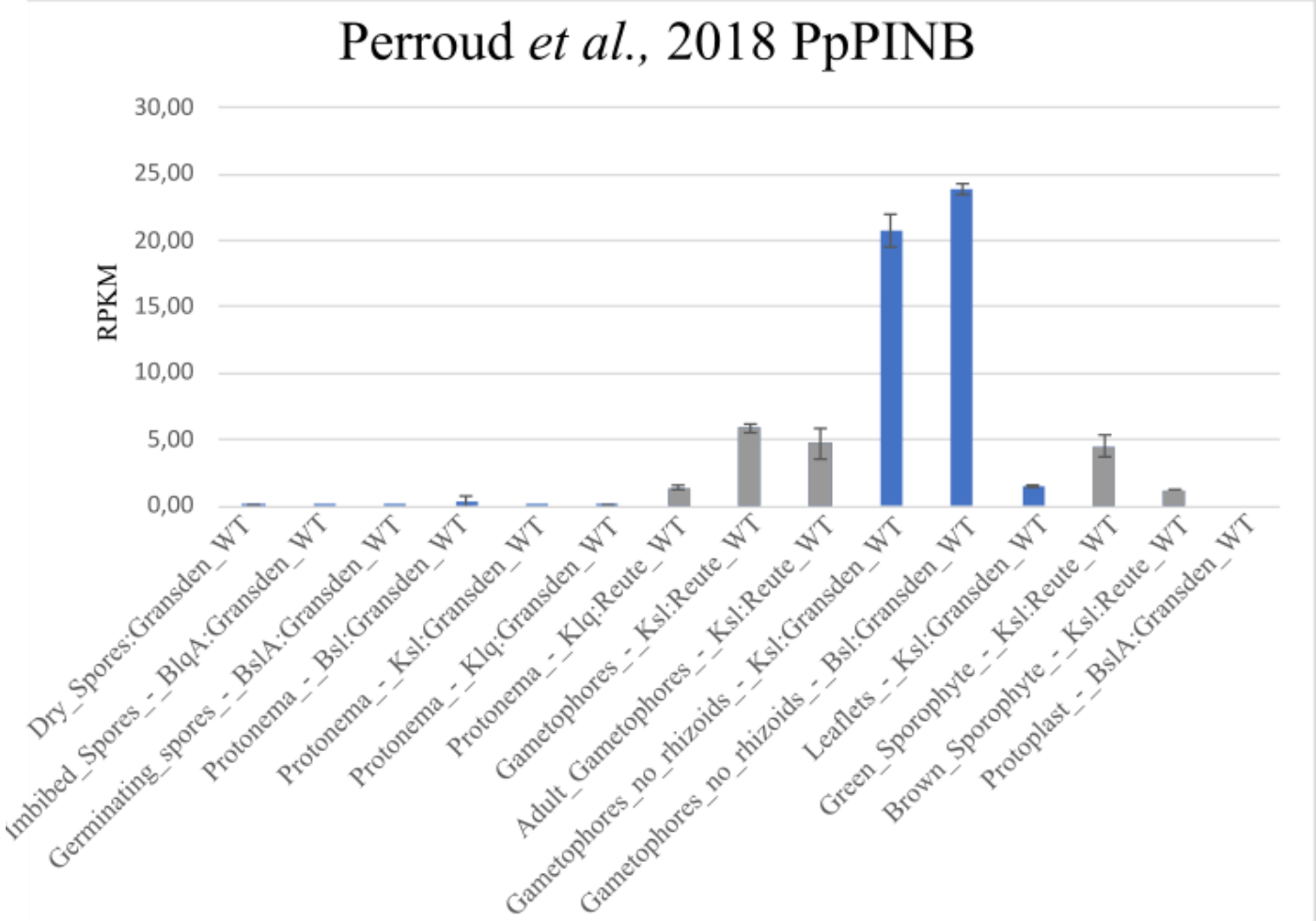
Perroud *et al.*, 2018 PpPINB
RPKM
30,00
25,00
20,00
15,00
10,00
5,00
0,00
Dry_Spores:Gransden_WT
Imbibed_Spores_-_BlqA:Gransden_WT
Germinating_spores_-_BslA:Gransden_WT
Protonema_-_Bsl:Gransden_WT
Protonema_-_Ksl:Gransden_WT
Protonema_-_Klq:Gransden_WT
Protonema_-_Klq:Reute_WT
Gametophores_-_Ksl:Reute_WT
Adult_Gametophores_-_Ksl:Reute_WT
Gametophores_no_rhizoids_-_Ksl:Gransden_WT
Gametophores_no_rhizoids_-_Bsl:Gransden_WT
Leaflets_-_Ksl:Gransden_WT
Green_Sporophyte_-_Ksl:Reute_WT
Brown_Sporophyte_-_Ksl:Reute_WT
Protoplast_-_BslA:Gransden_WT

1494

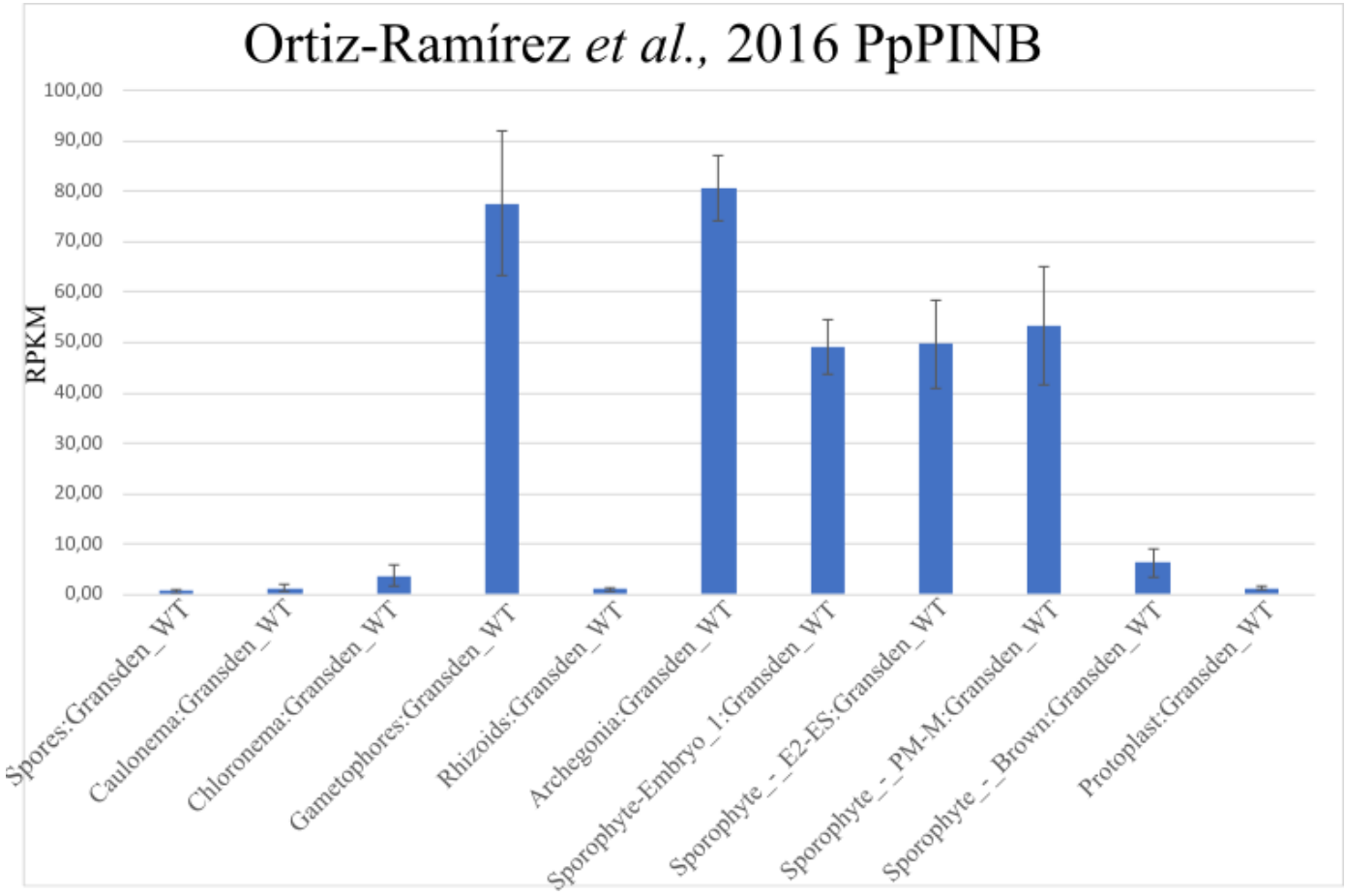
Ortiz-Ramírez *et al.*, 2016 PpPINB
RPKM
100,00
90,00
80,00
70,00
60,00
50,00
40,00
30,00
20,00
10,00
0,00
Spores:Gransden_WT
Caulonema:Gransden_WT
Chloronema:Gransden_WT
Gametophores:Gransden_WT
Rhizoids:Gransden_WT
Archegonia:Gransden_WT
Sporophyte-Embryo_1:Gransden_WT
Sporophyte_-_E2-ES:Gransden_WT
Sporophyte_-_PM-M:Gransden_WT
Sporophyte_-_Brown:Gransden_WT
Protoplast:Gransden_WT

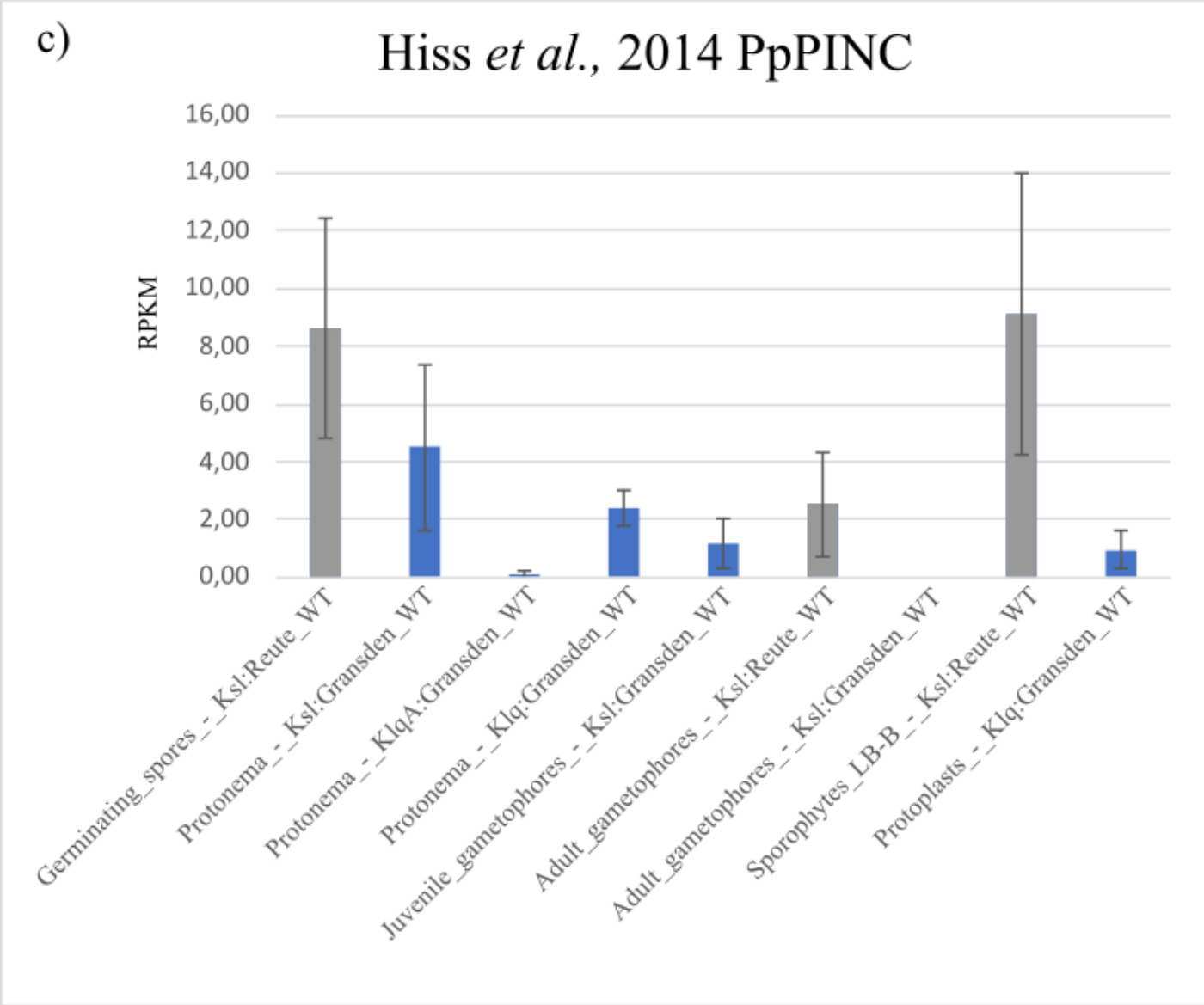
c)
Hiss et al., 2014 PpPINC
RPKM
16,00
14,00
12,00
10,00
8,00
6,00
4,00
2,00
0,00
Germinating_spores_-_Ksl:Reute_WT
Protonema_-_Ksl:Gransden_WT
Protonema_-_KlqA:Gransden_WT
Protonema_-_Klq:Gransden_WT
Juvenile_gametophores_-_Ksl:Gransden_WT
Adult_gametophores_-_Ksl:Reute_WT
Adult_gametophores_-_Ksl:Gransden_WT
Sporophytes_LB-B_-_Ksl:Reute_WT
Protoplasts_-_Klq:Gransden_WT

1498

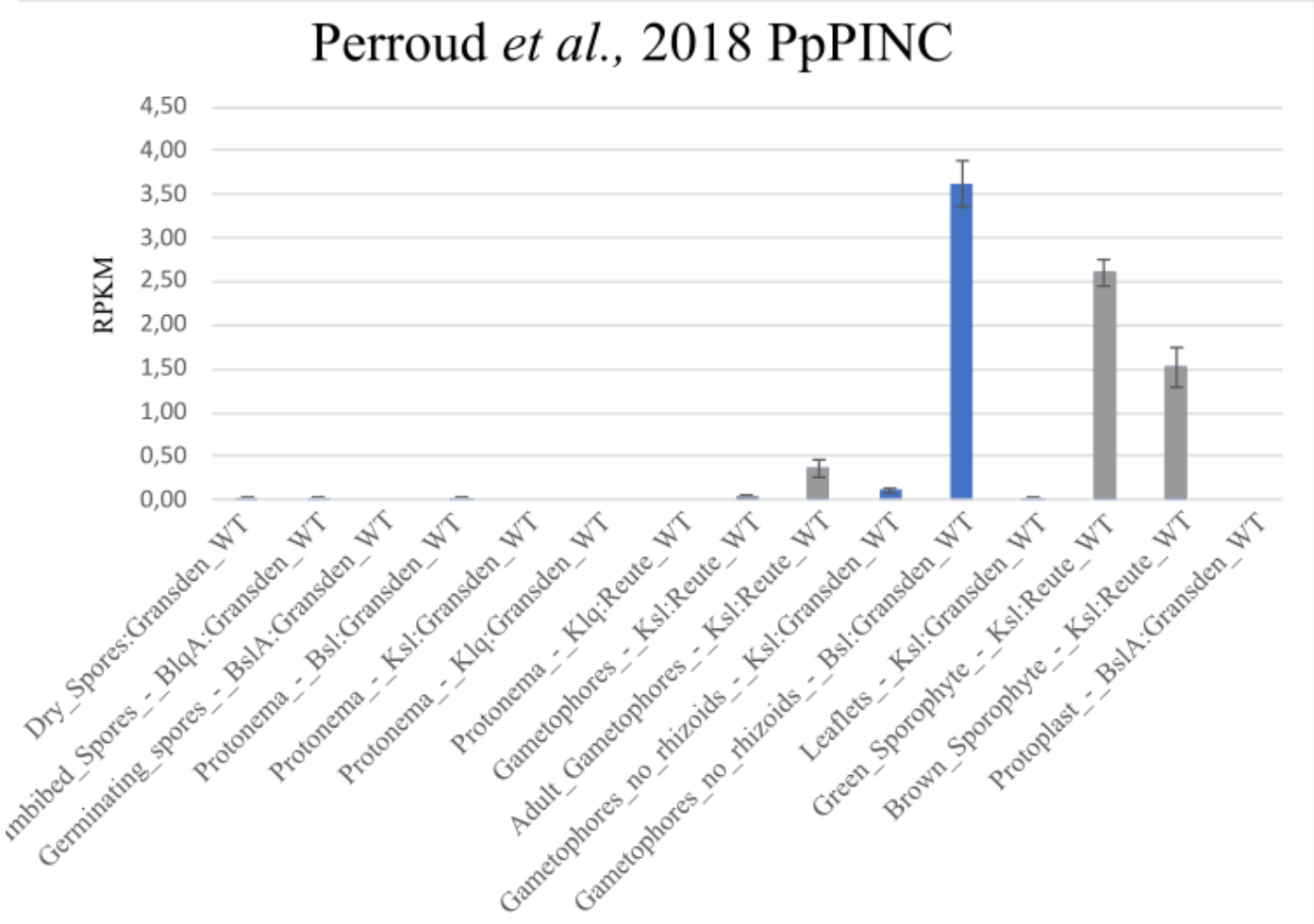
Perroud *et al.*, 2018 PpPINC
RPKM
4,50
4,00
3,50
3,00
2,50
2,00
1,50
1,00
0,50
0,00
Dry_Spores:Gransden_WT
mbibed_Spores_-_BlqA:Gransden_WT
Germinating_spores_-_BslA:Gransden_WT
Protonema_-_Bsl:Gransden_WT
Protonema_-_Ksl:Gransden_WT
Protonema_-_Klq:Gransden_WT
Protonema_-_Klq:Reute_WT
Protonema_-_Ksl:Reute_WT
Gametophores_-_Ksl:Reute_WT
Adult_Gametophores_-_Ksl:Gransden_WT
Gametophores_no_rhizoids_-_Bsl:Gransden_WT
Gametophores_no_rhizoids_-_Ksl:Gransden_WT
Leaflets_-_Ksl:Reute_WT
Green_Sporophyte_-_Ksl:Reute_WT
Brown_Sporophyte_-_Ksl:Reute_WT
Protoplast_-_BslA:Gransden_WT

1499

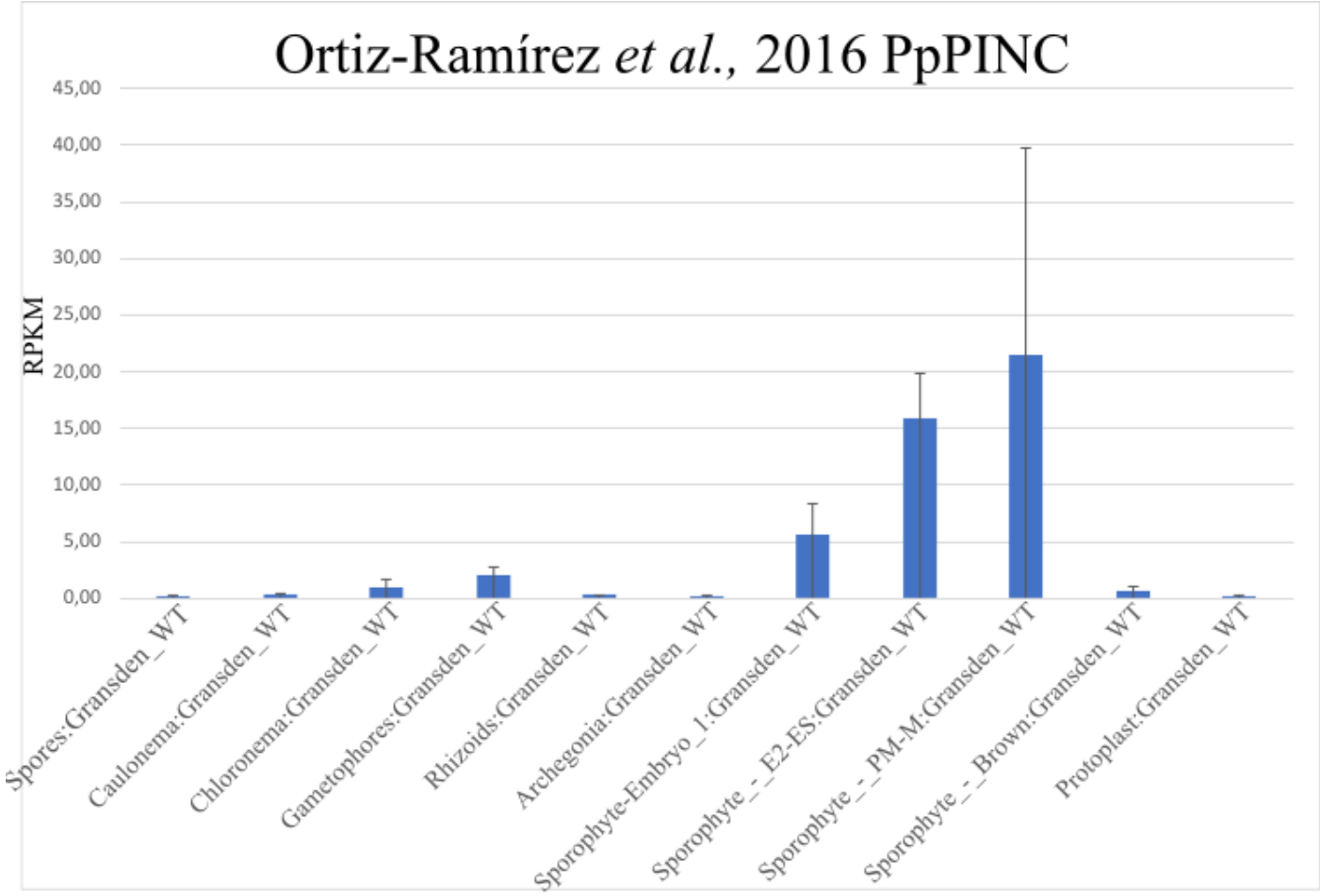

Supplemental Figure S2: Expression data of Physcomitrella PIN genes from PEATmoss database. Expression of *PpPINA*, *B* and *C* in different gene expression sets accessed via the PEATmoss database (Fernandez-Pozo *et al.*, 2020) in the two Physcomitrella ecotypes Gransden (blue bars) and Reute (grey bars), used data sets: Hiss *et al*. (2014), Perroud *et al*. (2018), and Ortiz-Ramirez *et al*. (2016). a) *PpPINA* b) *PpPINB* c) *PpPINC*. Blq = BCD liquid, BlqA = BCD (ammonium) liquid, Bsl = BCD solid, BslA = BCD (ammonium) solid, Klq = Knop liquid, Ksl = Knop solid, Sporophyte LB-B = light brown to brown sporophyte, Sporophyte PM-M = premeiotic to meiotic green sporophyte, sporophyte Embryo 1= first embryo stage, sporophyte E2-ES = early developing sporophyte. n = 3, RPKM = reads per kilobase per million, standard deviation values were not calculated but taken from the according data sets.

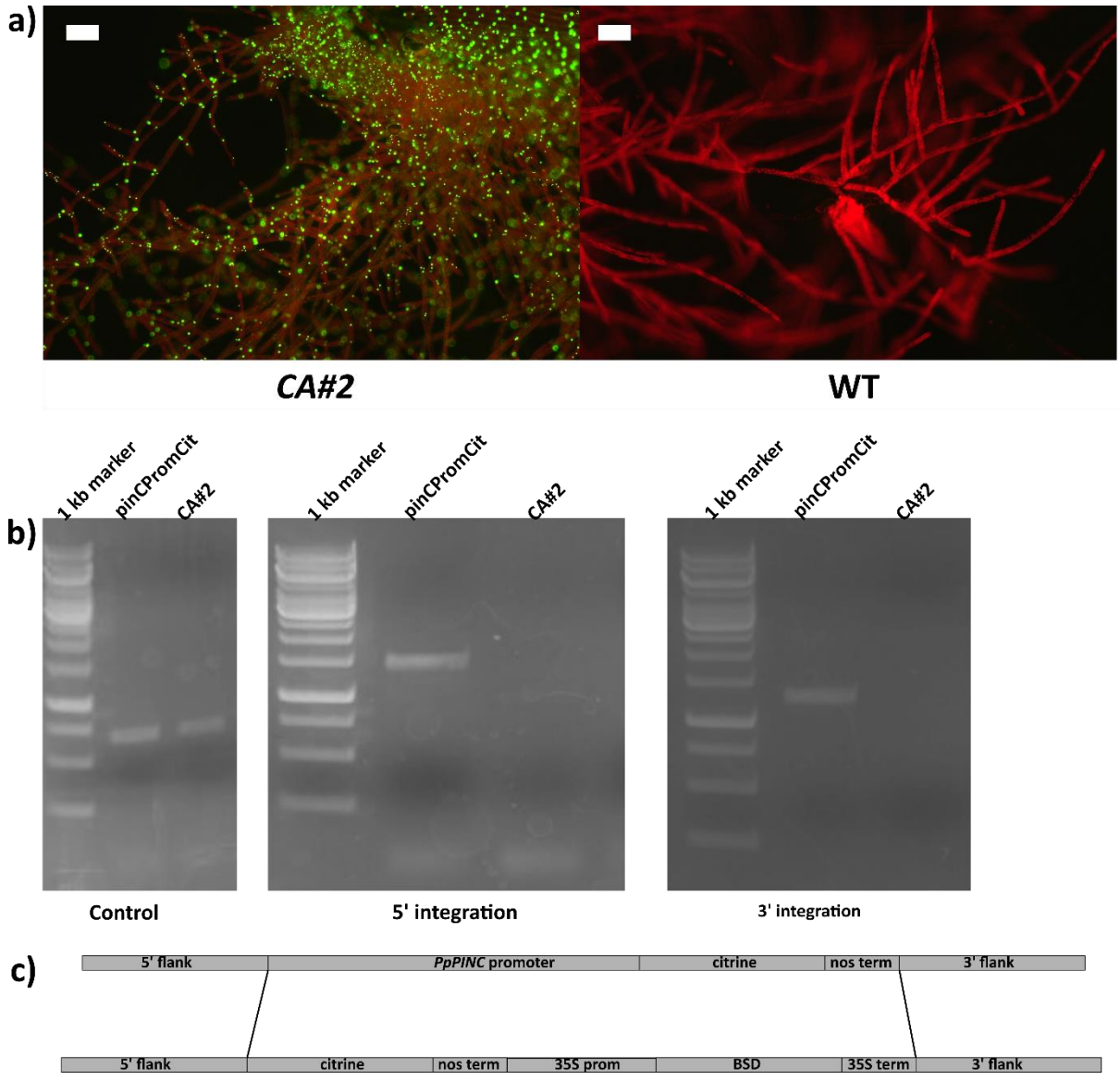

Supplemental Figure S3: Molecular evaluation of *pinCPromCit*. a) Fluorescent microscopy pictures of CA#2, parental line of *pinCPromCit* (left) and Physcomitrella WT (right) protonema and budding gametophore, scale bar = 100 µm. b) Control PCR using constitutive expressed gene Ef1α for *pinCPromCit* and *CA#2*, 3' integration (PCR product = 1.4 kb) and 5' integration (PCR product = 1.5 kb) of *PpPINC* promoter construct, no PCR product for *CA#2* parental line. c) Construct used for creating *pinCPromCit* by targeting the whole construct used in Wiedemann *et al*. (2018). BSD = selection marker, prom = promoter, term = terminator.

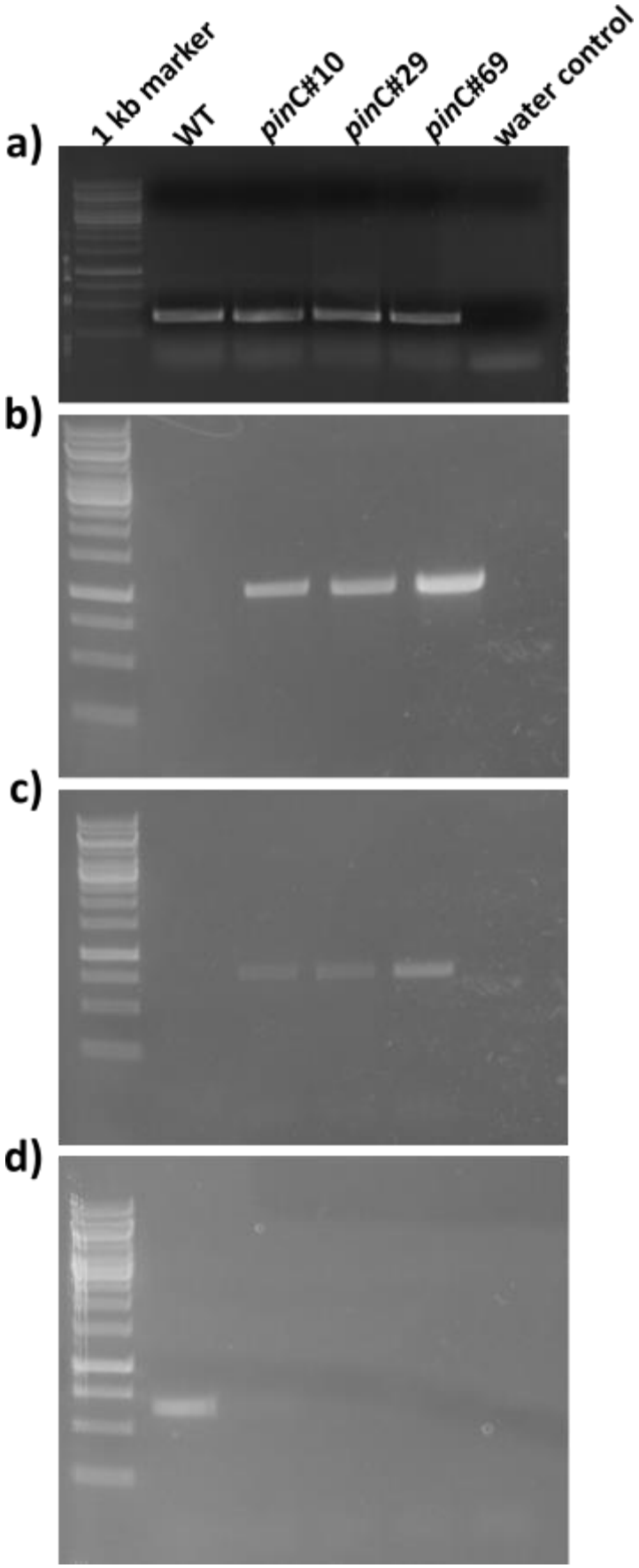

1526

1527

Supplemental Figure S4: Molecular analysis of Physcomitrella *pin*C mutant lines. a) Control PCR using the L21 gene (C45 primers). b) 5' integration of targeting construct (1 kb). c) 3' integration of targeting construct (770 bp). d) RT-PCR amplifying a region from exon 3 to exon 5 (700 bp).

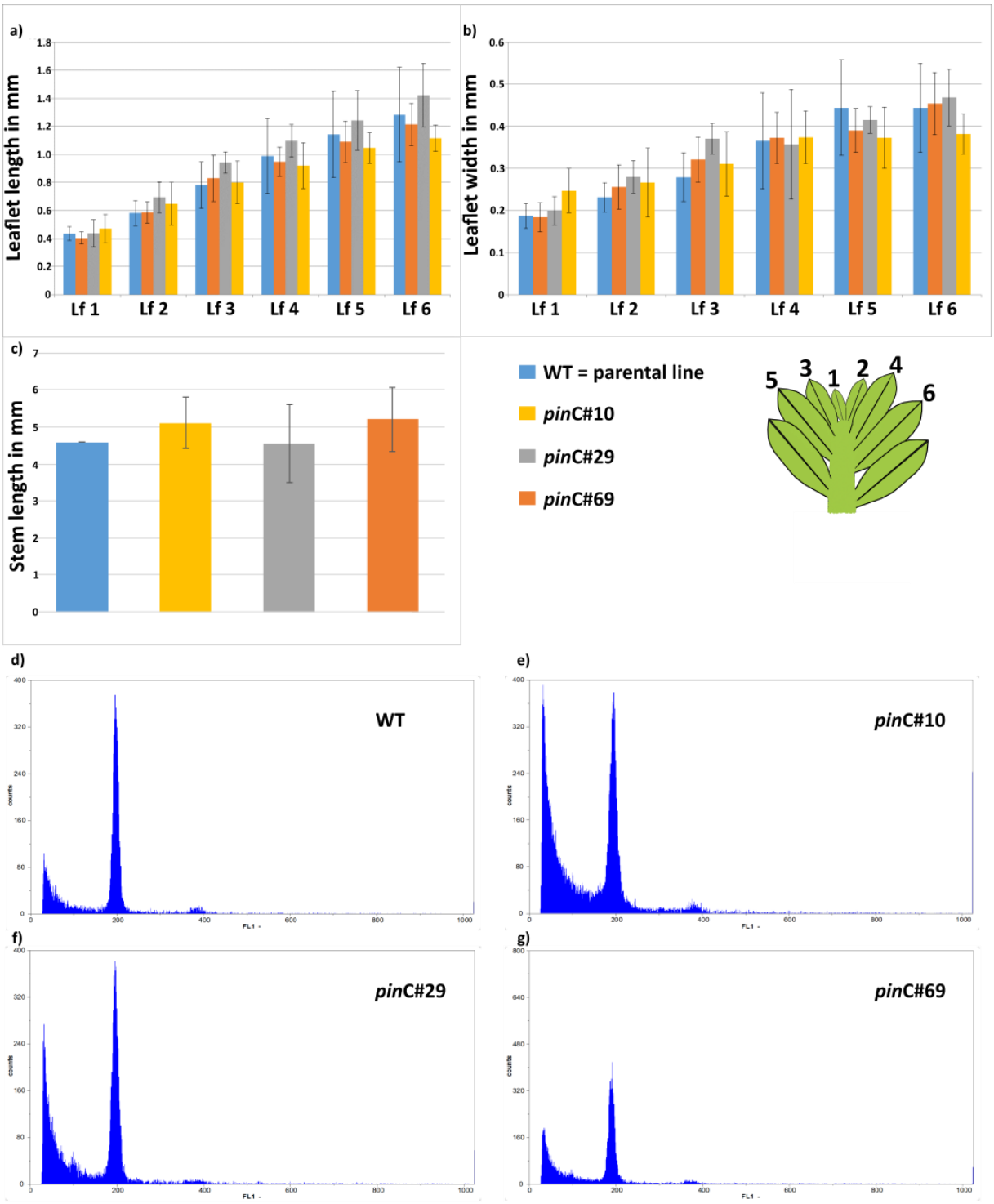

Supplemental Figure S5: Phenotypical characterization of vegetative tissue for Physcomitrella wild type (WT) and *pin*C mutant lines. a) Length and b) width of the first six phyllids of a gametophore. c) stem length d)-g) flow cytometric measurements confirmed haploidy of the generated *pin*C knockouts. Number of measured phyllids and stems a) + b) n= 7; c) WT: n = 13, *pin*C#10: n = 14, *pin*C#29: n = 16, *pin*C#69: n = 18.

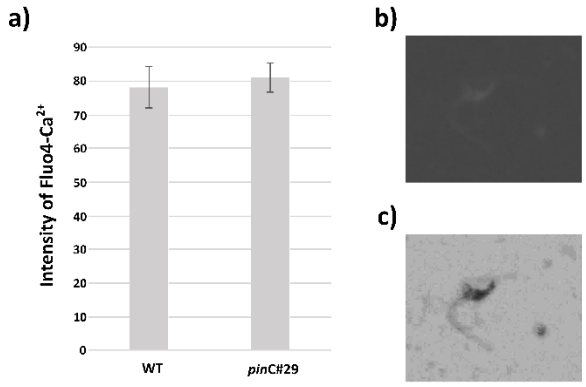

Supplemental Figure S6: Calcium concentration in Physcomitrella spermatozoids. No difference in Ca^{2+} concentration in Physcomitrella WT and mutant sperm cells. a) Intensity of single sperm cells after treatment with Fluo-4 showed no difference (assessed via student t-test). b) grey scale picture of fluorescence image of sperm cell treated with Fluo-4. c) negative image of b) to show sperm cell with flagellum. For a) n = 15 spermatozoids from three different antheridia were examined.

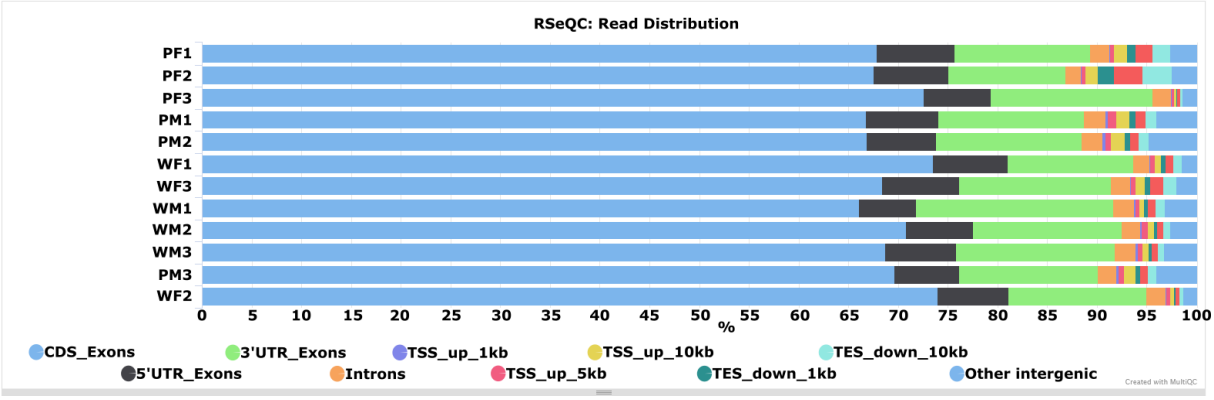

	% Assigned	M Assigned
PF1	47.7%	19.0
PF2	49.5%	25.6
PF3	69.8%	30.9
PM1	54.3%	22.9
PM2	60.1%	25.5
PM3	57.1%	39.8
WF1	61.2%	20.7
WF2	65.7%	30.3
WF3	56.9%	25.0
WM1	57.2%	21.9
WM2	61.5%	25.9
WM3	65.0%	26.3

Supplemental Figure S7: Quality control RNAseq. Read distribution in Physcomitrella WT and *pin*C mutant gametangia, WM = WT antheridia, WF = WT archegonia, PM = *pin*C#29 antheridia, PF = *pin*C#29 archegonia. CDS = coding sequence, UTR = untranslated region, TSS = transcription start sequence, TES = transcription end sequence. Quality control done with MultiQC (Galaxy Version 1.11+galaxy0).

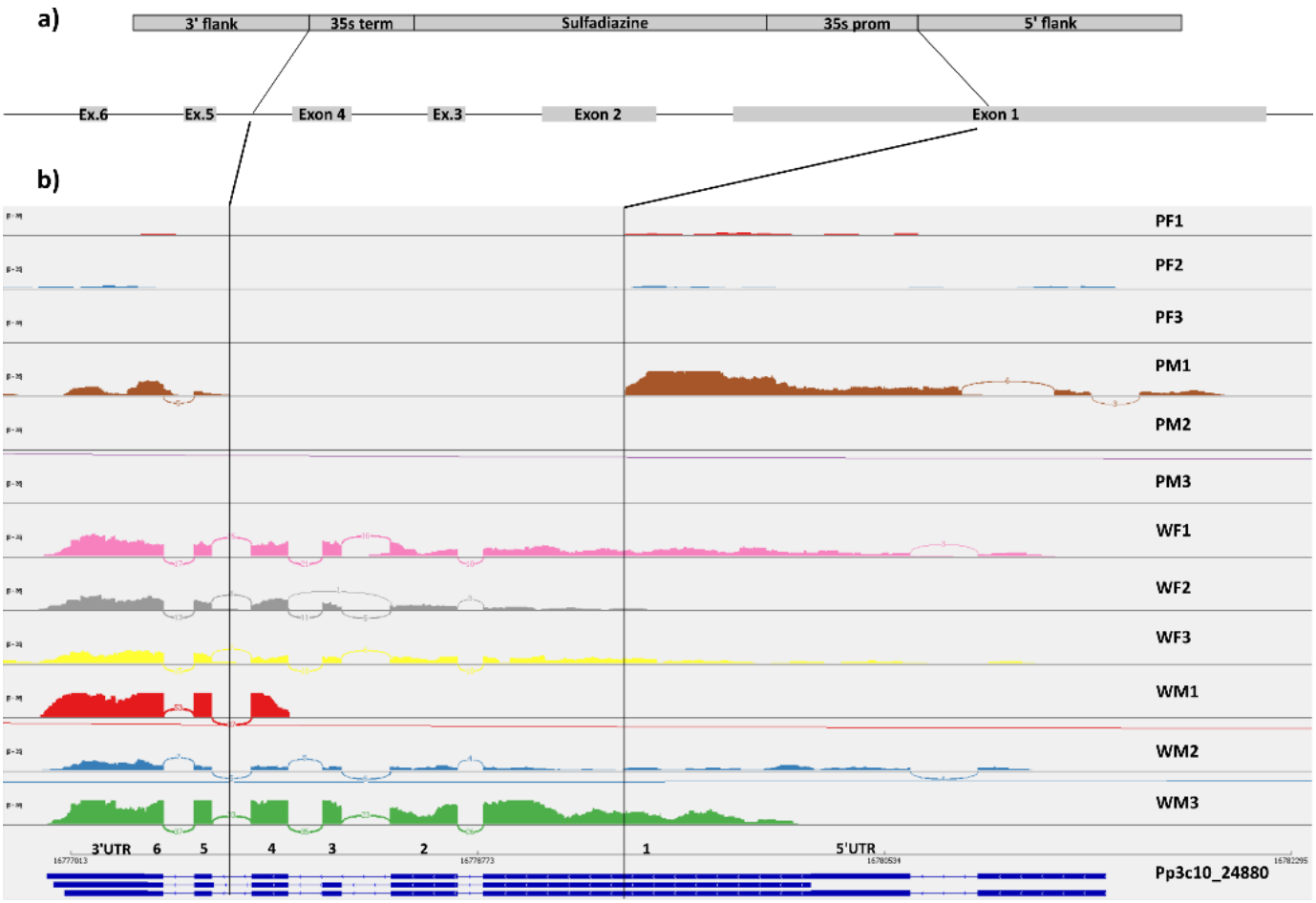

Supplemental Figure S8: Proof of *PpPINC* mutation in *pin*C#29. Sashimi plot showing integration of knockout construct in Physcomitrella WT background. a) Knockout construct for the *PINC* gene. Black lines indicate the integration into the gene starting from the middle of exon 1 to the intron between exon 4 and 5. b) Sashimi plot for the PINC gene in all samples. Continuous read through of mapped fragments only in WT samples, confirming knockout of the gene in the mutant.

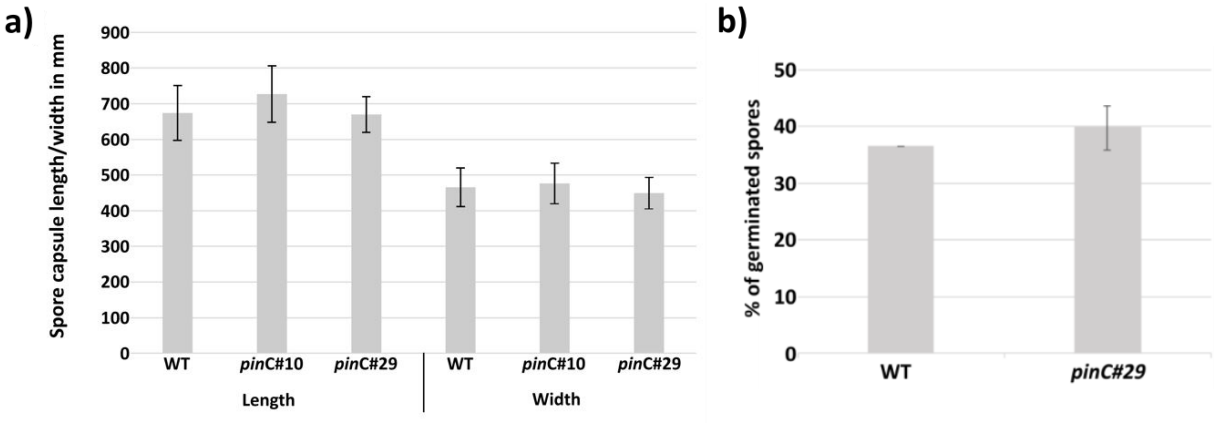

Supplemental Figure S9: **Size of spore capsules and spore germination rate.** a) Length and width of mature spore capsules from Physcomitrella WT n = 15, mutant *pin*C#10 and mutant #29, n = 16. b) Germination rate of spores three days after plating. n = 3 plates. Possible differences were tested with students t-test.

Supplemental Table S1: Primers used in Physcomitrella WT and mutant lines.

Name	Sequence	Comment
P3-KO Fw	5'-GGGATCCATGTTGGCCTACGCGTCTGT-3'	Amplified region for *pin*C knockout construct
P3-KO Rv	5'-GAAGCTTCTGGGGAGTTCAACACCATT-3'	
5PinCprom_f+CA5	5'- agcttaacgttagccactcTCCTTTGTGTGGAGTAGAG-3'	Gibson primers for amplification of PpPINC promoter region, (capital letters)
3PinCprom_r+Citrin	5'-CACGTCGACAGATCGTCAAGgcagaagttcatgggaggtgga-3'	
Pin3f_ex1-2	*5'*-ACGTGAACATTCCTCGGTTC-*3'*	RT-PCR, middle of exon 1 to exon 2 of PpPINC
Pin3r_ex2	*5'*-GTTCGGATTGCGAGTGAGTT-*3'*	
C45_fwd	*5'*-GGCTGGTCATGGGTTGCG-*3'*	cDNA reference gene
C45_rev	*5'*-GAGGTCAACTGTCTCGCC-*3'*	
35SPqPCR_f	5'-CCATTGCCCAGCTATCTGTC-3'	Determination of transgene *pin*C copy number via qPCR
35SPqPCR_r	5'-CATTGCGATAAAGGAAAGGC-3'	

Supplemental Table S2: Differentially expressed genes in Physcomitrella WT and mutant. Single genes found in comparisons of Physcomitrella a) mutant (PM) vs wildtype (WM) antheridia b) mutant (PF) vs wild type (WF) archegonia; BP = biological process, CC = cellular compartment, MF = molecular function.

a)

Upregulated genes mutant (PM) vs. wildtype (WM) antheridia					
geneID	Foldchange	p-Adjust	GO_annot_BP	GO_annot_MF	GO_annot_CC
Pp3c26_6020	2,61799094	0,00574099	single-multicellular organism process; anatomical structure development; ion transmembrane transport; single-organism developmental process	ion channel activity	cell part; integral component of membrane
Pp3c26_3990	2,60429982	3,58E-08	transmembrane transport	substrate-specific transmembrane transporter activity	chloroplast envelope; integral component of membrane

geneID	PM1	PM2	PM3	WM1	WM2	WM3
Pp3c26_6020	209	282	1259	15	50	32
Pp3c26_3990	676	735	822	79	101	101

Downregulated genes mutant (PM) vs. wildtype (WM) antheridia					
geneID	Foldchange	p-Adjust	GO_annot_BP	GO_annot_MF	GO_annot_CC
Pp3c9_8920	-2,14177862	0,00160142	dolichol biosynthetic process	amino acid binding	chloroplast stroma; chloroplast thylakoid membrane
Pp3c14_8940	-2,3368623	0,01313347	.	.	integral component of membrane
Pp3c20_22670	-2,48823907	0,00673352	positive regulation of transcription, DNA-templated	zinc ion binding; sequence-specific DNA binding; sequence-specific DNA binding transcription factor activity	nucleus
Pp3c1_22810	-2,68377153	0,00973054	cell wall modification:pectin catabolic process	pectinesterase activity:aspartyl esterase activity	cell wall:extracellular region
Pp3c19_15670	-2,68772125	0,00973054	cellular component organization or biogenesis; cellular process	.	cytoplasm

Pp3c3_4950	-2,71566077	0,009008	regulation of biological quality; regulation of transcription, DNA-templated; asymmetric cell division; leaf development; radial pattern formation	sequence-specific DNA binding; sequence-specific DNA binding transcription factor activity	nucleus
Pp3c3_11110	-3,07745056	4,01E-08	proteolysis	aspartic-type endopeptidase activity	.
Pp3c21_8410	-3,24497467	5,52E-05	peptidyl-tyrosine dephosphorylation	protein tyrosine phosphatase activity	.
Pp3c12_11710	-4,86650335	1,63E-14	.	.	.

geneID	PM1	PM2	PM3	WM1	WM2	WM3
Pp3c9_8920	1079	1248	2115	10980	5147	6717
Pp3c14_8940	531	119	190	1918	3043	2972
Pp3c20_22670	36	8	48	286	383	271
Pp3c3_11110	170	141	99	1975	1576	1902
Pp3c21_8410	1	5	7	100	197	253
Pp3c12_11710	232	115	230	71101	8547	41718
Pp3c1_22810	1	0	0	184	76	86
Pp3c19_15670	1	0	2	123	90	54
Pp3c3_4950	2	0	0	231	161	82

b)

Upregulated genes mutant (PF) archegonia vs. wildtype (WF) archegonia					
geneID	Foldchange	p-Adjust	GO_annot_BP	GO_annot_MF	GO_annot_CC
Pp3c11_4360	3,28704921	5,88E-11	proteolysis	serine-type endopeptidase activity	cell part

geneID	PF1	PF2	PF3	WF1	WF2	WF3
Pp3c11_4360	154	241	220	0	0	4

Downregulated genes mutant (PF) archegonia vs. wildtype (WF) archegonia					
geneID	Foldchange	p-Adjust	GO_annot_BP	GO_annot_MF	GO_annot_CC
Pp3c7_8820	-2,55854236	6,08E-07	.	.	.
Pp3c6_26100	-6,49563884	9,91E-73	.	metal ion binding	.

geneID	PF1	PF2	PF3	WF1	WF2	WF3
Pp3c7_8820	72	129	58	1134	1082	3960
Pp3c6_26100	0	0	0	989	1581	1305

1593

Supplemental Table S3: All DEG experiments, including table of single genes already identified in other publications.

See separate file.

Supplemental Table S4: Number of vital and aborted sporophytes counted in Physcomitrella WT and *pin*C mutant lines.

Line	Colonies	Gametophores	Vital Sporophytes	Aborted Sporophytes
WT	41	1029	43	9
*pin*C#10	30	1021	318	102
*pin*C#29	42	1370	401	503
*pin*C#69	32	1038	79	69